Membrane fouling development and biofilm-forming bacteria in anoxic/oxic-MBR under low organic loading rate conditions

低有機物負荷 A/O-MBR における膜ファウリングの発生機構とバイオフィルム形成細菌に関する研究

Doctoral thesis by Yuya Takimoto

Supervisor: Prof. Takashi Yamaguchi
Prof. Wataru Ogasawara
Associate Prof. Masashi Hatamoto
Associate Prof. Shinya Maki
Associate Prof. Tomonori Kindaichi

Department of Science of Technology Innovation
Nagaoka University of Technology
Kamitomioka 1603-1, Nagaoka, Niigata 940-2188, Japan

Contents

Chapter 1

General introduction

1.1. Background and objectives

Recently, urbanization and urban sprawl are expected to increase in the next century (Hibbs and Sharp, 2012), discharge of wastewater especially municipal sewage will increase. Membrane bioreactor (MBR) is one of the most innovative wastewater treatment system especially for treating municipal wastewater. Previous results showed that the MBR achieved not only high nutrient removal such as organic carbon, nitrogen and phosphorus but pathogen or virus removal in municipal wastewater (Rosenberger et al., 2002; Trussell et al., 2005; Chae and Shin, 2007; Ma et al., 2013; Wu et al., 2010). Moreover, install of the full-scale MBRs are drastically spread and continue to increase in the world (Xiao et al., 2019). However, membrane fouling which cause permeate flux decline remains as major issue of the widespread to use for various wastewater treatment in MBR. Especially, biofilm formation of the fouled membrane is severe problem. To date, membrane fouling have been understood to occur from three stages as follows; Firstly, adherence of microbes on the membrane surface and produce extracellular poly-substances (EPS) with fast TMP increase. Secondly, growth of attached microbes and micro-colony formation to three-dimensional structure and accumulation of foulants with slow TMP increase. Thirdly, continuous accumulation and formation of cake layer with fast TMP increase and lead to TMP jump (Gao et al., 2013).

In the full-scale MBR, generally, MBR was worked under low feed-to-microorganism conditions because of high concentrated sludge operation compared to conventional activated sludge process (Lobos et al., 2005), and no sludge discharge and limited COD were observed (Shen et al., 2012). Hence, it is necessary to investigate influence of low organic loading rate (OLR) condition on microbial community and membrane fouling in MBR in order to improve the reactor performance and control membrane fouling. Recently, many researchers have addressed to reveal microbial community corresponding membrane fouling development in the MBR since the high throughput sequencing technology had been developed (mentioned chapter 2).

Although system performance under starvation or prolonged starvation conditions were investigated in conventional activated sludge process and MBR process (Lobos et al., 2005; Zhang et al., 2009; Wu and Lee, 2011; Maqbool et al., 2017; Palmarin et al., 2020), microbial community and important bacteria related to system performance and membrane fouling in the condition are still unclear. Thus, the objective of this study was to investigate influence of extremely low OLR (prolonged starvation) conditions on membrane fouling development and microbial community in mixed liquor and to clarify the key bacteria related to membrane fouling development in anoxic/oxic (A/O)-MBR. In order to achieve the goal, four specific objectives were built as follows;

1. To evaluate the influence of extremely low OLR on membrane fouling development and bacteria response for characteristics of mixed liquor.

2. To explore the biofilm-forming bacteria on fouled membrane surface in low OLR MBR by comparing naturally developed biofilm in MBR under standard condition.
3. To clarify mechanisms of biofilm formation especially initiation and progression of biofilm development on the fouled membrane in low OLR MBR.
4. To explore the fouling causing bacteria and fouling mitigating bacteria compared between fouled MBR and fouling-mitigated MBR under low OLR conditions.

1.2. Outline of this thesis

This thesis organized six chapters in order to achieve the objectives (**Fig. 1.1**). In chapter 1, the background, objectives and outline of this thesis are introduced. In chapter 2, basic information regarding this thesis was provided.

In chapter 3, influence of low OLR condition in A/O-MBR on membrane fouling was evaluated and biofilm-forming bacteria in the A/O-MBR were identified to compare with naturally developed biofilm under standard condition. In chapter 4, fouled membranes during progression of membrane fouling under low OLR condition were monitored by non-destructive observation and pioneer bacteria for membrane fouling was estimated. In chapter 5, generation of dissolved organic matter derived from cell lysis on membrane fouling was evaluated and fouling causing and mitigating bacteria were estimated. Finally, the conclusion of this thesis and future outlook were discussed in chapter 6.

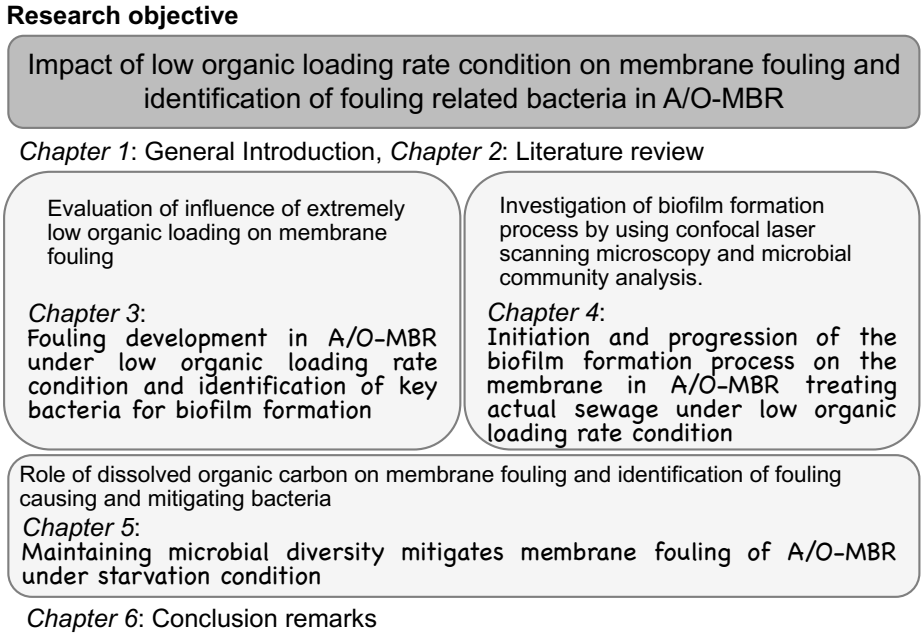

Fig. 1.1 Structure of this thesis

References

Chae, S. R., and Shin, H. S. (2007). Characteristics of simultaneous organic and nutrient removal in a pilot-scale vertical submerged membrane bioreactor (VSMBR) treating municipal wastewater at various temperatures. Process Biochemistry, 42(2), 193-198.

Gao, D., Fu, Y., & Ren, N. (2013a). Tracing biofouling to the structure of the microbial community and its metabolic products: A study of the three-stage MBR process. Water research, 47(17), 6680-6690.

Hibbs, B. J., & Sharp Jr, J. M. (2012). Hydrogeological impacts of urbanization. Environmental & Engineering Geoscience, 18(1), 3-24.

Lobos, J., Wisniewski, C., Heran, M., & Grasmick, A. (2005). Effects of starvation conditions on biomass behaviour for minimization of sludge production in membrane bioreactors. Water Science and Technology, 51(6-7), 35-44.

Ma, D., Gao, B., Hou, D., Wang, Y., Yue, Q., and Li, Q. (2013). Evaluation of a submerged membrane bioreactor (SMBR) coupled with chlorine disinfection for municipal wastewater treatment and reuse. Desalination, 313, 134-139.

Maqbool, T., Cho, J., & Hur, J. (2017). Spectroscopic descriptors for dynamic changes of soluble microbial products from activated sludge at different biomass growth phases under prolonged starvation. Water research, 123, 751-760.

Palmarin, M. J., Young, S., & Chan, J. (2020). Recovery of a hybrid and conventional membrane bioreactor following long-term starvation. Journal of Water Process Engineering, 34, 101027.

Rosenberger, S., Krüger, U., Witzig, R., Manz, W., Szewzyk, U., and Kraume, M. (2002). Performance of a bioreactor with submerged membranes for aerobic treatment of municipal waste water. Water Research, 36(2), 413-420.

Shen, Y. X., Xiao, K., Liang, P., Sun, J. Y., Sai, S. J., & Huang, X. (2012). Characterization of soluble microbial products in 10 large-scale membrane bioreactors for municipal wastewater treatment in China. Journal of Membrane Science, 415, 336-345.

Trussell, R. S., Adham, S., and Trussell, R. R. (2005). Process limits of municipal wastewater treatment with the submerged membrane bioreactor. *Journal of Environmental Engineering*, *131*(3), 410-416.

Wu, J., Li, H., and Huang, X. (2010). Indigenous somatic coliphage removal from a real municipal wastewater by a submerged membrane bioreactor. *Water research*, *44*(6), 1853-1862.

Wu, S. C., & Lee, C. M. (2011). Correlation between fouling propensity of soluble extracellular polymeric substances and sludge metabolic activity altered by different starvation conditions. Bioresource Technology, 102(9), 5375-5380.

Xiao, K., Liang, S., Wang, X., Chen, C., & Huang, X. (2019). Current state and challenges of full-scale membrane bioreactor applications: a critical review. Bioresource technology, 271, 473-481.

Zhang, H. F., Sun, B. S., Zhao, X. H., & Sun, J. M. (2009). Membrane fouling caused by soluble microbial products in an activated sludge system under starvation. Desalination and Water Treatment, 1(1-3), 180-185.

Chapter 2

Literature review

2.1. Advantages of membrane bioreactor (MBR) system

MBR is a promising biological wastewater treatment process which has microfiltration membrane submerged in activated sludge for separation of solid and liquid. Since submerged MBR was developed by Yamamoto et al. (1989), a lot of studies of MBR have focused on treatment of municipal wastewater and achieved high system performance on complete suspended solid removal, organic matter and nutrient removal, pathogen and virus removal efficiency with higher mixed liquor suspended solid (MLSS) concentration (Rosenberger et al., 2002; Trussell et al., 2005; Chae and Shin, 2007; Ma et al., 2013; Wu et al., 2010). Additionally, MBR system could save a space for sedimentation tank although conventional activated sludge process requires large scale treatment area. Thus, these advantages of MBR suggests that could treat high nutrient wastewater with shorter operational time.

Aerobic MBR consists anoxic and oxic tank (called anoxic/oxic (A/O)-MBR) to enhance denitrification in oxic tank by ammonium and nitrite oxidizing bacteria in oxic tank, denitrification in anoxic tank, and phosphorus removal by polyphosphate accumulating organisms, respectively (Chae and Shin, 2007; Sun et al., 2013). Although both of polymeric and ceramic membranes are used in MBR, most of MBR membrane were used polymeric materials such as polyvinylidene difluoride (PVDF) with approximately 0.1 μm pore due to low cost. Thus, A/O-MBR has potential of alternative municipal wastewater treatment system to conventional activated sludge process for achieving complete nutrient removal of municipal wastewater in full-scale plant around the world (Lyko et al., 2008; Xiang et al., 2014; Monclús et al., 2010). In fact, the development and application of full-scale MBR have been spread in the world (Xiao et al., 2019). However, membrane fouling remains as major issue of the MBR.

2.2. Membrane fouling development and the related substances (foulants)

2.2.1. Membrane fouling

A major issue of MBR is membrane fouling development during long term operation by clogging the membrane pores by organic or inorganic matter causing flux decrease. Membrane fouling was primary triggered by cake layer formation on the membrane surface and has divided into three parts (Meng et al., 2009); First is removable fouling which can remove accumulated matter on the membrane surface by physical cleaning. Second is irremovable fouling which cannot be removed by intermediate physical cleaning or backwashing. Third is irreversible fouling which requires chemical cleaning of foulants on the membrane surface (Fig. 2.1). Although chemical agents such as NaClO could remove almost all foulants (fouling causing substances on membrane surface) on the membrane surface, recently, it is clarify that NaClO exposure contributes generation of significant stress in bacteria and of dissolved organic matter (DOM) triggering severe or rapid membrane fouling development (Cai and Liu, 2018; Sun et al., 2018; Sun et al.,

2019), and significant damage of polymeric membrane. Moreover, on-line chemical cleaning also generated halogenated byproducts and the remained byproducts has potential for significant damage on aquatic environment (Zhang and Liu, 2020). Thus, we should focus on the fouling control strategy without using the chemical agents for saving the cost and environment.

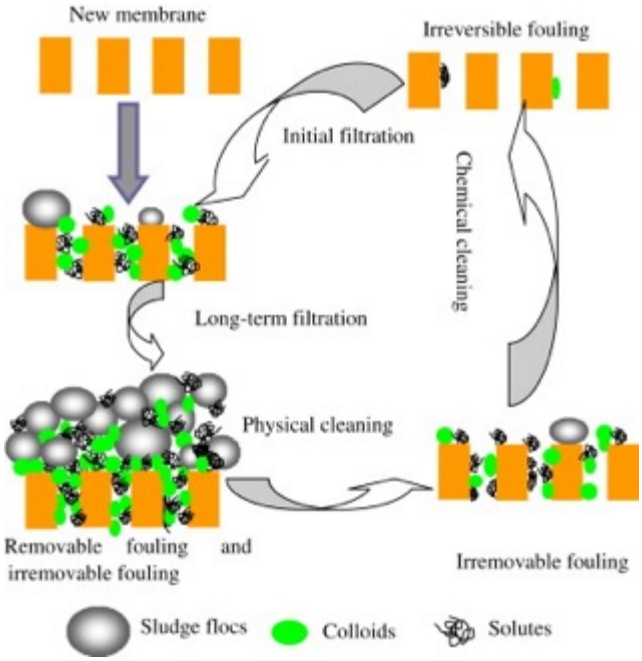

Fig. 2.1 Schematic diagram of removable, irremovable, and irreversible fouling formed on the membrane surface. (from Meng et al., 2009)

Generally, estimation of membrane fouling was divided into three stages derived from trans-membrane pressure (TMP) rise as following (Gao et al., 2013a); Initial stage: adhesion of microbes on the membrane surface and produce extracellular poly-substances (EPS) with fast TMP increase. Second stage: growth of attached microbes and micro-colony formation to three-dimensional structure and accumulation of foulants with slow TMP increase. Third stage: continuous accumulation and formation of cake layer with fast TMP increase and lead to TMP jump. Since the foulants including microbes, proteins, polysaccharides, and humic substances or inorganic substances play significant role on membrane fouling, Gao et al. (2013a) mentioned that Betaproteobacteria played important role on membrane fouling development rather than proteins. However, detailed function of each foulant, specially microbes are still unknown.

2.2.2. Microbial products on membrane fouling (SMP, EPS)

Behavior of soluble microbial products (SMP) and EPS in MBR have been revealed during MBR operation. A lot of researchers found the positive correlation between SMP or EPS concentrations

and membrane fouling development (increasing of TMP), suggesting that these substances plays a significant role on membrane fouling as foulants. Proteins and polysaccharide in EPS were recognized that more significant positive correlation with membrane fouling than other foulant and negative correlation with temperature and EPS of the mixed liquor showed more broad molecular weight (MW) than influent (Wang et al., 2009). In the mixed liquor of MBR, SMP had more positive correlation with membrane fouling than EPS (Wu and Huang, 2009). Shen at al. (2012) characterized SMP in full-scale MBR and described that polysaccharide was major component (approximately 60-70%) followed by humic acid (approximately 40%) and had broad MW from 1 kDa to over 100 kDa. In addition, proteins were minority in the mixed liquor of MBR. Conversely, some studies showed that proteins in bound EPS of activated sludge was major component than polysaccharide (Domínguez et al., 2010; Di Bella et al., 2011; Hang et al., 2012). Moreover, loosely-bound EPS had more correlation with membrane fouling development than tightly-bound EPS (Wang et al., 2009). Thus, although higher concentration of EPS and SMP had possible to develop membrane fouling with same level, it is suggested that the role of EPS and SMP was different on membrane fouling development. Banti et al. (2018) reported that SMP deposited within membrane pores gradually formed aggregates resulting membrane pore blocking and TMP rise. Moreover, SMP changed the membrane characteristics into hydrophilic surface even hydrophobic membrane surface and the approximately 60% of polysaccharide in the SMP retained in mixed liquor than proteins (less than 30%). Recently, size-exclusion chromatography-organic carbon detection-organic nitrogen detection (LC-OCD-OND) was developed to characterize humic and non-humic substances in aquatic environment (Huber et al., 2011). LC-OCD system have been applied to reveal foulant in MBR study. Some studies suggested that the concentration of biopolymer matter (higher molecules; >10 kDa) were correlated with fouling development (Ishizaki et al., 2016a; Díaz et al., 2016). Moreover, biopolymer clusters, mainly consisted by 5-50 μm size, are found on membrane surface neither cannot be found in activated sludge in MBR, and SMPs or colloidal organic matter attached and formed the clusters on membrane surface (Wang et al., 2008). Thus, the affinity of SMP component between the components or the component and membrane surface (or inside the membrane pore) is important parameter for membrane fouling development.

Membrane fouling is influenced not only by SMP concentrations but also the characteristics (Jiang et al., 2010). To date, it was reported that SMP is divided into two parts: biomass associated products (BAP) and utilization associated products (UAP) (Leudeking and Piret, 1959; Namkung and Rittmann, 1986). Recently, these microbial products are considered to important parameters on membrane fouling development (Ni et al., 2011). UAP, produced from active cell with lower MW, and BAP ,produced from decayed cell of EPS, were clearly different source (**Fig. 2.2**) (Shi et al., 2018). Jiang et al., (2010) clarified that higher abundance of lower MW in UAP fraction

produced in the cell proliferation stage was more significant on membrane fouling than BAP in spite of its lower MW. However, the detailed information of these function in complexed environment such as activated sludge of MBR is still lack due to difficulty of the BAP and UAP separation and the difference of operational conditions (influent characteristics, solid retention time (SRT), food-microorganism (F/M) ratio, or temperature) in each MBR. Hydrophobicity and hydrophilicity are also important parameters of activated sludge or foulant characteristics, and the detailed explanation was mentioned below (section 2.2.3).

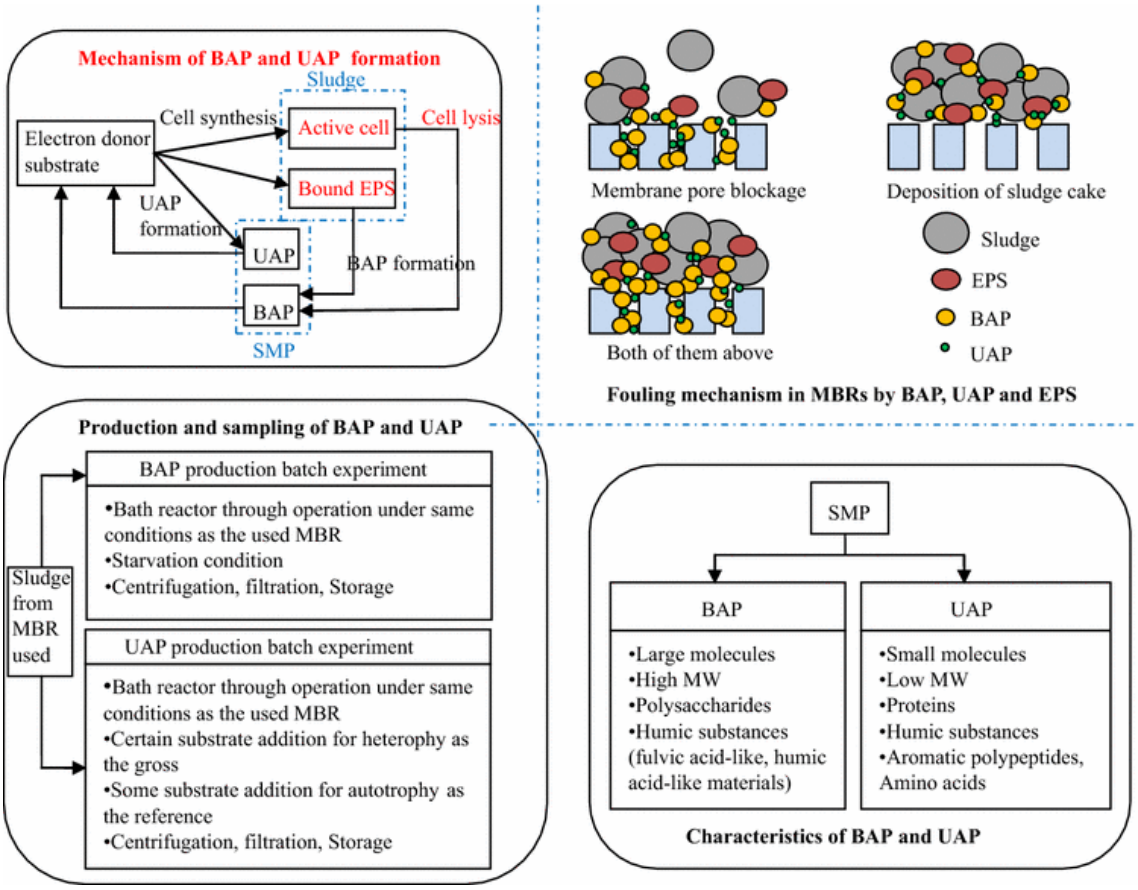

Fig. 2.2 Schematic diagram of the formation, sampling, characteristics and fouling mechanism of BAP and UAP. (from Shi et al., 2018)

2.2.3. Operational parameters on membrane fouling (Flux, SRT, temperature, OLR, membrane characteristics)

Various operational parameters of MBR which contributed membrane fouling development have been investigated. Suction flux is primary operating parameter affecting membrane fouling development. In general, as flux should be operated under sub-critical condition without critical flux condition and sub-critical flux is widely practiced to mitigate membrane fouling, thus, a lot of researchers have been focused on characterization of membrane fouling phenomenon under sub-critical condition. Ng and Ng, 2010 investigated membrane surface under sub-critical, critical, and super-critical conditions, they suggested that although protein and polysaccharide concentrations in SMP or EPS were constant during operation under sub-critical flux condition, proteins formed conditioning film (initial fouling layer) on the membrane surface and had largest effect on the TMP increase in all flux conditions. Under sub-critical flux condition, membrane fouling showed two stages; TMP gradually increased in first stage, second stage was TMP jump (Hwang et al., 2008). The abrupt TMP increase was mainly occurred by substantial production of EPS in lower layer of biofilm on the membrane surface because of an endogenous decay or microbial cell lysis in the lower layer, suggesting that stressful environment for the bacteria.

Solid retention time (SRT), temperature and organic loading rate (OLR) parameters could change the sludge characteristics and was investigated on membrane fouling. Longer SRT (50 day) with higher MLSS concentration mitigated membrane fouling than shorter SRT (13 day) and SMP concentration was considerably low under longer SRT conditions (Miyoshi et al., 2009). Although irreversible fouling was dominant in higher temperature and shorter SRT and had positive correlation with SMP concentration, in lower temperature, removable fouling was dominant in both SRT operation (Yao et al., 2011; Miyoshi et al., 2009). Al-Halbouni et al. (2008) showed that EPS generation in full-scale MBR was found to be inversely proportional to temperature seasonal change (**Fig. 2.3**). Thus, the fouling causing substances were found to be inversely proportional to SRT and temperature.

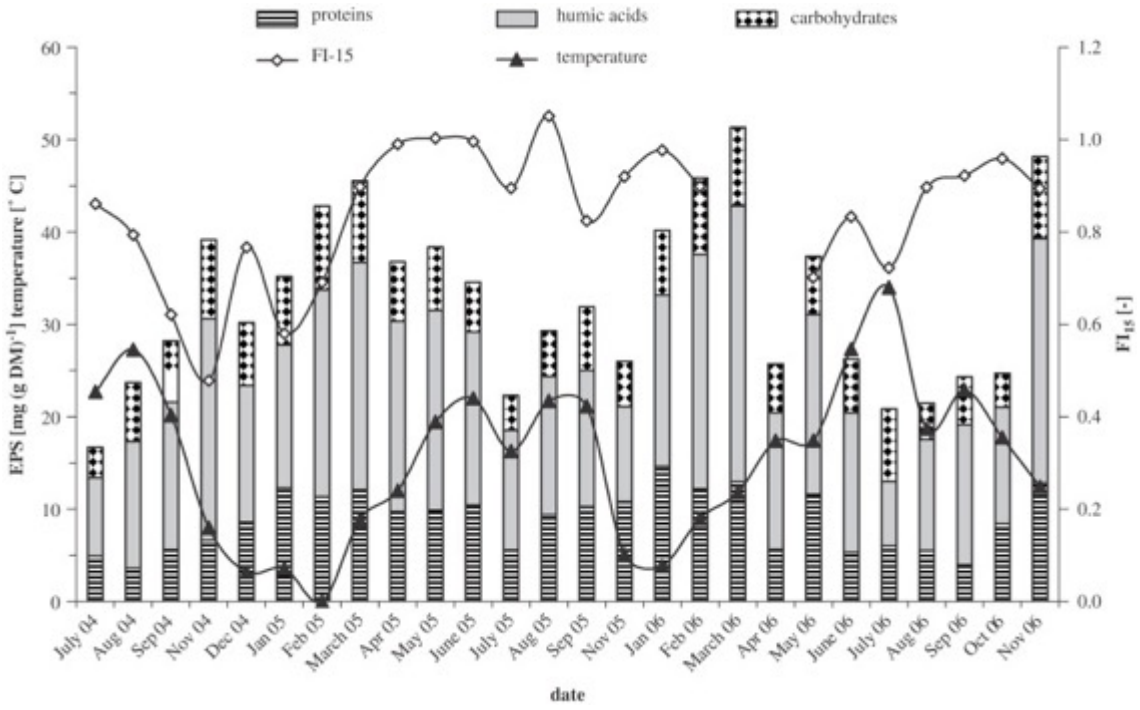

Fig. 2.3 Seasonal changes of bound EPS of activated sludge in full-scale MBR treating municipal wastewater. (from Al-Halbouni et al., 2008)

In a similar manner to flux, SRT, and temperature, organic loading rate (OLR) condition also plays significant role on membrane fouling development. Johir et al. (2012) investigated the influence of different OLR between 0.5 to 3.0 kg-COD·m^{-3}·day^{-1} with same MLSS concentration on sludge characteristics and membrane fouling. The report showed that lower OLR conditions mitigated membrane fouling and SMP generation than higher one, and suggested that bio-polymer in hydrophilic SMP contributes accumulation of foulant. Xia et al. (2010) also had showed that lower OLR condition (0.33 gCOD·$gVSS^{-1}$·day^{-1}) mitigated membrane fouling than higher OLR (0.52 gCOD·$gVSS^{-1}$·day^{-1}). Although longer SRT condition was recommended to achieve high nutrient removal and mitigate membrane fouling as mentioned above, much long SRT causes starvation and prolonged starvation caused BAP generation leading severe membrane fouling (Wu and Lee, 2011). Moreover, generally, MBR was worked under low F/M conditions because of high MLSS operation compared to conventional activated sludge process (Lobos et al., 2005). In fact, no sludge discharge and limited COD were observed in actual larger-scale MBR (Shen et al., 2012). Also, the rain event has possible for changing influent property into low strength wastewater in combined sewer system (Stricker et al., 2003; Wilén et al., 2006), thus, it is important to investigate influence of low OLR (starvation in many cases) condition on microbial community and membrane fouling in MBR.

The flat sheet and hollow fiber modules are normally used for submerged MBR system (Judd, 2008). There are various characteristics of membrane materials and surfaces. Generally, the submerged membranes are made from ceramic or polymeric materials. Ceramic membrane study have been expanding due to their advantages from polymeric materials such as strong mechanical, thermal, and chemical stability (Li et al., 2020). Jeong et al. (2018) reported that alumina-based ceramic membrane (super-hydrophilicity) had stable filtration against hydrophobic sludge characteristics (i.e. proteins dominant) compared to PVDF polymeric membrane with hydrophobic surface due to hydrophobic-hydrophilic repulsion although the SMP concentrations of bulk sludge in ceramic MBR were higher than PVDF MBR. To prevent hydrophobic membrane fouling, recently, polymeric membrane has modified to hydrophilic surface. Mater et al. (2016) investigated four different membrane materials on EPS and membrane fouling. Although they reported that the more hydrophilic membrane showed higher negative charged surface, lower foulant accumulation and lowest TMP, EPS transition on the membrane surface was same in all membranes. However, many studies suggested contradictory results between hydrophobicity and hydrophilicity of dissolved organic matter on membrane fouling (Xia et al., 2010; Zhang et al., 2015). Thus, Mu et al. (2019) have focused on relative degrees of hydrophobicity of the foulants, and reported that the nominally moderate hydrophobic/philic fractions played most contributor on membrane fouling development. In addition, some researchers indicated that it is important to investigate the surface structure such as roughness on membrane fouling, certain roughness could mitigate membrane fouling (Mater et al., 2016; Zhang et al., 2015). Therefore, it is difficult to address membrane fouling in terms of hydrophobicity/hydrophilicity, we might pay attention to not only degrees of hydrophobicity of sludge or foulants but also molecular weight of the foulants and surface structure (i.e. porosity or roughness).

2.3. Microbial community in mixed liquor and fouling layer of MBR

2.3.1. 16S rRNA genes analysis technology

In the recent decade, high throughput sequencing technology based on 16S rRNA genes have been applied to investigate the bacterial community in mixed liquor, gel layer and cake layer of MBR, and have proposed the new insights for fouling causing bacteria and biofilm-forming or fouling mitigating bacteria. These fouling related bacteria estimated by using 16S rRNA genes high throughput sequencing were listed in **Table 2.1**.

2.3.2. Fouling related bacteria

Fouling related bacteria is divided into three groups in this thesis; biofilm-forming bacteria, fouling causing bacteria, and fouling mitigating bacteria.

Firstly, the biofilm-forming bacteria could be identified from biofilm or cake layer as the abundance of these bacteria were increased in biofilm compared with the activated sludge community. Previous studies suggested that these bacteria related to secretion of EPS or SMP and adhesion on the membrane surface as pioneer of colonization and biofilm formation (Hong et al., 2019; Gao et al., 2013b; Choi et al., 2017; Liu et al., 2018; Ziegler et al., 2016; Takada et al., 2018). Interestingly, Neoh et al. (2017) suggested that OD1 known as Parcubacteria in candidate phyla radiation was dominant in the biofilm although minority in the mixed liquor of MBR and might relate to complex carbon degradation and biofilm formation.

Secondly, the fouling causing bacteria could be identified from mixed liquor or biofilm. These bacteria was also related to EPS secretion and became predominant in fouled MBR (Han et al., 2018; Choi et al., 2017). Ishizaki et al. (2016b) have revealed that the colony of fouling causing bacteria showed high water, hydrophilic organic matter, and carbohydrate contents.

Thirdly, the fouling mitigating bacteria could be identified from mixed liquor or biofilm. These bacteria were related to less EPS generation in mixed liquor (Sepehri and Sarrafzadeh, 2018), degradation of foulant in the biofilm (Gao et al., 2013b) and mixed liquor (Han et al., 2018). In addition, *Simplispira*, *Aminobacter*, *Pirallula* and *Chitinophagaceae* increased its abundance in fouling-mitigated MBR after addition of magnetic powder (Liu et al., 2018). However, the detailed function of these bacteria is still unknown in fouling-mitigated MBR. Recently, quorum quenching bacteria was applied as fouling control technology in MBR in order to mitigate membrane fouling development for degradation of quorum sensing auto inducer such as acyl-homoserine lactone (Weerasekara et al., 2014).

Almost all fouling related bacteria belonged Alpha, Beta, or Gammaproteobacteria (**Table 2.1**). Especially, Gammaproteobacteria was related to membrane fouling development. Conversely, *Chitinophagaceae* was recognized as both contradictory role of secretion of EPS and degradation of large molecules. This fact suggested that response of these bacteria might be changed for depending on the wastewater and analyzing of lower taxonomy is necessary for understanding the role of these bacteria in depth. Moreover, synthetic wastewater have been used to investigate fouling related bacteria and membrane fouling phenomenon even now. Therefore, it is important to practical use of actual municipal wastewater for revealing phenomenon of membrane fouling and response of fouling related bacteria in the future research of MBR field.

Table 2.1 Biofilm-forming bacteria, fouling causing bacteria, and fouling mitigating bacteria in MBR based on 16S rRNA genes sequencing in MBRs.

Bacteria	Class	Sample	Function	Reactor type (membrane type)	Membrene material	Wastewater	Operational condition	References
Estimated biofilm-forming bacteria								
Rhodanobacter sp. (*Rhodanobacteraceae*) *Pseudommonas* sp. *(Pseudomonadaceae)* *Tatlockia* sp. *(Legionellaceae)*	γ-proteobacteria	Biofilm	Adhesion to membrane in early-stage, EPS production	Lab-scale MBR (flat sheet)	0.2 μm chlorinated PE	Synthetic	10.8 LMH (constand flux mode); 80 kPa (constant TMP mode)	Hong et al., 2019
Thiothrix sp. *(Thiotrichaceae)*	γ-proteobacteria	Biocake	Disruptive foaming	Lab-scale A/O-MBR (hollow fiber)	0.4 μm PE	Synthetic	9.09 LMH	Gao et al., 2014
Rhizobiales *Aquabacterium* sp. *(Comamonadaceae)*	α-proteobacteria β-proteobacteria	Biocake	Secretion of extracellular polysaccharide Pioneer of membrane attachment	Lab-scale A/O-MBR (hollow fiber)	0.4 μm PE	Synthetic	0.27 m/day; 283, 293, 303 K	Gao et al., 2013b
γ-proteobacteria, *Anaerolineae*		Cake layer	Microbial colonization and biofilm formation	Full-scale MBR (hollow fiber)	0.4 μm no description	Domestic, industrial	SRT 12-15 d; HRT 12 h	Choi et al., 2017
Planctomycetes		Biofilm	Attachment on the membrane	Lab-scale MBR (hollow fiber)	0.1 μm PVDF	Synthetic	11.25 LMH; addition of magnetic powder	Liu et al., 2018
Limnohabitans (Comamonadaceae) *Hydrogenophaga (Comamonadaceae)* *Malikia (Comamonadaceae)*	β-proteobacteria	Early biofilm	Pioneer of membrane biofilm	Pilot-scale MBR (flat sheet)	0.2 μm PP	Actual influent	3 kPa (constant TMP), 8 LMH (start point)	Ziegler et al., 2016
Carnobacterium (Carnobacteriaceae) *Chlostridiales* *Exiguobacterium (Bacillaceae)*	Bacilli	Cake layer	Initial attachment and maturation	Full-scale MBR (flat sheet)	0.4 μm chlorinated PE	WWTP in Osaka	Approximately 0.5 m/day	Takada et al., 2018
OD1		Biofilm	Complex carbon degradation, biofilm formation	Pilot-scale MBR (flat sheet)	0.4 μm chlorinated PE	Palm oil mill effluent (high strength)	3.2 m^3/h; HRT 15 h	Neoh et al., 2017
Micavibrio *Ca.* Saccharibacteria	α-proteobacteria	Bioflm	Adhesion to membrane in early-stage	Lab-scale MBR (flat sheet)	20 kDa polysulfone	Municipal	9.5 LMH; HRT 26 h	Rehmen et al., 2020
OD1, TM6, *Xanthomonadaceae*, *Neisseriaceae*		Biofilm, cake layer	Pionner bacteria for membrane attachment	Lab-scale MBR (flat sheet)	0.2 μm chlorinated PVC	Manicipal	12 LMH; HRT 6 h; SRT 60 day; 12°C	This study
Estimated fouling causing bacteria								
Ferruginibacter (Chitinophagaceae) γ-proteobacteria	Sphingobacteriia	Activated sludge	Secretion and exportation of EPS	Lab-scale A/O-MBR (flat sheet)	0.2 μm PVDF	Municipal	10 LMH; 7-15°C	Han et al., 2018
Caldilineaceae	Caldilineae	Cake layer, bulk sludge	Filamentous bulking and EPS secretion	Full-scale MBR (hollow fiber)	0.4 μm no description	Domestic, industrial	SRT 12-15 d; HRT 12 h	Choi et al., 2017
Xanthomonadaceae *Microbacteriaceae*	γ-proteobacteria Actinobacteria	Attached biomass	High water, hydrophilic organic matter, and carbohydrate contents	Pilot-scale MBR (hollow fiber)	0.3 μm PTFE	Municipal wastewater	Cultivation by R2A agar	Ishizaki et al., 2016
Xanthomonadaceae	γ-proteobacteria	Bulk sludge	EPS production	Lab-scale MBR (flat sheet)	0.2 μm chlorinated PVC	Manicipal	12 LMH; HRT 6 h; SRT 60 day; 12°C	This study
Estimated fouling mitigating bacteria								
Nitrifiers		Activated sludge	Less EPS, SMP generation	Lab-scale activated sludge reactor		Synthetic	NH4+ rich or glucose rich feed	Sepehri and Sarrafzadeh, 2018
Saprospiraceae	Sphingobacteriia	Biocake	Degradation of protein	Lab-scale A/O-MBR (hollow fiber)	0.4 μm PE	Synthetic	0.27 m/day 283, 293, 303 K	Gao et al., 2013b
Chloroflexi		Activated sludge	Degradation of carbohydrates in SMP	Lab-scale A/O-MBR (flat sheet)	0.2 μm PVDF	Municipal	10 LMH; 7-15°C	Han et al., 2018
Simplicispira (Comamonadaceae) *Aminobacter (Phyllobacteriaceae)* *Pirellula (Planctomycetaceae)* *Chitinophagaceae*	β-proteobacteria α-proteobacteria Planctomycetes Sphingobacteriia	Bulk sludge	Degradation of large molecules and less membrane fouling	Lab-scale MBR (hollow fiber)	0.1 μm PVDF	Synthetic	11.25 LMH; addition of magnetic powder	Liu et al., 2018
Rhodococcus sp. BH4 (*Nocardiaceae*)	Actinobacteria	In microporus membrane vessel	AHL-lactonase producing (quorum quenching)	Lab-scale MBR (hollow fiber)	0.1 μm PVDF	Synthetic	30 LMH	Weerasekara et al., 2014
Chitinophagaceae, Ca. Prominaofilum		Bulk sludge	BAP degradation	Lab-scale MBR (flat sheet)	0.2 μm chlorinated PVC	Municipal	12 LMH; HRT 6 h; SRT 60 day; 12°C	This study

References

Banti, D. C., Samaras, P., Tsioptsias, C., Zouboulis, A., & Mitrakas, M. (2018). Mechanism of SMP aggregation within the pores of hydrophilic and hydrophobic MBR membranes and aggregates detachment. Separation and Purification Technology, 202, 119-129.

Cai, W., & Liu, Y. (2018). Oxidative stress induced membrane biofouling and its implications to on-line chemical cleaning in MBR. Chemical Engineering Journal, 334, 1917-1926.

Chae, S. R., and Shin, H. S. (2007). Characteristics of simultaneous organic and nutrient removal in a pilot-scale vertical submerged membrane bioreactor (VSMBR) treating municipal wastewater at various temperatures. Process Biochemistry, 42(2), 193-198.

Choi, J., Kim, E. S., & Ahn, Y. (2017). Microbial community analysis of bulk sludge/cake layers and biofouling-causing microbial consortia in a full-scale aerobic membrane bioreactor. Bioresource technology, 227, 133-141.

Di Bella, G., Torregrossa, M., & Viviani, G. (2011). The role of EPS concentration in MBR foaming: analysis of a submerged pilot plant. Bioresource technology, 102(2), 1628-1635.

Díaz, O., Vera, L., González, E., García, E., & Rodríguez-Sevilla, J. (2016). Effect of sludge characteristics on membrane fouling during start-up of a tertiary submerged membrane bioreactor. Environmental Science and Pollution Research, 23(9), 8951-8962.

Domínguez, L., Rodríguez, M., & Prats, D. (2010). Effect of different extraction methods on bound EPS from MBR sludges. Part I: influence of extraction methods over three-dimensional EEM fluorescence spectroscopy fingerprint. Desalination, 261(1-2), 19-26.

Gao, D., Fu, Y., & Ren, N. (2013a). Tracing biofouling to the structure of the microbial community and its metabolic products: A study of the three-stage MBR process. Water research, 47(17), 6680-6690.

Gao, D. W., Wen, Z. D., Li, B., & Liang, H. (2013b). Membrane fouling related to microbial community and extracellular polymeric substances at different temperatures. Bioresource technology, 143, 172-177.

Gao, D. W., Wen, Z. D., Li, B., & Liang, H. (2014). Microbial community structure characteristics associated membrane fouling in A/O-MBR system. Bioresource technology, 154, 87-93.

Han, X., Zhou, Z., Mei, X., Ma, Y., & Xie, Z. (2018). Influence of fermentation liquid from waste activated sludge on anoxic/oxic-membrane bioreactor performance: Nitrogen removal, membrane fouling and microbial community. Bioresource technology, 250, 699-707.

Hong, P. N., Noguchi, M., Matsuura, N., & Honda, R. (2019). Mechanism of biofouling enhancement in a membrane bioreactor under constant trans-membrane pressure operation. Journal of Membrane Science, 592, 117391.

Huber, S. A., Balz, A., Abert, M., & Pronk, W. (2011). Characterisation of aquatic humic and non-humic matter with size-exclusion chromatography–organic carbon detection–organic nitrogen detection (LC-OCD-OND). Water research, 45(2), 879-885.

Hwang, B. K., et al. (2008). Correlating TMP increases with microbial characteristics in the bio-cake on the membrane surface in a membrane bioreactor. Environmental science & technology, 42(11), 3963-3968.

Ishizaki, S., Terada, K., Miyake, H., & Okabe, S. (2016a). Impact of anodic respiration on biopolymer production and consequent membrane fouling. Environmental science & technology, 50(17), 9515-9523.

Ishizaki, S., Fukushima, T., Ishii, S., & Okabe, S. (2016b). Membrane fouling potentials and cellular properties of bacteria isolated from fouled membranes in a MBR treating municipal wastewater. Water research, 100, 448-457.

Jeong, Y., Kim, Y., Jin, Y., Hong, S., & Park, C. (2018). Comparison of filtration and treatment performance between polymeric and ceramic membranes in anaerobic membrane bioreactor treatment of domestic wastewater. Separation and Purification Technology, 199, 182-188.

Jiang, T., Kennedy, M. D., Schepper, V. D., Nam, S. N., Nopens, I., Vanrolleghem, P. A., & Amy, G. (2010). Characterization of soluble microbial products and their fouling impacts in membrane bioreactors. Environmental science & technology, 44(17), 6642-6648.

Johir, M. A., Vigneswaran, S., Sathasivan, A., Kandasamy, J., & Chang, C. Y. (2012). Effect of organic loading rate on organic matter and foulant characteristics in membrane bio-reactor. Bioresource Technology, 113, 154-160.

Judd, S. (2008). The status of membrane bioreactor technology. Trends in biotechnology, 26(2), 109-116.

Li, C., Sun, W., Lu, Z., Ao, X., & Li, S. (2020). Ceramic nanocomposite membranes and membrane fouling: A review. Water research, 175, 115674.

Liu, Y., Liu, Q., Li, J., Ngo, H. H., Guo, W., Hu, J., ... & Hou, Y. (2018). Effect of magnetic powder on membrane fouling mitigation and microbial community/composition in membrane bioreactors (MBRs) for municipal wastewater treatment. Bioresource technology, 249, 377-385.

Lobos, J., Wisniewski, C., Heran, M., & Grasmick, A. (2005). Effects of starvation conditions on biomass behaviour for minimization of sludge production in membrane bioreactors. Water Science and Technology, 51(6-7), 35-44.

Luedeking, R., & Piret, E. L. (1959). A kinetic study of the lactic acid fermentation. Batch process at controlled pH. Journal of Biochemical and Microbiological Technology and Engineering, 1(4), 393-412.

Lyko, S., Wintgens, T., Al-Halbouni, D., Baumgarten, S., Tacke, D., Drensla, K., Janot, A., Dott, W., Pinnekamp, J., and Melin, T. (2008). Long-term monitoring of a full-scale municipal membrane bioreactor—characterisation of foulants and operational performance. Journal of membrane science, 317(1-2), 78-87.

Ma, D., Gao, B., Hou, D., Wang, Y., Yue, Q., and Li, Q. (2013). Evaluation of a submerged membrane bioreactor (SMBR) coupled with chlorine disinfection for municipal wastewater treatment and reuse. Desalination, 313, 134-139.

Matar, G., Gonzalez-Gil, G., Maab, H., Nunes, S., Le-Clech, P., Vrouwenvelder, J., & Saikaly, P. E. (2016). Temporal changes in extracellular polymeric substances on hydrophobic and hydrophilic membrane surfaces in a submerged membrane bioreactor. Water research, 95, 27-38.

Meng, F., Chae, S. R., Drews, A., Kraume, M., Shin, H. S., and Yang, F. (2009). Recent advances in membrane bioreactors (MBRs): membrane fouling and membrane material. Water research, 43(6), 1489-1512.

Miyoshi, T., Tsuyuhara, T., Ogyu, R., Kimura, K., & Watanabe, Y. (2009). Seasonal variation in membrane fouling in membrane bioreactors (MBRs) treating municipal wastewater. Water Research, 43(20), 5109-5118.

Monclús, H., Sipma, J., Ferrero, G., Rodriguez-Roda, I., & Comas, J. (2010). Biological nutrient removal in an MBR treating municipal wastewater with special focus on biological phosphorus removal. Bioresource technology, 101(11), 3984-3991.

Mu, S., Wang, S., Liang, S., Xiao, K., Fan, H., Han, B., ... & Huang, X. (2019). Effect of the relative degree of foulant "hydrophobicity" on membrane fouling. Journal of Membrane Science, 570, 1-8.

Namkung, E., & Rittmann, B. E. (1986). Soluble microbial products (SMP) formation kinetics by biofilms. Water Research, 20(6), 795-806.

Neoh, C. H., Yung, P. Y., Noor, Z. Z., Razak, M. H., Aris, A., Din, M. F. M., & Ibrahim, Z. (2017). Correlation between microbial community structure and performances of membrane bioreactor for treatment of palm oil mill effluent. Chemical Engineering Journal, 308, 656-663.

Ng, T. C. A., & Ng, H. Y. (2010). Characterisation of initial fouling in aerobic submerged membrane bioreactors in relation to physico-chemical characteristics under different flux conditions. Water research, 44(7), 2336-2348.

Ni, B. J., Rittmann, B. E., & Yu, H. Q. (2011). Soluble microbial products and their implications in mixed culture biotechnology. Trends in biotechnology, 29(9), 454-463.

Rehman, Z. U., Fortunato, L., Cheng, T., & Leiknes, T. (2020). Metagenomic analysis of sludge and early-stage biofilm communities of a submerged membrane bioreactor. Science of The Total Environment, 701, 134682.

Rosenberger, S., Krüger, U., Witzig, R., Manz, W., Szewzyk, U., and Kraume, M. (2002). Performance of a bioreactor with submerged membranes for aerobic treatment of municipal waste water. Water Research, 36(2), 413-420.

Sepehri, A., & Sarrafzadeh, M. H. (2018). Effect of nitrifiers community on fouling mitigation and nitrification efficiency in a membrane bioreactor. Chemical Engineering and Processing-Process Intensification, 128, 10-18.

Shen, Y. X., Xiao, K., Liang, P., Sun, J. Y., Sai, S. J., & Huang, X. (2012). Characterization of soluble microbial products in 10 large-scale membrane bioreactors for municipal wastewater treatment in China. Journal of Membrane Science, 415, 336-345.

Shi, Y., Huang, J., Zeng, G., Gu, Y., Hu, Y., Tang, B., ... & Shi, L. (2018). Evaluation of soluble microbial products (SMP) on membrane fouling in membrane bioreactors (MBRs) at the fractional and overall level: a review. Reviews in Environmental Science and Bio/Technology, 17(1), 71-85.

Stricker, A. E., Lessard, P., Héduit, A., & Chatellier, P. (2003). Observed and simulated effect of rain events on the behaviour of an activated sludge plant removing nitrogen. Journal of Environmental Engineering and Science, 2(6), 429-440.

Sun, F. Y., Wang, X. M., and Li, X. Y. (2013). An innovative membrane bioreactor (MBR) system for simultaneous nitrogen and phosphorus removal. Process Biochemistry, 48(11), 1749-1756.

Sun, H., Liu, H., Han, J., Zhang, X., Cheng, F., & Liu, Y. (2018). Chemical cleaning-associated generation of dissolved organic matter and halogenated byproducts in ceramic MBR: ozone versus hypochlorite. Water research, 140, 243-250.

Sun, M., Yan, L., Zhang, L., Song, L., Guo, J., & Zhang, H. (2019). New insights into the rapid formation of initial membrane fouling after in-situ cleaning in a membrane bioreactor. Process Biochemistry, 78, 108-113.

Takada, K., Shiba, T., Yamaguchi, T., Akane, Y., Nakayama, Y., Soda, S., ... & Ike, M. (2018). Cake layer bacterial communities during different biofouling stages in full-scale membrane bioreactors. Bioresource technology, 259, 259-267.

Trussell, R. S., Adham, S., and Trussell, R. R. (2005). Process limits of municipal wastewater treatment with the submerged membrane bioreactor. *Journal of Environmental Engineering*, *131*(3), 410-416.

Wang, X. M., & Li, X. Y. (2008). Accumulation of biopolymer clusters in a submerged membrane bioreactor and its effect on membrane fouling. Water research, 42(4-5), 855-862.

Wang, Z., Wu, Z., & Tang, S. (2009). Extracellular polymeric substances (EPS) properties and their effects on membrane fouling in a submerged membrane bioreactor. Water research, 43(9), 2504-2512.

Weerasekara, N. A., Choo, K. H., & Lee, C. H. (2014). Hybridization of physical cleaning and quorum quenching to minimize membrane biofouling and energy consumption in a membrane bioreactor. Water research, 67, 1-10.

Wilén, B. M., Lumley, D., Mattsson, A., & Mino, T. (2006). Rain events and their effect on effluent quality studied at a full scale activated sludge treatment plant. Water science and technology, 54(10), 201-208.

Wu, J., & Huang, X. (2009). Effect of mixed liquor properties on fouling propensity in membrane bioreactors. Journal of Membrane Science, 342(1-2), 88-96.

Wu, J., Li, H., and Huang, X. (2010). Indigenous somatic coliphage removal from a real municipal wastewater by a submerged membrane bioreactor. *Water research*, *44*(6), 1853-1862.

Wu, S. C., & Lee, C. M. (2011). Correlation between fouling propensity of soluble extracellular polymeric substances and sludge metabolic activity altered by different starvation conditions. Bioresource Technology, 102(9), 5375-5380.

Xiang, H. U., Li, X. I. E., Hojae, S. H. I. M., ZHANG, S., & Dianhai, Y. A. N. G. (2014). Biological nutrient removal in a full scale anoxic/anaerobic/aerobic/pre-anoxic-MBR plant for low C/N ratio municipal wastewater treatment. Chinese Journal of Chemical Engineering, 22(4), 447-454.

Xiao, K., Liang, S., Wang, X., Chen, C., & Huang, X. (2019). Current state and challenges of full-scale membrane bioreactor applications: a critical review. Bioresource technology, 271, 473-481.

Yamamoto. K., Hiasa, M., Mahmood, T., Matsuo, T. (1989). Direct solid-liquid separation using hollow fiber membrane in an activated sludge aeration tank. Water Science and Technology, 21 (4-5), 43-54.

Yao, M., Ladewig, B., & Zhang, K. (2011). Identification of the change of soluble microbial products on membrane fouling in membrane bioreactor (MBR). Desalination, 278(1-3), 126-131.

Zhang, M., Liao, B. Q., Zhou, X., He, Y., Hong, H., Lin, H., & Chen, J. (2015). Effects of hydrophilicity/hydrophobicity of membrane on membrane fouling in a submerged membrane bioreactor. Bioresource technology, 175, 59-67.

Zhang, X., & Liu, Y. (2020). Potential toxicity and implication of halogenated byproducts generated in MBR online-cleaning with hypochlorite. Journal of Chemical Technology & Biotechnology, 95(1), 20-26.

Ziegler, A. S., McIlroy, S. J., Larsen, P., Albertsen, M., Hansen, A. A., Heinen, N., & Nielsen, P. H. (2016). Dynamics of the fouling layer microbial community in a membrane bioreactor. PLoS One, 11(7), e0158811.

Chapter 3

Fouling development in A/O-MBR under low organic loading condition and identification of key bacteria for biofilm formations

Yuya Takimoto, Masashi Hatamoto, Takashi Ishida, Takahiro Watari and Takashi Yamaguchi (2018). Fouling development in A/O-MBR under low organic loading condition and identification of key bacteria for biofilm formations. *Scientific reports*, *8*(1), 1-9.

3.1. Background and objectives

Large-scale membrane bioreactors (MBRs) have been developed for treating municipal wastewater and their capacity has been greatly increased (Meng et al., 2017). MBR can achieve high removal efficiency for nutrients and complete removal of suspended solids from treated water because of a combined system involving activated sludge with membrane filtration. Moreover, the MBR has the potential to simplify and reduce the footprint of a wastewater treatment system. However, membrane fouling remains a major issue in MBRs; it is caused by membrane clogging and contribute to decrease suction flux. The membrane fouling has been divided into two classes: reversible and irreversible fouling. The latter, contributed to biofouling, is caused by microbial products derived from bacterial metabolism and lysis (Meng et al., 2009). Microbial products such as extracellular polymer substances (EPS) and soluble microbial product (SMP) had potential to induce mature biofilm formation, causing serious fouling associated with high membrane resistance (Sun et al., 2008; Meng et al., 2007).

To date, bacteria related to biofilm formation have been determined in various MBRs treating several kinds of wastewater. The relationship between fouling development and bacterial species that show high productivity of foulants such as EPS, SMPs, and auto-inducers, has been studied and reported previously (Malaeb et al., 2013; Ishizaki et al., 2017). Higher bacterial relative abundance, microbial community diversity, and productivity of foulants probably has an significant role in biofilm formation (Ishizaki et al., 2016; Gao et al., 2014). Furthermore, the attachment and growth of pioneer bacteria belonging to Betaproteobacteria and Gammaproteobacteria on the membrane surface plays a key role on biofilm formation and might cause severe fouling (Miura et al., 2007; Lim et al., 2012). Thus, characterization of fouling-related bacteria is important for the optimization of MBR operational conditions and fouling control. However, reports on bacteria related to biofilm formation detected on the fouled membrane surface in MBRs treating municipal wastewater are limited (Miura et al., 2007; Huang et al., 2008; Jo et al., 2016). In addition, the existence of common biofilm-forming bacteria among various MBRs under different conditions is still unclear.

Although various fouling control techniques have been reported, no anti-biofouling method has not been widely accepted yet, because the wastewater and operational conditions differ in each MBR (Lee et al., 2016; Gkotsis et al., 2017; Wang et al., 2014). In addition, a reactor operation and a fouling control technic are usually based on rules of thumb by operators in each

MBR plant without engineering and scientific knowledge. Considering the reactor parameters, many studies have focused on the EPS and SMP derived major microbes in the fouled MBR, and these components were found to increase under high organic loading rates or low temperature conditions (Johir et al., 2012; Ma et al., 2013). Membrane fouling was also found to be caused by EPS production in long term starvation conditions (Wu and Lee, 2011). Thus, considering the positive correlation between membrane fouling and microbial cell lysis occurring under starvation conditions, microbial lysis seems to be an important factor as an origin of biofilm formation in the membrane fouling development in the MBR.

The study of chapter 3 aimed to confirm an extremely low organic loading rate condition induce membrane fouling and to estimate the biofilm-forming bacteria in an operating A/O-MBR treating actual municipal wastewater under the condition. Moreover, to elucidate the common biofilm-forming bacteria, the microbial community was compared to that in naturally induced biofouling in an A/O-MBR under the stably normal conditions. The similarity in bacterial types identified in two fouled reactors operated under different conditions was determined. The present study provides a new perspective on biofilm-forming bacteria in a biofilm of a fouled membrane surface.

3.2. Materials and methods

3.2.1. A/O-MBR operational condition

Two lab-scale A/O-MBR systems designated R_L and R_N, consisting of a 6 L anoxic tank and a 6 L aerobic tank, were used for the experiment in parallel (**Fig. 3.1**). The membrane module with 0.11 m^2 filtration area and a chlorinated polyvinyl chloride (CPVC) flat sheet with 0.20 μm mean pore size (KUBOTA Co., Ltd., Japan) were submerged in the aerobic tank. Aeration was supplied by a diffuser at the bottom of the reactor. Anoxic and aerobic internal recycling was conducted to remove the phosphate and nitrogen. Municipal sewage after sedimentation was used as an influent into the anoxic tank. **Table 3.1** shows the characteristics of the municipal sewage.

The hydraulic retention time (HRT) of the reactors was 8.0 h with a solid retention time (SRT) of 60 d. Each reactor was operated under the following conditions: A membrane suction cycle of 9 min on and 1min off was adopted and an average membrane operating flux of 11.8 $L \cdot m^{-2} \cdot h^{-1}$ (LMH) with an aeration rate of 5.0 L/min was set. Conventional activated sludge (AS) taken from a sewage treatment facility, was seeded and the initial mixed liquor suspended solids

(MLSS) concentration was approximately 4300 mg/L in each MBR. Both reactors were operated under the standard conditions of 0.42 kg-COD·m^{-3}·day^{-1} until the reactor showed a stable performance. To induce membrane fouling, the permeate effluent of the R_L reactor was used to recycle into the anoxic tank to generate a low organic lading rate (OLR) starvation condition (0.002 kg-COD·m^{-3}·day^{-1}). To compensate the 200 mL of sampling of AS from the R_L reactor every day, 200 ml of sewage was fed as an influent, accounting for 0.002 kg-COD·m^{-3}·day^{-1}. On the other hand, the R_N reactor was continued to operate under standard conditions (0.42 kg-COD·m^{-3}·day^{-1}).

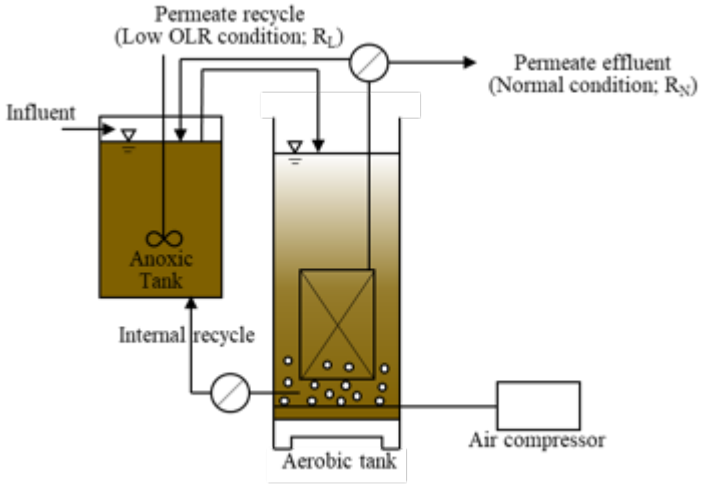

Fig. 3.1 Schematic diagram of the A/O-MBR used in this study. A permeate effluent was recycled to the anoxic tank under the low OLR condition (R_L).

Table 3.1 Characteristics of the raw influent sewage used in this study.

Parameters	Units	Average±SD (N=22)
Temperature	°C	16.1±2.9
pH	-	6.8±0.2
Soluble CODcr	mg/L	156±54
NH_4^+	mg-N/L	24±5
NO_3^-	mg-N/L	0.13±0.05
Total nitrogen	mg-N/L	28±7
Total phosphorus	mg-P/L	2.4±0.6

3.2.2. Analytical methods

Temperature, pH, and dissolved oxygen (DO) of the AS in the aerobic tank and the oxidation-reduction potential (ORP) of AS in the anoxic tank were measured on-site using a portable pH, DO meter (DM-32P, TOA DKK, Japan), and ORP meter (HM-31P, TOA DKK, Japan), respectively. The permeate flow rate (30 minutes) was also measured on-site using a measuring cylinder. The transmembrane pressure (TMP) of each reactor was measured using a pressure transducer (ZSE50F, SMC, Japan) located in the permeate line. Dissolved COD, MLSS, ammonium, nitrite, nitrate, total nitrogen (TN) and total phosphate (TP) of samples were measured. Dissolved COD and TN were measured using water-quality analyzer (DR2800, Hach, USA). Ammonium, nitrite and nitrate concentrations were measured by HPLC (LC-20ADsp, SHIMADZU Co., Ltd. Japan). All samples were filtered using 0.2 μm filter paper.

3.2.3. Biofilm sampling

After development of membrane fouling, the fouled membrane was taken from the aerobic tank and the membrane surface was rinsed with distilled water to remove the activated sludge attached to the membrane. The loosely bonded sludge cake on the fouled membrane surface was softly exfoliated and sampled as a membrane sludge (MS) sample using a thin plastic plate. Finally, the tightly bonded biofilm on the fouled membrane surface was sampled as a biofilm (BF) sample using a spatula. The samples were stored at -20 °C until DNA extraction.

3.2.4. 16S rRNA genes analysis

The AS in the aerobic tank and the MS and BF on the membrane surface were used for microbial analysis. Genomic DNA from each sample was extracted using the FastDNA Spin Kit for Soil (MP Biomedicals, Santa Ana, CA). A forward universal bacterial primer Univ515F (5′-GTGCCAGCMGCCGCGGTAA-3′) and a reverse universal primer Univ806R (5′-GGACTACHVGGGTWTCTAAT-3′) were used in this study to amplify the bacterial 16S rRNA genes. PCR was performed using the following conditions: one cycle of 94 °C for 3 min, 25 cycles of 94 °C for 45 s, 50 °C for 60 s and 72 °C for 90 s, and a final cycle 72 °C for 10 min. The PCR products were purified using QIAquick PCR Purification Kit (QIAGEN, Germany), and 16S rRNA genes sequencing was performed as described by Caporaso et al. (2012). DNA was sequenced using the MiSeq Reagent Kit v2 and the MiSeq System (Illumina Inc., San Diego, CA).

3.2.5. Data analysis

All data were analyzed using the QIIME software (version 1.9.1) (Caporaso et al., 2010). Operational taxonomic units (OTUs) were selected at 97% identity using UCLUST. Taxonomic classification was assigned using BLAST based on the Greengenes database ver. 13_8. The relative species of predominant OTUs were searched using BLAST in the NCBI database (http://blast.ncbi.nlm.nih.gov/Blast.cgi). To compare the metabolisms and functional enzymes between the AS and BF samples, the Phylogenetic Investigation of Communities by Reconstruction of Unobserved States (PICRUSTs) based on the KEGG database was used (Langille et al., 2013). A principal component analysis (PCA) plot with significant mean proportion differences for virginal datasets was created using Sequence Tag-based Analysis of Microbial Population dynamics (STAMP) software. The raw sequence data obtained in this study were deposited in the sequence read archive in the DDBJ database under the accession numbers DRA006840.

3.3. Results and discussion

3.3.1. Fouling development and reactor performance

Both reactors were operated for about 6 months under standard conditions. After 6 months operation, the membrane modules in the reactor were physically washed and removed reversible foulants with ultra-pure water using urethane sponges. Then, both reactors were moved to the experimental study. In this study, the first day was defined as after about 3 weeks from the membrane wash. The R_L reactors showed the following performance after being operated at 3 weeks from membrane cleaning under standard conditions: TMP (8 kPa), flux (0.28 m/day), MLSS concentration (10200 mg/L), COD removal rate (82%), and TN removal rate (64%). On the other hand, the R_N reactor showed the following performance: TMP (6.2 kPa), flux (0.27 m/day), MLSS concentration (10300 mg/L), COD removal rate (83%), and TN removal rate (68%). After each MBR achieved a stable operational condition (upon operation at 3 weeks after washing), the R_L reactor was started to operate under the low OLR condition in order to induce membrane fouling development caused by microbial lysis. The R_N reactor was continued to operate under stable condition.

The performances of both MBRs under different conditions are shown in **Fig. 3.2**. Both MBRs in the initial phase reached approximately 80% dissolved COD removal, (data not shown).

The removal efficiency of dissolved COD in the R_L and R_N reactor was stable until the final phase. However, the TN removal ratio of the R_L reactor began to deteriorate soon after initiating the low OLR operation (**Fig. 3.2A, B**). Although the TN and TP in the R_N reactor was stable until the final phase, their concentrations continued to increase during the operational term for the R_L reactor. A/O-MBR has high removal efficiency for nitrogen and phosphorus to possess the phosphorus accumulating organisms (PAOs) and denitrifying bacteria (Fu et al., 2009). In this study, the removal efficiency for nitrogen and phosphorus was decreased in the R_L reactor. The average TN and TP concentrations in the influent were 27.9±7.4 mg-N/L and 2.4±0.6mg-P/L, respectively. Thus, the amount of nitrogen and phosphorus that flowed into the R_L reactor in a day was calculated only 5.6 mg-N/day and 0.5 mg-P/day on an average, respectively. However, the increasing rate of nutrient concentration far exceeded the amount of that in only the influent sewage of the R_L reactor. Therefore, the accumulated TN and TP were considered from the retained sludge in the R_L reactor. These results also implied that nucleic acids and microbial products derived from microbial lysis induced by low OLR conditions were released in the R_L reactor. Accordingly, the MLSS of the R_L reactor was decreased to 7570 mg/L at the final phase from 10200 mg/L at the initial phase (**Fig. 3.3**). The degradation of MLSS in the R_L reactor also suggested that microbial lysis occurred in the R_L reactor. On the other hand, in the R_N reactor, the TP was temporary accumulated and the MLSS concentration was drastically decreased from 59 days to 66 days. This result might suggest that microbial lysis also occurred in the R_N reactor as the TMP jump was observed and endogenous substances generated by the lysis might affect membrane fouling development.

The progression of fouling in each reactor was evaluated by monitoring the increase in TMP and the decrease of flux (**Fig. 3.2C, D**). In the R_N reactor, the operation was stably continued for 2 months, and a drastic increase in TMP was observed at 64 days and flux was decreased from 0.27 m/day to 0.16 m/day with the TMP reaching 60 kPa after 86 days of operation. In contrast, a sudden increase of TMP to 40 kPa and decrease of flux of 0.28 m/day to 0.17 m/day was confirmed after 17 days after the low OLR condition was initiated in the R_L reactor. These results show that membrane fouling was developed under extremely the low organic loading rate condition (OLR: 0.002 kg-COD$\cdot m^{-3}\cdot day^{-1}$) of the R_L reactor. In the previous study, although higher fouling development at a high organic loading rate was reported (Xia et al., 2010),

induction of rapid and severe fouling development was confirmed at a low organic loading rate condition in this study.

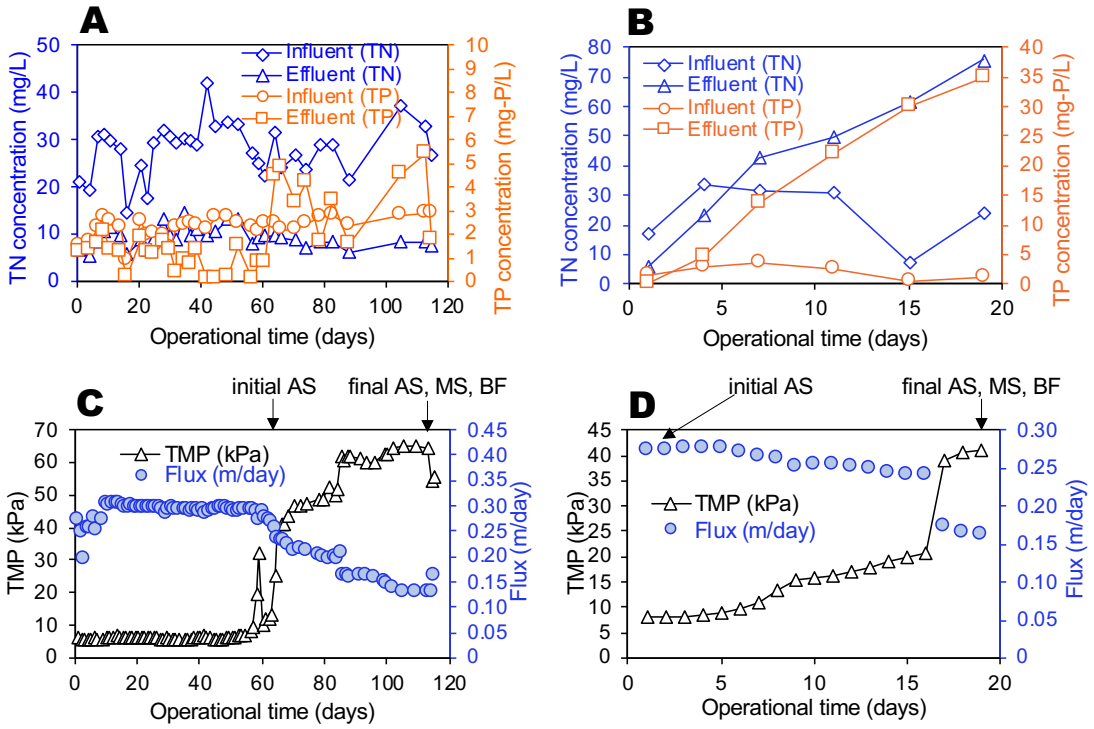

Fig. 3.2 Performances of each reactor under different conditions. (A) and (B) shows the performance of TN and TP removal in the R_N reactor and R_L reactor, respectively. (C) and (D) shows the TMP and flux profiles during each operational condition after stable operational term in the R_N reactor (C) and the R_L reactor (D). Arrows indicate the sampling points for microbial analysis and the sample name.

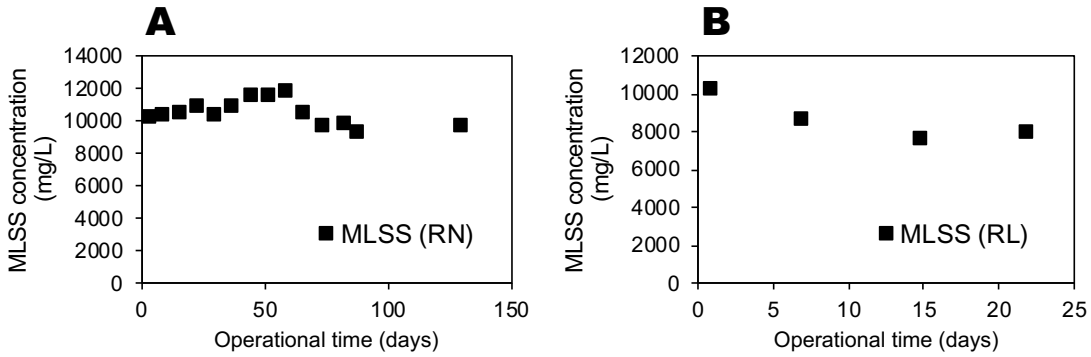

Fig. 3.3 Changes in the MLSS concentration of the aerobic tank. (A): R_N reactor, (B): R_L reactor.

The development of fouling behavior has been described as occurring in three or two stages (Gao et al., 2014; Wang et al., 2008). The changes in TMP in this study were also divided into three stages, especially R_L reactor was more clear than R_N reactor (**Fig. 3.2C, D**). In the R_L reactor, the first stage from the first day to the 8th day was considered as initial fouling, or the first step of fouling. The second step was from the 9th day to the 16th day, and the third step was from the 17th day considering as the final stage of membrane fouling. A TMP jump was observed and flux was drastically decreased in the third step. In the third step, visible biofilm formation was observed on the membrane surface. On the other hand, the TMP behavior in the R_N reactor indicated that there are two fouling stages (**Fig. 3.2C**). Since the R_N reactor was stably operated, the first step of the R_N reactor was longer than that for the R_L reactor. The second step might be from the 54th day. The visible biofilm was also observed in the final step. In conclusion, membrane fouling involving biofilm formation was developed after microbial lysis had occurred. These results indicate that membrane fouling is related to microbial lysis and that fouling might induce abrupt biofilm formation.

3.3.2. Comparison of microbial communities at a higher taxonomic level among AS, MS, and BF in each reactor

Microbial samples from AS, MS, and BF were collected before and after fouling development (**Fig. 3.2C, D**). The MiSeq sequencing profile was drawn using the QIIME software to analyze the top 10 of the microbial community at the phylum or class level in the initial AS, final AS, MS, and BF during the operational term in each reactor (**Fig. 3.4**). Bacteroidetes, Alphaproteobacteria, Betaproteobacteria, Deltaproteobacteria, and Gammaproteobacteria was the predominant bacterial phylum or class in the AS of each reactor. Chlorobi was the predominant bacterial phylum in the AS of the R_N reactor. The remaining phylogenetic groups of the AS were Epsilonproteobacteria, TM6, OD1, and Actinobacteria phylum. The predominant phylum or class composition of the AS detected in each reactor was similar to the bacteria observed in the AS of the MBR treating municipal wastewater (Wan et al., 2011; Hu et al., 2012), because this study used actual sewage as the influent.

There were clear differences between the AS and BF in each reactor, with respect to the distribution of the phylum TM6, OD1, and Gammaproteobacteria class. In the BF of the R_L reactor, the compositions of TM6 (20.1%), Actinobacteria (6.8%) and Betaproteobacteria (11.6%), and

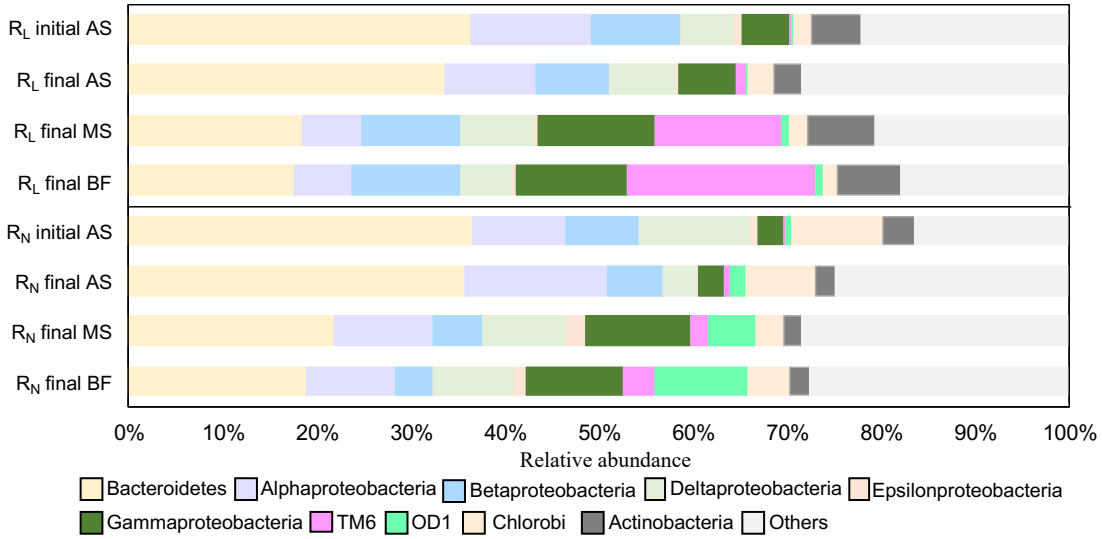

Fig. 3.4 Compositional changes in the microbial community structure of the both MBRs under different conditions at the phylum or class level. AS; activated sludge in oxic tank, MS; membrane cake sludge on membrane surface, BF; biofilm on membrane surface.

Gammaproteobacteria (11.7%) were significantly higher than that in the final AS. In the BF of the R_N reactor, the composition of OD1 (9.8%) and TM6 (3.3%), Deltaproteobacteria (8.6%) and Gammaproteobacteria (10.4%) was higher than that in the final AS. The microbial community structure of the cake layer was insignificantly correlated with the dominant bacteria of the mixed liquor in the MBR (Wu et al., 2011; Choi et al., 2017). The distribution of Proteobacteria in the BF was changed from that in the final AS in each reactor. In addition, the composition of TM6 in the BF of the R_L reactor and TM6, OD1 in the BF of the R_N reactor were increased from the MS of the fouled membrane in each reactor. These results indicated that the increased bacterial phylum or class in the BF were seemed to relate with initial biofilm formation. In fact, Betaproteobacteria and Gammaproteobacteria are known as pioneers of fouling development (Miura et al., 2007; Lim et al., 2012). Moreover, filamentous bacteria such as some Actinobacteria species have been reported as fouling-related bacteria (Chen et al., 2015) due to the morphology, which could be a reason for the increased Actinobacteria composition in the BF of the R_L reactor. On the other hand, the composition of Bacteroidetes was significantly decreased in the BF from the AS in each reactor. This is consistent with a previous study that reported Bacteroidetes to be decreased in the cake sludge from activated sludge (Choi et al., 2017).

At the family level microbial community, clear difference were found between AS and BF in each reactor. Although families *Rhodocyclaceae* and *Comamonadaceae* commonly existed in

the AS and BF samples of each reactor, family *Xanthomonadaceae* compositions of the BF were higher than final AS in each reactor. The family *Xanthomonadaceae* was reported as fouling-causing bacteria (Ishizaki et al., 2016). Thus, these results suggested that these bacterial groups with higher relative abundance than AS might be biofilm-forming bacteria.

3.3.3. Comparison of microbial community structure at the OTU level

Employing MiSeq sequencing, 742-1840 OTUs were obtained from each sample. To compare the microbial community of each sample, community profiles were visualized using a PCA plot. **Fig. 3.5** shows the PCA plot of the microbial community at the OTU level obtained from the AS, MS, and BF in each reactor. Since the distances on the plot between the initial and final AS microbial community of each reactor under the different conditions were close, no clear differences in microbial community were found between the initial and final AS of each reactor. This indicates that the microbial community structure was stable during the experimental period. In contrast, the final BF and MS plot in each reactor was differed from with each final and initial AS plot, suggesting that unique microbial communities were developed on the membrane surface as a biofilm. In addition, the microbial structure of the BF in the R_L and R_N reactors was significantly different at the OTU level. The major bacterial species involved in biofilm formation might be thus differ in each reactor.

PICRUSt analysis shows the composition difference between the BF and AS with respect to predictive functional genes related to biofilm formation and enzymes (**Fig. 3.6**). The percentage of the motility quorum-sensing regulator (MqsR) gene in the BF of R_L reactor was increased compared to that in the AS (**Fig. 3.6A**). In addition, the percentage of acyl homoserine lactone (AHL) synthase, which generates a kind of auto-inducer molecules, was increased in the BF of each reactor compared to the AS (**Fig. 3.6B**). MqsR is correlated with an increase in biofilm formation (Barrios et al., 2006) and AHL is also reported to correlate with biofilm formation and bacterial growth (Ren et al., 2013). Thus, these findings suggest that the unique microbial community developed on the membrane surface might affect the function of biofilm communities. In conclusion, the difference in microbial communities between the BF and AS was influenced by unique bacteria such as the biofilm-forming bacteria in each reactor.

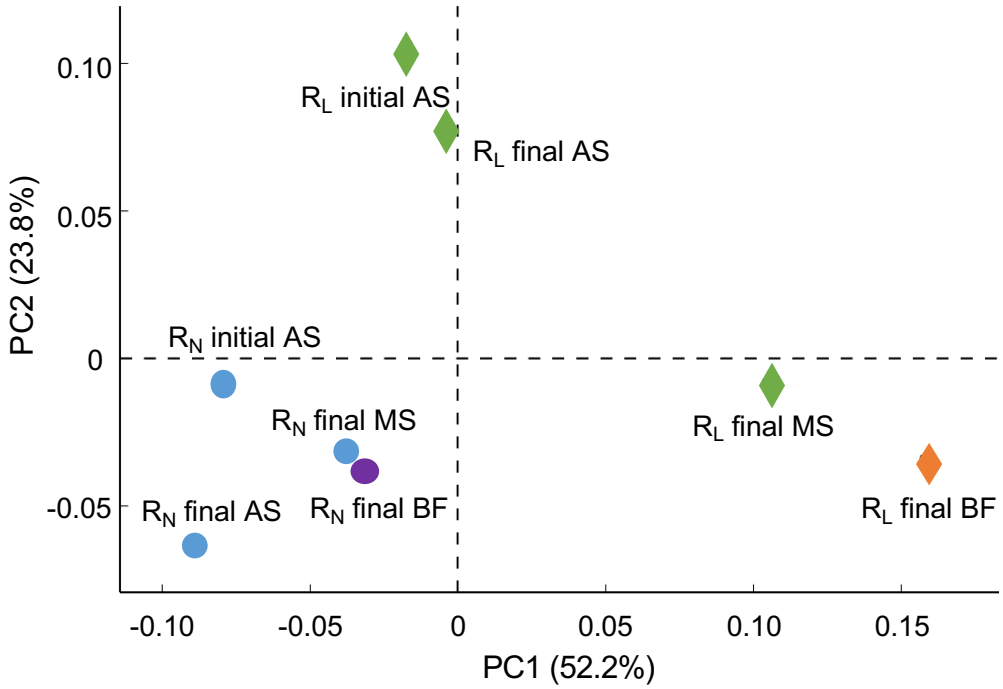

Fig. 3.5 Comparison of the AS, MS and BF microbial community in both MBRs under different conditions described by a principal composition analysis (PCA) plot obtained from OTUs.

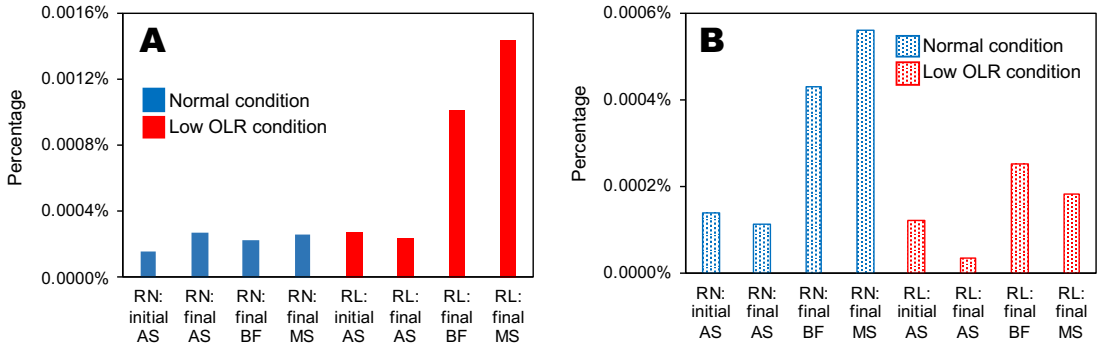

Fig. 3.6 Prediction of functional genes according to PICRUSt analysis of the initial and final AS, final MS and BF in each reactor. A: a motility quorum-sensing regulator gene, B: an acyl homoserine lactone synthase (auto-inducer) gene.

3.3.4. Biofilm-forming bacteria in both reactors under different conditions

The top 10 ranked OTUs of BF samples are shown in **Table 3.2**, and were selected based on increasing ratios based on the final AS in each reactor (**Fig. 3.7**). In the BF of the R_N reactor, the most dominant OTU (denovo3418) was *Dokdonella* sp., which showed a high increasing ratio in the final AS and possesses lipase activities (Inaba et al., 2017). In previous studies on biofilms or granular sludge, these bioaggregates were considered to comprise proteins, polysaccharides, lipids and microbial cells (Lawrence et al., 2003; Chen et al., 2007). In fact, some predictive lipase percentage in the BF was higher compared to the final AS in both reactors in this study (**Table 3.3**). These results imply that the biofilm maturation was facilitated by the presence of particular bacteria, which possess enzymatic activities such as lipases and proteases, and formed lower molecules present in biofilms, such as SMPs. The OTUs assigned to the uncultured bacterial phyla TM6 (denovo6461), OD1(denovo5772, denovo6080), and GN02 (denovo798) were subsequently predominant in the R_N reactor. OD1 was detected in the biofilm on the membrane surface of fouled MBR and might be related to biofilm formation (Ishizaki et al., 2016; Neoh et al., 2017). The remaining OTUs of normal BF were uncultured *Myxococcales* (denovo3208) and *Polyangium* (denovo6607) belonging to order *Myxococcales* and myxobacteria have been reported to produce colloid to form biofilm and cause fouling (Gao et al., 2013). The *Saprospira* sp. (denovo6316) is related to cell lysis (Saw et al., 2012), and thus, its presence might facilitate the assimilation of microbes in the biofilm.

Conversely, in the BF of the R_L reactor, OTU assigned to the candidate phylum TM6 (denovo6461) was the most dominant. McLean et al. (2013) reported that TM6 bacteria were detected in a biofilm from a sink drain in a hospital restroom. In addition, the previous study suggested that TM6 was the predominant bacteria in an anaerobic MBR reactor (Xie et al., 2014). These reports indicate that TM6 might survive in an anoxic or anaerobic environment. Mature biofilms form a partial anoxic or anaerobic zone located between the membrane surface and the membrane sludge cake, which could be a reason for the increased TM6 composition. Moreover, TM6 and candidate phyla radiation group such as OD1 (known as Parcubacteria) showed ultrasmall cell size (less than 0.2 μm) (Bruno et al. 2017) and these cell size suggested that the candidate phyla might deposit into the membrane pores and form an aggregate leading pore clogging and increasing TMP. Unclassified *Neisseriaceae* (denovo5366, 2742, 4166: total detection rate; 5.390%) belonging to Betaproteobacteria ranked next in predominance.

Betaproteobacteria are also reported to play an important role in mature biofilm formation in MBRs (Miura et al., 2007). *Conexibacter* (denovo6762: 2.113%) which was detected in biocathode biofilms (Zhang et al., 2017), might be related to biofilm formation. In addition, *Legionella* sp. (denovo3909, 1332: total 1.348%) was present in a protozoan host and survived within a biofilm matrix (Lau and Ashbolt, 2009; Murga et al., 2001). The difference of predominant OTUs in the BF of each reactor might depend on the operational condition of the A/O-MBR, but some similar bacterial groups were observed.

The top 5 shared OTUs in BF samples from both R_N and R_L reactors that showed increased detection ratio compared to that in the final AS are shown in **Table 3.4**. Both BFs showed a higher detection ratio for OTUs classified as uncultured bacterial groups of the candidate phylum TM6 (denovo6461), uncultured Deltaproteobacteria (denovo5106), and uncultured *Myxococcales* (denovo3208). Interestingly, among the top 5 most abundant OTUs in both BF samples, 4 OTUs from the BF of R_L reactor showed a higher abundance rate than that of the BF of R_N reactor. This result suggested that the low OLR condition could promote biofilm formation, which is similar microbial compositions of normally formed biofilm.

A TMP jump is induced by the existence of an anoxic zone in the interior of a biofilm (Cho and Fane, 2002; Jin et al., 2006). A previous study reported that bacteria belonging to TM6, *Desulfatiglans* and *Rudaea* thrived under anaerobic or oxic conditions (McLean et al., 2013; Li et al., 2015; Ma et al., 2016). We considered this was the reason for the high abundance of TM6, *Desulfatiglans* and *Rudaea* (**Table 3.2, 3.4**). Our findings show that various microorganisms such as biofilm forming bacteria, which mainly include uncultured bacteria, biofilm-utilizing bacteria, and the partner, were present in both biofilms. However, the relationship between temporal bacterial growth and biofilm formation is still unclear. Thus, the bacterial species involved in biofilm formation and TMP behavior should be investigated simultaneously in future studies. In addition, biofilms show complex interactions among bacterial microorganisms as well as eukaryotic microorganisms (Jeong et al., 2016). Thus, an investigation of the microorganism network including the metazoans and protozoans in biofilms is required.

Table 3.2 The top 10 increased OTUs in BF compared with the final AS of each reactor*.

OTU ID	Phylogenetic affiliation	Relative abundance
Normal BF (R_N)		
denovo6461	Candidate division TM6 phylum	2.44%
denovo3418	*Dokdonella* sp. (class Gammaproteobacteria)	5.41%
denovo5772	Candidate division OD1 phylum	1.93%
denovo798	Candidate division GN02 phylum	0.88%
denovo3208	Uncultured Myxococcales (class Deltaproteobacteria)	0.93%
denovo6607	*Polyangium* sp. (class Deltaproteobacteria)	0.79%
denovo6080	Candidate division OD1 phylum	0.78%
denovo5106	Uncultured Deltaproteobacteria	0.93%
denovo658	*Desulfatiglans* sp. (class Deltaproteobacteria)	0.69%
denovo6316	*Saprospira* sp. (phylum Bacteroidetes)	0.56%
Low OLR BF (R_L)		
denovo6461	Candidate division TM6 phylum	19.4%
denovo5106	Uncultured Deltaproteobacteria	2.60%
denovo5366	Unclassified *Neisseriaceae* (class Betaproteobacteria)	3.48%
denovo6762	*Conexibacter* sp. (phylum Actinobacteria)	2.11%
denovo2742	Unclassified *Neisseriaceae* (class Betaproteobacteria)	1.04%
denovo6851	Unclassified *Rubrobacteria* (phylum Actinobacteria)	1.33%
denovo3909	*Legionella* sp. (class Gammaproteobacteria)	0.69%
denovo516	*Rudaea* sp. (class Gammaproteobacteria)	1.51%
denovo4166	Unclassified *Neisseriaceae* (class Betaproteobacteria)	0.87%
denovo1332	*Legionella* sp. (class Gammaproteobacteria)	0.66%

*The ratio of the increase was calculated by STAMP software and the results are presented in supplementary **Fig. 3.7**.

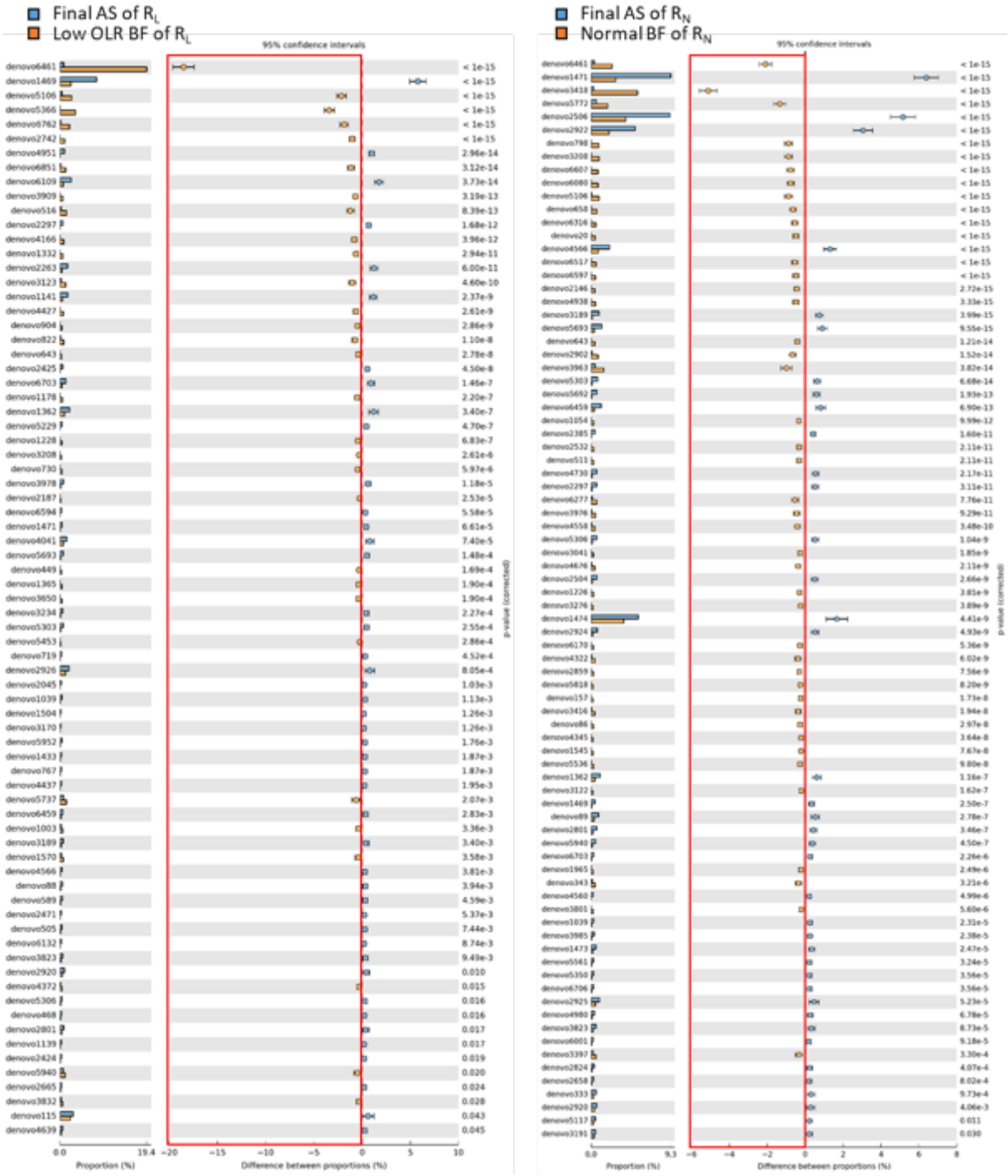

Fig. 3.7 Increased OTUs of BF compared with the final AS community in each reactor calculated by STAMP software.

Table 3.3 The predictive lipase percentages in AS or BF samples according to PICRUSt analysis.

Sample name	Initial AS	Final AS	Final BF	Final MS
R_N reactor				
phospholipase A1 [EC:3.1.1.32]	0.0073%	0.0059%	0.0131%	0.0148%
outer membrane lipase/esterase	0.0006%	0.0005%	0.0008%	0.0011%
phospholipase D [EC:3.1.4.4]	0.0002%	0.0001%	0.0004%	0.0003%
R_L reactor				
phospholipase A1 [EC:3.1.1.32]	0.0084%	0.0078%	0.0162%	0.0154%
outer membrane lipase/esterase	0.0012%	0.0024%	0.0060%	0.0059%
phospholipase D [EC:3.1.4.4]	0.0002%	0.0002%	0.0006%	0.0006%

Table 3.4 The top 5 most abundant shared OTUs in BF samples between the RN and RL reactors selected as increasing bacteria compared with the final AS in each reactor*.

OTU ID	Phylogenetic affiliation	Relative abundance	
		Normal BF (R_N)	Low OLR BF (R_L)
denovo6461	Candidate division TM6 phylum	2.44%	19.4%
denovo5106	Uncultured Deltaproteobacteria	0.93%	2.60%
denovo3208	Uncultured Myxococcales (class Deltaproteobacteria)	0.93%	0.31%
denovo643	*Thalassolituus* (class Gammaproteobacteria)	0.41%	0.42%
denovo4372	*Fischerella* (phylum Cyanobacteria)	0.29%	0.53%

*The ratio of the increase was calculated using STAMP software and the results are presented in supplementary **Fig. 3.7**.

3.4. Summary of chapter 3

In the A/O-MBR operated under low organic loading rate condition (R_L reactor; OLR: 0.002 kg-COD·m^{-3}·day^{-1}), membrane fouling and biofilm were developed rapidly compared to the A/O-MBR under normal conditions (R_N reactor; OLR: 0.42 kg-COD·m^{-3}·day^{-1}). The microbial community composition between the bulk AS and BF was considerably different, and characteristic bacteria found in BF were thought to important for biofilm formation on the membrane surface in A/O-MBR. Candidate TM6 showed specific presence on the fouled membrane surface as a biofilm in the R_L reactor. On the other hand, Candidate OD1 was the predominant phylum in the fouled membrane surface of the R_N reactor. In addition, biofilms might be formed by the same process in both reactors. However, correlation of the bacterial species involved in biofilm formation and TMP behavior should be investigated in future studies.

References

Barrios, A. F. G., Zuo, R., Hashimoto, Y., Yang, L., Bentley, W. E., & Wood, T. K. Autoinducer 2 controls biofilm formation in Escherichia coli through a novel motility quorum-sensing regulator (MqsR, B3022). J. Bacteriol. 188, 305-316, doi: 10.1128/JB.188.1.305-316.2006 (2006).

Bruno, A., Sandionigi, A., Rizzi, E., Bernasconi, M., Vicario, S., Galimberti, A., ... & Casiraghi, M. (2017). Exploring the under-investigated "microbial dark matter" of drinking water treatment plants. Scientific reports, 7, 44350.

Caporaso, J. et al. Ultra-high-throughput microbial community analysis on the Illumina HiSeq and MiSeq platforms. ISME J. 6, 1621, doi: 10.1038/ismej.2012.8 (2012).

Caporaso, J. G. et al. QIIME allows analysis of high-throughput community sequencing data. Nature Methods. 7, 335, doi: 10.1038/nmeth.f.303 (2010).

Chen, M. Y., Lee, D. J., Tay, J. H., & Show, K. Y. Staining of extracellular polymeric substances and cells in bioaggregates. Appl. Microbiol. Biotechnol. 75, 467-474, doi: 10.1007/s00253-006-0816-5 (2007).

Chen, C. H., Fu, Y., & Gao, D. W. Membrane biofouling process correlated to the microbial community succession in an A/O MBR. Bioresour. Technol. 197, 185-192, doi: 10.1016/j.biortech.2015.08.092 (2015).

Cho, B. D., & Fane, A. G. Fouling transients in nominally sub-critical flux operation of a membrane bioreactor. J. Membr. Sci. 209, 391-403, doi: 10.1016/S0376-7388(02)00321-6 (2002).

Choi, J., Kim, E. S., & Ahn, Y. Microbial community analysis of bulk sludge/cake layers and biofouling-causing microbial consortia in a full-scale aerobic membrane bioreactor. Bioresour. Technol. 227, 133-141, doi: 10.1016/j.biortech.2016.12.056 (2017).

Fu, Z., Yang, F., An, Y., & Xue, Y. Simultaneous nitrification and denitrification coupled with phosphorus removal in an modified anoxic/oxic-membrane bioreactor (A/O-MBR). Biochem. Eng. J. 43, 191-196, doi: 10.1016/j.bej.2008.09.021 (2009).

Gao, D., Fu, Y., & Ren, N. Tracing biofouling to the structure of the microbial community and its metabolic products: A study of the three-stage MBR process. Water Res. 47, 6680-6690, doi: 10.1016/j.watres.2013.09.007 (2013).

Gao, D. W., Wen, Z. D., Li, B., & Liang, H. Microbial community structure characteristics associated membrane fouling in A/O-MBR system. Bioresour. Technol. 154, 87-93, doi: 10.1016/j.biortech.2013.11.051 (2014).

Gkotsis, P. K., Batsari, E. L., Peleka, E. N., Tolkou, A. K., & Zouboulis, A. I. Fouling control in a lab-scale MBR system: comparison of several commercially applied coagulants. J. Environ. Manag. 203, 838-846, doi: 10.1016/j.jenvman.2016.03.003 (2017).

Hu, M., Wang, X., Wen, X., & Xia, Y. Microbial community structures in different wastewater treatment plants as revealed by 454-pyrosequencing analysis. Bioresour. Technol. 117, 72-79, doi: 10.1016/j.biortech.2012.04.061 (2012).

Huang, L. N., De Wever, H., & Diels, L. Diverse and distinct bacterial communities induced biofilm fouling in membrane bioreactors operated under different conditions. Environ. Sci. Technol. 42, 8360-8366, doi: 10.1021/es801283q (2008).

Inaba, T., Hori, T., Aizawa, H., Ogata, A., & Habe, H. Architecture, component, and microbiome of biofilm involved in the fouling of membrane bioreactors. npj Biofilms Microbiomes. 3, 5, doi: 10.1038/s41522-016-0010-1 (2017).

Ishizaki, S., Fukushima, T., Ishii, S., & Okabe, S. Membrane fouling potentials and cellular properties of bacteria isolated from fouled membranes in a MBR treating municipal wastewater. Water Res. 100, 448-457, doi: 10.1016/j.watres.2016.05.027 (2016).

Ishizaki, S., Sugiyama, R., & Okabe, S. Membrane fouling induced by AHL-mediated soluble microbial product (SMP) formation by fouling-causing bacteria co-cultured with fouling-enhancing bacteria. Sci. Rep. 7, 8482, doi: 10.1038/s41598-017-09023-5 (2017).

Jeong, S. Y., Yi, T., Lee, C. H., & Kim, T. G. Spatiotemporal dynamics and correlation networks of bacterial and fungal communities in a membrane bioreactor. Water Res. 105, 218-230, doi: 10.1016/j.watres.2016.09.001 (2016).

Jin, Y. L., Lee, W. N., Lee, C. H., Chang, I. S., Huang, X., & Swaminathan, T. Effect of DO concentration on biofilm structure and membrane filterability in submerged membrane bioreactor. Water Res. 40, 2829-2836, doi: 10.1016/j.watres.2006.05.040 (2006).

Jo, S. J., Kwon, H., Jeong, S. Y., Lee, C. H., & Kim, T. G. Comparison of microbial communities of activated sludge and membrane biofilm in 10 full-scale membrane bioreactors. Water Res. 101, 214-225, doi: 10.1016/j.watres.2016.05.042 (2016).

Johir, M. A., Vigneswaran, S., Sathasivan, A., Kandasamy, J., & Chang, C. Y. Effect of organic loading rate on organic matter and foulant characteristics in membrane bio-reactor. Bioresour. Technol. 113, 154-160, doi: 10.1016/j.biortech.2011.12.002 (2012).

Langille, M. G. et al. Predictive functional profiling of microbial communities using 16S rRNA marker gene sequences. Nature Biotechnol. 31, 814-821, doi: 10.1038/nbt.2676 (2013).

Lau, H. Y., & Ashbolt, N. J. The role of biofilms and protozoa in Legionella pathogenesis: implications for drinking water. J. Appl. Microbial. 107, 368-378, doi: 10.1111/j.1365-2672.2009.04208.x (2009).

Lawrence, J. R. et al. Scanning transmission X-ray, laser scanning, and transmission electron microscopy mapping of the exopolymeric matrix of microbial biofilms. Appl. Environ. Microbiol. 69, 5543-5554, doi: 10.1128/AEM.69.9.5543-5554.2003 (2003).

Lee, S. et al. Crossing the border between laboratory and field: bacterial quorum quenching for anti-biofouling strategy in an MBR. Environ. Sci. Technol. 50, 1788-1795, doi: 10.1021/acs.est.5b04795 (2016).

Li, Z. et al. Anaerobic mineralization of 2, 4, 6-tribromophenol to CO2 by a synthetic microbial community comprising Clostridium, Dehalobacter, and Desulfatiglans. Bioresour. Technol. 176, 225-232, doi: 10.1016/j.biortech.2014.10.097 (2015).

Lim, S., Kim, S., Yeon, K. M., Sang, B. I., Chun, J., & Lee, C. H. Correlation between microbial community structure and biofouling in a laboratory scale membrane bioreactor with synthetic wastewater. Desalination. 287, 209-215, doi: 10.1016/j.desal.2011.09.030 (2012).

Ma, Z. et al. Effect of temperature variation on membrane fouling and microbial community structure in membrane bioreactor. Bioresour. Technol. 133, 462-468, doi: 10.1016/j.biortech.2013.01.023 (2013).

Ma, S. J. et al. Effects of DO levels on surface force, cell membrane properties and microbial community dynamics of activated sludge. Bioresour. Technol. 214, 645-652, doi: 10.1016/j.biortech.2016.04.132 (2016).

Malaeb, L., Le-Clech, P., Vrouwenvelder, J. S., Ayoub, G. M., & Saikaly, P. E. Do biological-based strategies hold promise to biofouling control in MBRs?. Water Res. 47, 5447-5463, doi: 10.1016/j.watres.2013.06.033 (2013).

McLean, J. S. et al. Candidate phylum TM6 genome recovered from a hospital sink biofilm provides genomic insights into this uncultivated phylum. Proc. Natl. Acad. Sci. USA 110, E2390-E2399, doi: 10.1073/pnas.1219809110 (2013).

Meng, F., Zhang, S., Oh, Y., Zhou, Z., Shin, H. S., & Chae, S. R. Fouling in membrane bioreactors: an updated review. *Water Res*. **114,** 151-180, doi: 10.1016/j.watres.2017.02.006 (2017).

Meng, F., Zhang, H., Yang, F., & Liu, L. Characterization of cake layer in submerged membrane bioreactor. Environ. Sci. Technol. 41, 4065-4070, doi: 10.1021/es062208b (2007).

Meng, F., Chae, S. R., Drews, A., Kraume, M., Shin, H. S., & Yang, F. Recent advances in membrane bioreactors (MBRs): membrane fouling and membrane material. *Water Res*. **43,** 1489-1512, doi: 10.1016/j.watres.2008.12.044 (2009).

Miura, Y., Watanabe, Y., & Okabe, S. Membrane biofouling in pilot-scale membrane bioreactors (MBRs) treating municipal wastewater: impact of biofilm formation. Environ. Sci. Technol. 41, 632-638, doi: 10.1021/es0615371 (2007).

Murga, R., Forster, T. S., Brown, E., Pruckler, J. M., Fields, B. S., & Donlan, R. M. Role of biofilms in the survival of Legionella pneumophila in a model potable-water system. Microbiology. 147, 3121-3126, doi: 10.1099/00221287-147-11-3121 (2001).

Neoh, C. H. et al. Correlation between microbial community structure and performances of membrane bioreactor for treatment of palm oil mill effluent. Chem. Eng. J. 308, 656-663, doi: 10.1016/j.cej.2016.09.063 (2017).

Ren, T. T., Li, X. Y., & Yu, H. Q. Effect of N-acyl-homoserine lactones-like molecules from aerobic granules on biofilm formation by Escherichia coli K12. Bioresour. Technol. 129, 655-658, doi: 10.1016/j.biortech.2012.12.043 (2013).

Saw, J. H. et al. Complete genome sequencing and analysis of Saprospira grandis str. Lewin, a predatory marine bacterium. Stand. Genomic Sci. 6, 84, doi: 10.4056/sigs.2445005 (2012).

Sun, F. Y., Wang, X. M., & Li, X. Y. Visualisation and characterisation of biopolymer clusters in a submerged membrane bioreactor. J. Membr. Sci. 325, 691-697, doi: 10.1016/j.memsci.2008.08.048 (2008).

Wan, C. Y., De Wever, H., Diels, L., Thoeye, C., Liang, J. B., & Huang, L. N. Biodiversity and population dynamics of microorganisms in a full-scale membrane bioreactor for municipal

wastewater treatment. Water Res. 45, 1129-1138, doi: 10.1016/j.watres.2010.11.008 (2011).

Wang, Z., Wu, Z., Yin, X., & Tian, L. Membrane fouling in a submerged membrane bioreactor (MBR) under sub-critical flux operation: membrane foulant and gel layer characterization. J. Membr. Sci. 325, 238-244, doi: 10.1016/j.memsci.2008.07.035 (2008).

Wang, Z., Meng, F., He, X., Zhou, Z., Huang, L. N., & Liang, S. Optimisation and performance of NaClO-assisted maintenance cleaning for fouling control in membrane bioreactors. *Water Res*. **53,** 1-11, doi: 10.1016/j.watres.2013.12.040 (2014).

Wu, B., Yi, S., & Fane, A. G. Microbial behaviors involved in cake fouling in membrane bioreactors under different solids retention times. Bioresour. Technol. 102, 2511-2516, doi: 10.1016/j.biortech.2010.11.045 (2011).

Wu, S. C., & Lee, C. M. Correlation between fouling propensity of soluble extracellular polymeric substances and sludge metabolic activity altered by different starvation conditions. *Bioresour. Technol.* **102,** 5375-5380, doi: 10.1016/j.biortech.2010.11.093 (2011).

Xia, S. et al. The effect of organic loading on bacterial community composition of membrane biofilms in a submerged polyvinyl chloride membrane bioreactor. *Bioresour. Technol*. **101,** 6601-6609, doi: 10.1016/j.biortech.2010.03.082 (2010).

Xie, Z., Wang, Z., Wang, Q., Zhu, C., & Wu, Z. An anaerobic dynamic membrane bioreactor (AnDMBR) for landfill leachate treatment: Performance and microbial community identification. *Bioresour. Technol.* **161,** 29-39, doi: 10.1016/j.biortech.2014.03.014 (2014).

Zhang, G., Feng, S., Jiao, Y., Lee, D. J., Xin, Y., & Sun, H. Cathodic reducing bacteria of dual-chambered microbial fuel cell. *Int. J. Hydrogen Energy.* **42,** 27607-27617, doi: 10.1016/j.ijhydene.2017.06.095 (2017).

Chapter 4

Initiation and progression of the biofilm formation process on the membrane in A/O-MBR treating actual sewage under low organic loading rate conditions

4.1 Background and objectives

Biofilm development is thought of the major cause of membrane fouling to decrease permeability (Yun et al., 2006; Hwang et al., 2012; Sweity et al., 2011). Thus, understanding biofilm formation process is key information to control biofilm development for the prevention or mitigation of membrane fouling.

It is widely accepted that the general biofilm formation process is divided into multiple stages, which includes the reversible and irreversible attachment of bacteria to the surface, cell-cell adhesion and proliferation, growth to maturity of the biofilm and finally detachment by degradation of extracellular substances (Vuong and Otto, 2002). In the case of MBR, the conditioning film formation on the membrane surface is first step to modify the physico-chemical properties of membrane and interact with surface appendages evident of pili, fimbriae, glycocalyx, and EPSs on the bacterial cell (Vanysacker et al., 2014). Conditioning film was mainly consisted by extracellular polymeric substances (EPSs) and soluble microbial products (SMPs) including microbial by-products such as proteins, lipoproteins, polysaccharides and other macromolecules (Aslam et al., 2018). The stage of bacterial attachment facilitates further biofilm formation, it is important to investigate this stage for membrane fouling control (Blanpain-Avet et al., 2011; Toyofuku et al., 2016). In addition, some pioneer bacteria is firstly attached on the conditioning film. Previously, Betaproteobacteria and Alphaproteobacteria might be recognized as pioneer bacteria (Ziegler et al., 2016). The shear force by aeration is strong to remove the activated sludge from the membrane surface in the initial stage of biofilm formation and this might facilitate selection pressures of specific bacteria species in activated sludge. In the next stage of initial bacteria adhesion, pioneer bacteria might form microcolonies and produce EPS matrix to make favorable conditions for the attachment of other bacteria and macromolecules. Finally, accumulated biomaterials induce biofilm maturation (i.e. cake layer) and lead to severe membrane fouling development.

Investigation of biofilm progression is important to improve our understanding of biofilm development in MBRs. Characterization of biofilm formation at different stages has been studied in terms of microbial community composition and biofilm image analysis. Previously, confocal laser scanning microscopy (CLSM) imaging or scanning electron microscope (SEM) imaging techniques provides the biofilm characteristics including morphological information, cell and EPS abundance or proportion, thickness and so on. Hwang et al. (2012) revealed that SEM the

membrane surface was covered by cake layer and the distribution of polysaccharides and live cells on the cake layer by using SEM and CLSM observation. Recently, some reports investigated the biofilm by using combination of CLSM and microbial community analysis (Inaba et al., 2017; Gu et al., 2018). To date, however, there have been limited investigations of the relationships between the biofilm formation process and the microbial community of AS and biofilm in MBRs treating real sewage.

The aim of chapter 4 was to elucidate the relationship between microbial community structure of biofilm and AS at each biofilm formation stage in terms of microbial colonization and biofilm growth in MBR treating actual sewage under low organic loading rate condition. To achieve this goal, non-destructive visualization by CLSM and SEM analysis was applied to analyze biofilm. In addition, 16S rRNA gene sequencing of biofilm and AS on fouling progression was applied to reveal the key player for biofilm formation.

4.2. Materials and methods

4.2.1. MBR operational conditions

Two laboratory-scale anoxic/oxic (A/O)–MBRs (R1 and R2) were used for treating actual sewage. The MBRs consisted of 6 L of anoxic and oxic tank. Actual sewage after sedimentation was used as influent into the reactor. The flat sheet membrane (chlorinated polyvinyl chloride: CPVC) with an area of 0.11 m^2 and mean pore size of 0.20 μm (KUBOTA Co.Ltd., Osaka, Japan) was submerged in the oxic tank. The aeration was applied by a diffuser at the bottom of the oxic tank at 5 L/min. Internal recycling of mixed liquor from the oxic tank into the anoxic tank was conducted to enhance denitrification.

A/O-MBRs were operated with hydraulic retention time of 8.0 h and a solid retention time of 60 days under the standard conditions. The average temperature of activated sludge in oxic tank was 11.8±0.6°C. The operation cycle of the membrane unit was as follows: a cycle of 9 min of filtration followed by 1 min of relaxation, and average permeate flux of 11.8 $L \cdot m^{-2} \cdot h^{-1}$. Returned AS taken from the municipal sewage treatment plant was seeded and mixed liquor suspended solids (MLSS) concentration was controlled to approximately 10,000 mg/L in each reactor. Both reactors were operated under 0.42 kg-soluble chemical oxygen demand (sCOD)$\cdot m^{-3} \cdot day^{-1}$ as the standard organic loading rate (OLR) condition for 15 days and then the low OLR condition (0.002 $kg \cdot sCOD \cdot m^{-3} \cdot day^{-1}$) was started in each reactor to induce membrane fouling

development. In order to create low OLR environment and keep permeate flux, permeate effluent was recycled into anoxic tank. The detail of the condition was already described in chapter 3.

4.2.2. Analytical methods

Temperature, pH, and dissolved oxygen (DO) in the oxic tank were measured on-site using a portable pH and DO meter (DM-32P, TOA DKK, Tokyo, Japan). The TMP between the pump and the membrane was monitored by a pressure transducer (ZSE50F, SMC, Tokyo, Japan). sCOD was measured with a water quality analyzer (DR2800, Hach, CO, USA) and ammonium-nitrogen (NH_4^+-N) was measured by high performance liquid chromatography (LC-20ADsp, Shimadzu, Kyoto, Japan).

4.2.3. Biofilm sampling and microscopic analysis

The membrane unit was taken from the oxic tank and then the membrane surface was gently rinsed with ultrapure water. Approximately 200 mm^2 of membrane pieces was cut and the membrane pieces were immediately immersed in phosphate buffered saline and stored at 4 °C for CLSM and SEM analyses. The membrane pieces were sampled on day 21 (early-stage biofilm), day 24 (middle-stage biofilm) and day 31 (mature-stage biofilm) in the R1 reactor, whereas samples were taken on day 21 (middle-stage biofilm) and day 31 (mature-stage biofilm) from the R2 reactor for CLSM analysis. LIVE/DEAD BacLight Bacterial Viability Kit (Thermo Fisher Scientific, MA, USA) was used for live and dead cell staining of the membrane pieces. The membrane pieces were stained for 15 min with SYTO9 and propidium iodide at final concentrations of 5 and 15 μM, respectively. The stained membrane biofilms were visualized by CLSM (A1, Nikon, Tokyo, Japan) using 488 nm and 561 nm lasers for SYTO9 (live cell) and propidium iodide (dead cell), respectively. A tabletop SEM (TM3030Plus, Hitachi, Tokyo, Japan) was used with low vacuum mode for non-destructive analysis of the membrane biofilm. The membrane pieces were put on the cool stage and maintained at −20°C during obsevations.

4.2.4. 16S rRNA gene sequence analysis

The membrane unit was taken out from the oxic tank and the surface was rinsed with ultrapure water to remove the cake layer and then the tightly bound layer biofilms were sampled by scrubbing using a spatula. The activated sludge was sampled from oxic tank at the same time.

The samples were stored at −20°C until DNA extraction. Genomic DNA was extracted using the FastDNA Spin Kit for Soil (MP Biomedicals, CA, USA). 16S rRNA gene sequencing was performed as following Caporaso et al. (2012). Briefly, the universal primer pair Univ515F (5′-GTGCCAGCMGCCGCGGTAA-3′) and Univ806R (5′-GGACTACHVGGGTWTCTAAT-3′) were used to amplify the 16S rRNA genes including V4 region. PCR was performed using the following conditions: one cycle of 94 °C for 3 min, 25 cycles of 94 °C for 45 s, 50 °C for 60 s and 72 °C for 90 s, and a final cycle of 72 °C for 10 min. The PCR products were purified using QIAquick PCR Purification Kit (QIAGEN, Hilden, Germany). MiSeq Reagent Kit v2 and the MiSeq System (Illumina Inc., CA, USA) were used for DNA sequencing.

4.2.5. Sequence data analysis

Sequence data were analyzed with QIIME software (version 1.9.1) (Caporaso et al., 2010). Operational taxonomic units (OTUs) were selected at 97% identify using UCLUST. Taxonomic classification was assigned using BLAST based on the Greengenes database ver. 13_8. The most closely-related species of predominant OTUs were searched using BLAST in NCBI database (http://blast.ncbi.nlm.nih.gov/Blast.cgi). A principal component analysis (PCA) plot with significant mean proportion differences for virginal datasets was created using Sequence Tag-based Analysis of Microbial Population dynamics (STAMP) software (Takimoto et al., 2018).

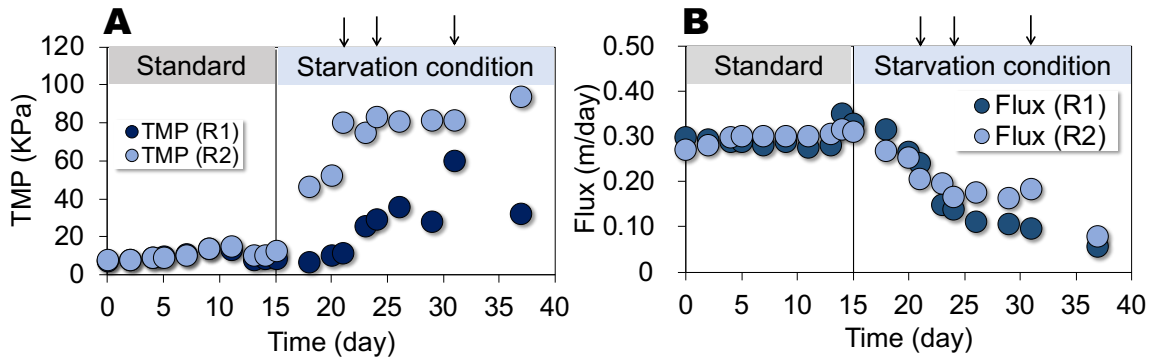

Fig. 4.1 Transition of TMP (A) and flux (B) of two A/O-MBRs under standard condition and low OLR condition. The low OLR condition was started at day 15 after standard condition. Arrows indicate the day of membrane sampling on day 21, 24, and 31 from each reactor.

4.3. Results

4.3.1. Reactor performance and biofouling development

Two reactors were operated under standard conditions to stabilize the reactor performances for over 5 weeks at room temperature. During the stabilization period, sCOD removal rate showed that R1 and R2 was 78.7% and 84.6%, respectively; NH_4^+-N removal was approximately 100% for each reactor. The mean MLSS concentration was 11200 mg/L in R1 and 11000 mg/L in R2 under standard conditions.

Before starting low OLR conditions, the membrane was physically washed by using an urethane sponge and ultrapure water for both reactors. Then low OLR conditions were started in both A/O-MBRs to induce membrane fouling development. After the low OLR operations, the MLSS concentration gradually decreased to 5100 and 4300 mg/L for R1 and R2, respectively. As shown in chapter 3, low OLR conditions might cause MLSS decrease and cell lysis. The flux and TMP drastically changed on 20 and 18 days of low OLR conditions in R1 and R2, respectively. During the period of decreasing permeability, membrane fouling developed and thus, we defined the day 21 membrane sample as early-stage biofilm, day 24 as middle-stage biofilm, and day 31 as mature-stage biofilm in R1; and day 21 membrane sample as middle-stage biofilm and day 24 as mature-stage biofilm in R2.

4.3.2. Biofilm analysis by CLSM

In the early-stage biofilm (**Fig. 4.2A**), red stained cell shape and non-cell shape (dead cell) were dispersed on the whole membrane surface. In contrast, only a few green stained cell (live cell) was detected in the early-stage biofilm. Thus, the attachment of live cells on membrane surface were limited in this stage. In the middle-stage biofilm, live cells colonized some small areas and dead cells were widely dispersed on the membrane surface but did not clearly show cell shapes (**Fig. 4.2B, C**). The red stained area might be a conditioning film with small live cells colonized on the surface. It is generally reported that major components of EPSs are proteins and polysaccharides and also contain humic acids, nucleic acids, lipids, and uronic acids (Lin et al., 2014). Thus, cell components including DNA and RNA could be released from lysed cells and initial biofilm could be stained as dead cells. Microcolony-like shape in a gel layer were clearly observed by SEM analysis (**Fig. 4.3**).

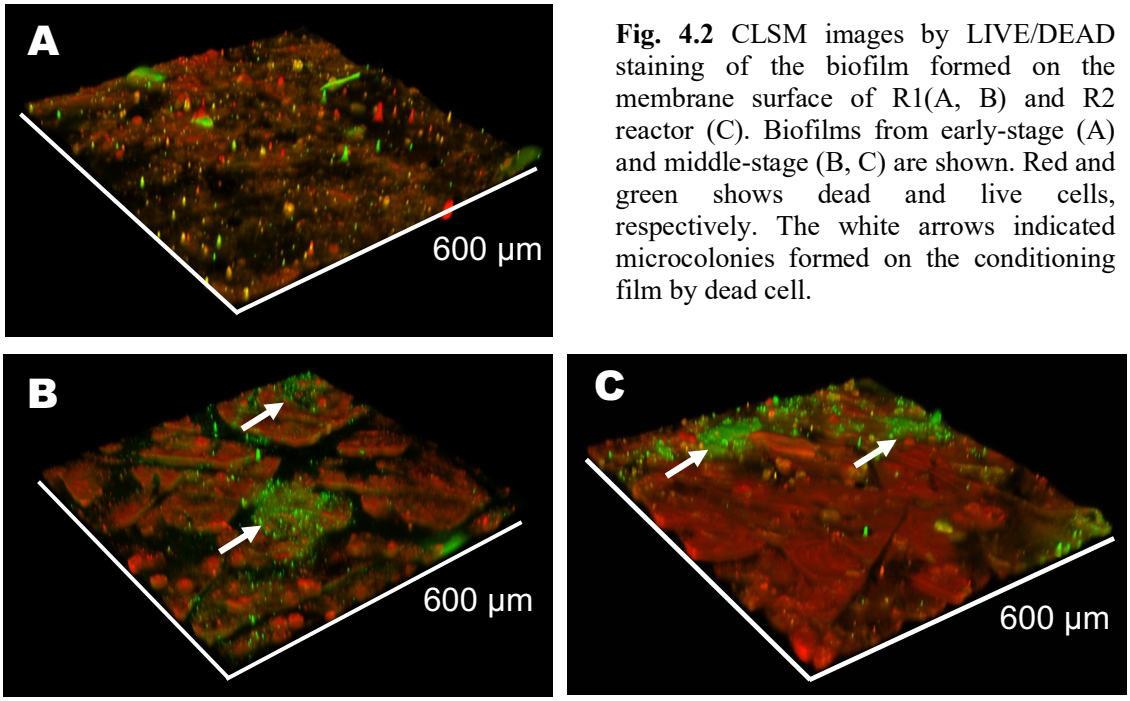

Fig. 4.2 CLSM images by LIVE/DEAD staining of the biofilm formed on the membrane surface of R1(A, B) and R2 reactor (C). Biofilms from early-stage (A) and middle-stage (B, C) are shown. Red and green shows dead and live cells, respectively. The white arrows indicated microcolonies formed on the conditioning film by dead cell.

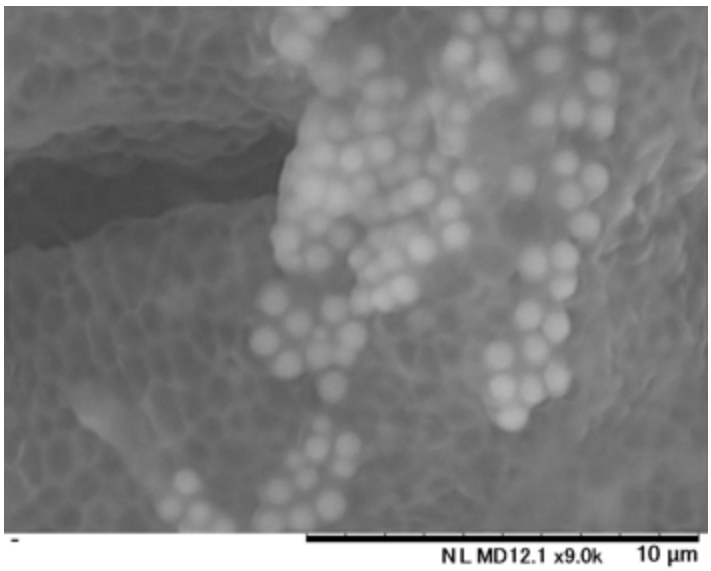

Fig. 4.3 SEM (using low vacuum and cool stage condition) microphotograph of middle stage biofilm on the membrane surface. The membrane surface was covered by a gel layer and microcolonies were formed and immobilized in the gel layer on the membrane surface.

4.3.3. Microbial community analysis

There were clear differences between the AS and biofilm microbial communities as shown in **Figs. 4.4 and 4.5**. Betaproteobacteria, Deltaproteobacteria, and Bacteroidetes were the dominant phyla and classes in the AS and biofilm microbial communities (**Fig. 4.4**). These bacteria were also found in AS in other sewage treatment plants (Zhang et al., 2012; Hatamoto et al., 2017). Almost relative abundance of phylum and class in activated sludge were stably maintained during

low OLR operation. The PCA also showed that the microbial community of AS did not significantly change compared to biofilm community during low OLR operation (**Fig. 4.5)**

In contrast, the microbial community changed between middle biofilm (24 day) and mature biofilm (31 day) samples. The biofilm community in middle stage was more different from mature stage. In other words, the mature biofilm community was approached to AS community. Betaproteobacteria was the most dominant bacteria in middle-stage biofilm and accounted for 37% and 42% of the total community in R1 and R2, respectively, followed by Bacteroidetes and Deltaproteobacteria. Particularly, the relative abundance of Chlamydiae, OD1, and Cyanobacteria in biofilm were significantly different from activated sludge community. Although Betaproteobacteria, Deltaproteobacteria and OD1 decreased in biofilm maturation, Alphaproteobacteria, Gammaproteobacteria, Bacteroidetes, Chlamydiae, and Cyanobacteria increased the relative abundance in biofilm maturation.

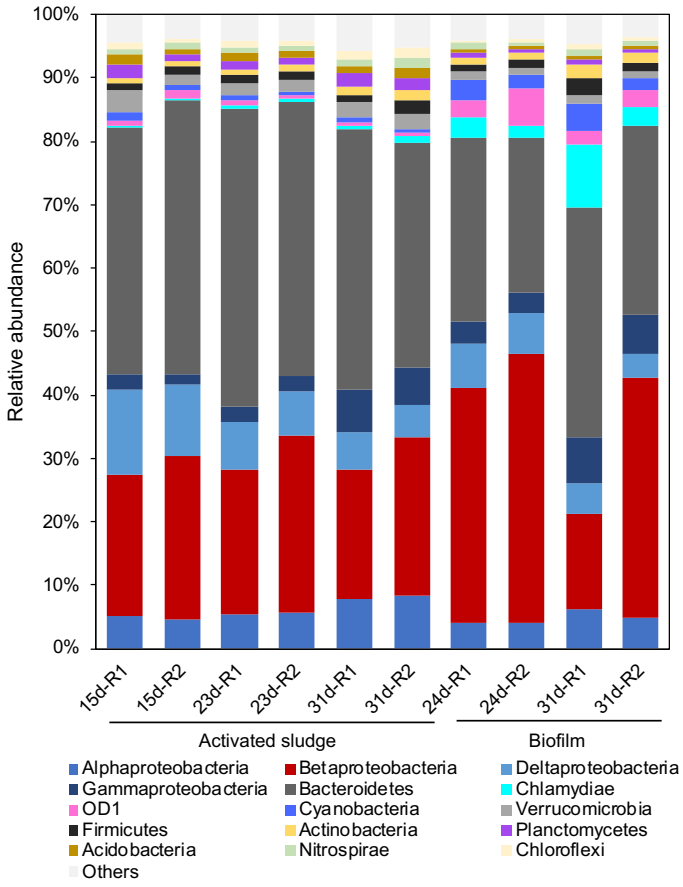

Fig. 4.4 Microbial community structure (phylum and class level) of activated sludge in aerobic tank and biofilm on the membrane surface in each reactor during low organic loading rate conditions. 15d-R1 indicate R1 reactor on 15 days during the experimental term.

Changes in the top 10 OTUs detected in AS and biofilm samples of both reactors are shown in **Table 4.1**. In AS community, unclassified *Neisseriaceae* (No.1) and *Kofleria* sp. (No.6) continuously decreased during low OLR operation. The relative abundance of the other bacteria in AS community were constant. In contrast, unclassified *Neisseriaceae* (No.1) was most dominant in middle stage biofilm and then decreased for biofilm maturation, although the bacteria was minority in AS community. *Parachlamydia* sp. (No.4) was also more abundant in the biofilm compared to the AS community. *Parachlamydia* sp. in AS community accounted for 0.3% in both reactors on day 23 whereas the OTU increased to 2.5% in R1 and 1.4% in R2 of middle biofilm on 24 day. Although *Melanibacteria* (No.10) was minor bacteria in AS community, the relative abundance increased middle biofilm and biofilm maturation. The relative abundance of *Solitalea* sp. (No.2), *Dechloromonas* ap. (No.3), and unclassified *Melanobacteria* (No.10) in middle biofilm increased to biofilm maturation.

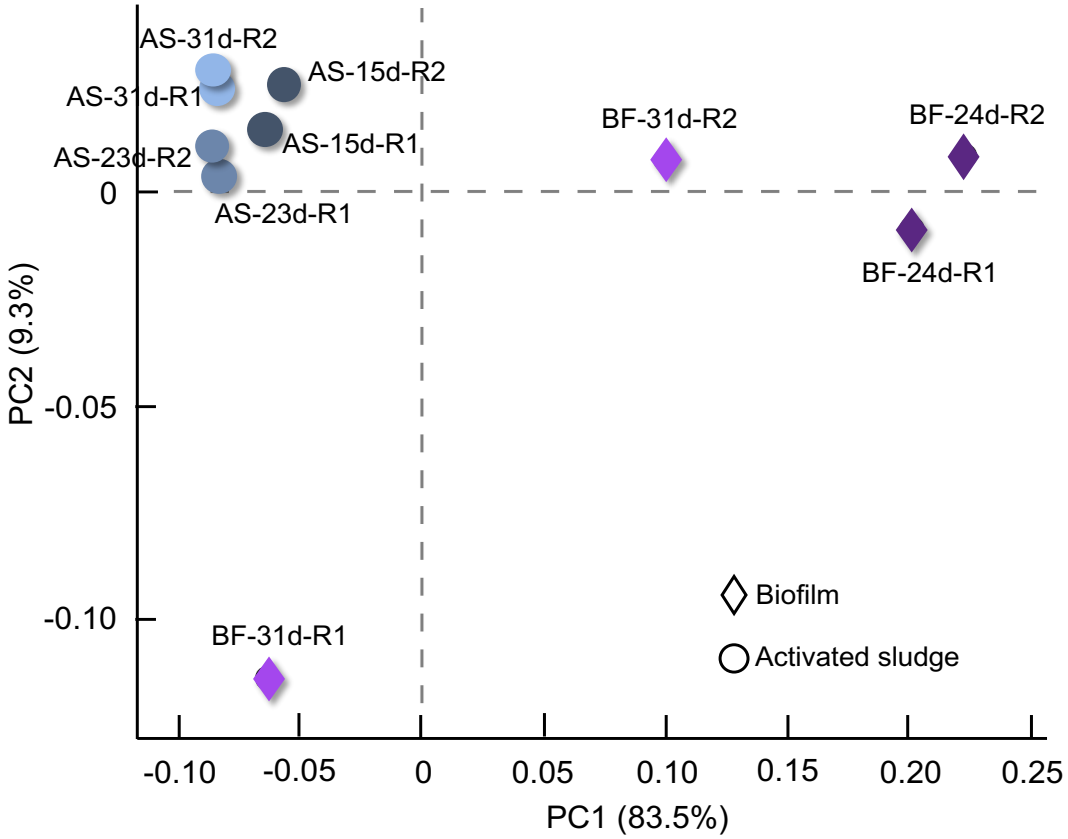

Fig. 4.5 Principal component analysis plot of biofilm and AS microbial community structures in both reactors during the low OLR operation. AS and biofilm samples were named as "AS-date-reactor number" and "BF-date-reactor", respectively.

Table 4.1 Representative operational taxonomic units (OTUs) in activated sludge and biofilms in R1 and R2 reactor under low organic loading rate conditions.

			Sample name	Activated sludge						Biofilm				
			Sampling day	15 day		23 day		31 day		24 day		31 day		
			Reactor	R1	R2	R1	R2	R1	R2	R1	R2	R1	R2	
No.	Phylum (Class)	Family	Genera											
1	(Betaproteobacteria)	*Neisseriaceae*	Unclassified	1.3	2.2	0.0	0.1	0.0	0.0	26.7	28.7	0.4	16.8	30%
2	Bacteroidetes	*Sphingobacteriaceae*	*Solitalea*	2.3	1.3	4.8	4.5	1.7	1.2	4.3	3.3	10.4	2.4	25%
3	(Betaproteobacteria)	*Azonexaceae*	*Dechloromonas*	2.9	4.3	5.6	8.3	6.1	9.0	1.8	2.3	3.6	4.8	20%
4	Chlamydiae	*Parachlamydiaceae*	*Parachlamydia*	0.1	0.2	0.3	0.3	0.2	0.6	2.5	1.4	8.1	2.1	15%
5	Bacteroidetes	*Chitinophagaceae*	*Terrimonas*	5.9	6.1	7.6	7.2	6.8	6.2	3.8	3.2	3.2	4.5	10%
6	(Deltaproteobacteria)	*Kofleriaceae*	*Kofleria*	5.3	5.3	2.5	2.0	0.0	0.1	3.5	3.6	2.0	0.9	5%
7	Bacteroidetes	*Prolixibacteraceae*	*Puteibacter*	4.1	2.9	4.1	3.4	5.1	3.5	2.0	1.5	2.6	2.1	3%
8	(Betaproteobacteria)	*Casimicrobiaceae*	*Casimicrobium*	3.5	3.1	3.0	3.0	2.1	1.0	0.8	0.8	1.2	1.1	2%
9	(Betaproteobacteria)		*Ca.* Accumulibacter	3.0	2.6	1.8	2.3	2.3	3.1	1.2	1.3	1.6	1.7	1%
10	Cyanobacteria	*Melainabacteria*	Unclassified	0.7	0.3	0.4	0.3	0.5	0.4	1.8	1.1	3.0	1.0	0%

*Values in the table indicate relative abundance (%) in the samples.

4.4. Discussion

Generally, the properties of the conditioning film can be drastically changed by adsorption of a variety of chemicals (Vanysacker et al., 2014). Hwang et al. (2013) showed that the conditioning film had the ability to enhance or impair bacterial adhesion depending on the surface. Fortunato et al. (2019) reported that a thick biofilm gradually developed on the membrane surface during MBR operation and that dead cell layer were found under the live cell layer. These studies suggested that released extracellular DNA by cell death formed a conditioning film. As shown in **Fig. 4.2**, dead bacteria and the red-stained area, which did not show clear cell shapes, were dispersed on the membrane surface. BAP including EPSs and extracellular DNA might be released from dead cells under low OLR conditions and form the conditioning film as initial biofilm on the membrane surface in this study. Miura et al. (2007) also reported similar trends in biofilm formation from pilot-scale hollow fiber MBRs treating municipal wastewater. In the matured biofilm, live cells were grown to vertical and horizontal direction based on the dead cell layer (**Fig. 4.6**). This biofilm structure indicated that bacteria in the bottom layer of the matured biofilm was influenced by low concentration of nutrient and DO and lead to cell lysis. Previous study suggested that eDNA is necessary to stabilize mature biofilm (Sena-Vélez et al., 2016). Thus, the dead cells might have key roles on not only initial adhesion to the membrane but also biofilm maturation and severe bio-fouling development.

As indicated in the PCA plots (**Fig. 4.5**) and the biofilm maturation on the membrane surface in the CLSM observation (**Figs. 4.2 and 4.6)**, AS gradually adhered to the mature biofilm and some bacteria penetrated the inner biofilm. Thus, these bacteria remained on the biofilm against physical washing with pure water of membrane surface for biofilm sampling. In fact, the

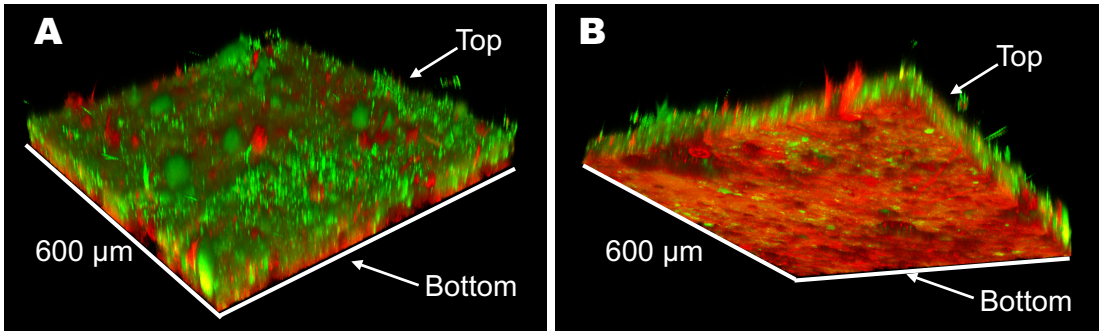

Fig. 4.6 3D CLSM images from top (A) and bottom (B) view of mature biofilm on the membrane surface in the R1 reactor at 31 days. Live cells were stained as green and dead cells were stained as red by LIVE/DEAD staining. Area of observed image: 600 μm × 600 μm × 125 μm.

microbial community structure of the biofilm approached that of the AS microbial community structure. This phenomenon was also found in a full-scale MBR treating wastewater (Takada et al., 2018). Since it was considered that some bacteria in AS community were just attached on the matured biofilm, the predominant bacteria found in the mature biofilm might not be important for biofilm formation process. Thus, it is important to investigate the microbial community and pioneer bacteria in early stage biofilm because those bacteria play a critical role in colonization and biofilm maturations on the membrane surface.

Many studies investigating the microbial structure in biofilm and AS showed that the microbial community in the biofilm drastically changed during the operation period whereas the microbial community in AS was relatively unchanged (Miura et al., 2007; Ziegler et al., 2016; Gao et al., 2013). Dominant bacteria in AS and biofilm in this study, such as Betaproteobacteria were reported as co-dominant bacteria in biofilm and AS in an MBR as well as in early biofilm at low TMP (Miura et al., 2007; Luo et al., 2017). OD1 was also found in a previous report and might play an important role in biofilm development (Takimoto et al., 2018; Neoh et al., 2017). The extremely low OLR conditions might induce cell lysis (Takimoto et al., 2018), thus, the proportions of the decreased bacteria (No.1 and No.6) were disappeared by cell lysis and then their dead cells attached to the membrane surface and formed the conditioning film (**Fig. 4.2**). Although *Neisseriaceae* and *Kofleria* sp. in AS community disappeared on 23 and 31 day in both reactors, respectively, the relative abundance of *Neisseriaceae* drastically increased on the middle biofilm. Thus, the drastic increase of *Neisseriaceae* is not simple reason that attachment of dead cell on the membrane surface. It could be considered that unclassified *Neisseriaceae* was one of the pioneer bacteria attached to the membrane surface in the beginning of low OLR conditions and played a crucial role in biofilm development. Unclassified *Neisseriaceae*, a member of Betaproteobacteria, was identified as a key bacteria in biofilm formation (Miura et al., 2007). One species, *Neisseria gonorrhoeae* that belongs to family *Neisseriaceae*, is a known human pathogen and biofilm forming bacteria (Greiner et al., 2005). However, this study was the first time that unclassified *Neisseriaceae* were identified as key player for biofilm formation on the membrane surface for sewage treatment. *Parachlamydia* belongs to class Chlamydiae, which was reported to grow by infecting eukaryotic host cells and major human pathogens (Horn, 2008). As the protozoa, metazoan, and fungi are existed in AS of oxic tank, it is considered that the low OLR condition affects these eukaryotic organisms to cell lysis. In fact, some protozoa cells decreased

during low OLR operations (data not shown). Thus, these parasitic bacteria might increased the abundance on the biofilm to utilize substances, which were released as BAP from eukaryotic organisms and were attached on the membrane surface, in low OLR environment. In addition, it is reported that hygienically relevant microorganisms could reside in biofilms in drinking water distribution networks (Wingender and Flemming, 2011). Therefore, the biofilms in sewage treatment systems might also become suitable microbial habitats for the bacteria. Thus, these facts indicated that *Parachlamydia* sp. was associated with biofilm development and might play an important role in the maturation process of the biofilm. Certain bacteria increased the relative abundance in biofilm such as *Solitalea* sp., *Dechloromonas* sp., and *Kofleria* sp. known as denitrifying bacteria (Li et al., 2015; Ma et al., 2016; Li et al., 2019). Presence of such denitrifiers also suggests that existence of partial anoxic zone inside the biofilm by biofilm maturation. Thus, these denitrifies might be important role on biofilm maturation.

4.5. Summary of chapter 4

In this study, two A/O-MBRs were operated under extremely low OLR conditions and severe membrane fouling was developed in both reactors. In the middle stage of biofilm formation, microcolonies formed by live cells leading permeability deterioration. Unclassified *Neisseriaceae* was most dominant bacteria in middle stage biofilm. The results of this study indicated that specific pioneer bacteria might play a role in forming microcolonies and then triggering further biofilm development. Certain heterotrophic bacteria such as *Parachlamydia* sp. and denitrifiers might be related to biofilm maturation. In conclusion, preventing colonization and growth control of early to middle stage biofilm development could be an effective strategy for mitigation of membrane fouling.

References

Aslam, M., Ahmad, R., Kim, J., (2018). Recent developments in biofouling control in membrane bioreactors for domestic wastewater treatment. Sep. Purif. Technol. 206, 297–315. https://doi.org/10.1016/j.seppur.2018.06.004

Blanpain-Avet, P., Faille, C., Delaplace, G., Bénézech, T., (2011). Cell adhesion and related fouling mechanism on a tubular ceramic microfiltration membrane using Bacillus cereus spores. J. Memb. Sci. 385-386, 200-216https://doi.org/10.1016/j.memsci.2011.09.041

Caporaso, J.G., Kuczynski, J., Stombaugh, J., Bittinger, K., Bushman, F.D., Costello, E.K., Fierer, N., Peña, A.G., Goodrich, J.K., Gordon, J.I., Huttley, G.A., Kelley, S.T., Knights, D., Koenig, J.E., Ley, R.E., Lozupone, C.A., Mcdonald, D., Muegge, B.D., Pirrung, M., Reeder, J., Sevinsky, J.R., Turnbaugh, P.J., Walters, W.A., Widmann, J., Yatsunenko, T., Zaneveld, J., Knight, R., (2010). QIIME allows analysis of high- throughput community sequencing data Intensity normalization improves color calling in SOLiD sequencing. Nat. Methods. 7, 335–336. https://doi.org/10.1038/nmeth0510-335

Caporaso, J.G., Lauber, C.L., Walters, W.A., Berg-Lyons, D., Huntley, J., Fierer, N., Owens, S.M., Betley, J., Fraser, L., Bauer, M., Gormley, N., Gilbert, J.A., Smith, G., Knight, R., (2012). Ultra-high-throughput microbial community analysis on the Illumina HiSeq and MiSeq platforms. ISME J. 6, 1621–1624. https://doi.org/10.1038/ismej.2012.8

Chen, J., Zhang, M., Li, F., Qian, L., Lin, H., Yang, L., Wu, X., Zhou, X., He, Y., Liao, B.Q., (2016). Membrane fouling in a membrane bioreactor: High filtration resistance of gel layer and its underlying mechanism. Water Res. 102, 82–89. https://doi.org/10.1016/j.watres.2016.06.028

Gao, D., Fu, Y., Ren, N., (2013). Tracing biofouling to the structure of the microbial community and its metabolic products: A study of the three-stage MBR process. Water Res. 47, 6680–6690. https://doi.org/10.1016/j.watres.2013.09.007

Greiner, L.L., Edwards, J.L., Shao, J., Rabinak, C., Entz, D., Apicella, M.A., (2005). Biofilm formation by Neisseria gonorrhoeae. Infect. Immun. 73, 1964–1970. https://doi.org/10.1128/IAI.73.4.1964-1970.2005

Gu, Y. Q., Li, T. T., & Li, H. Q. (2018). Biofilm formation monitored by confocal laser scanning microscopy during startup of MBBR operated under different intermittent aeration modes. Process biochemistry, 74, 132-140.

Hatamoto, M., Kaneko, T., Takimoto, Y., Ito, T., Miyazato, N., Maki, S., Yamaguchi, T., Aoi, T., (2017). Microbial community structure and enumeration of Bacillus species in activated sludge. J. Water Environ. Technol. 15, 233–240. https://doi.org/10.2965/jwet.17-037

Horn, M., (2008). Chlamydiae as Symbionts in Eukaryotes . Annu. Rev. Microbiol. 62, 113–131. https://doi.org/10.1146/annurev.micro.62.081307.162818

Hwang, B.K., Lee, C.H., Chang, I.S., Drews, A., Field, R., (2012). Membrane bioreactor: TMP rise and characterization of bio-cake structure using CLSM-image analysis. J. Memb. Sci. 419-420, 33-41.https://doi.org/10.1016/j.memsci.2012.06.031

Hwang, G., Liang, J., Kang, S., Tong, M., Liu, Y., (2013). The role of conditioning film formation in Pseudomonas aeruginosa PAO1 adhesion to inert surfaces in aquatic environments. Biochem. Eng. J. 76, 90–98. https://doi.org/10.1016/j.bej.2013.03.024

Inaba, T., Hori, T., Aizawa, H., Ogata, A., Habe, H. (2017). Architecture, component, and microbiome of biofilm involved in the fouling of membrane bioreactors. npj Biofilms and Microbiomes, 3(1), 1-8.

Judd, S. (2008). The status of membrane bioreactor technology. Trends in biotechnology, 26(2), 109-116.

Li, Y., Zhang, Y., Xu, Z., Quan, X., & Chen, S. (2015). Enhancement of sludge granulation in anaerobic acetogenesis by addition of nitrate and microbial community analysis. Biochemical Engineering Journal, 95, 104-111.

Li, F., An, X., Feng, C., Kang, J., Wang, J., & Yu, H. (2019). Research on Operation Efficiency and Membrane Fouling of A2/O-MBR in Reclaimed Water Treatment. Membranes, 9(12), 172.

Lin, H., Zhang, M., Wang, F., Meng, F., Liao, B.Q., Hong, H., Chen, J., Gao, W., (2014). A critical review of extracellular polymeric substances (EPSs) in membrane bioreactors: Characteristics, roles in membrane fouling and control strategies. J. Memb. Sci. 460, 110–125. https://doi.org/10.1016/j.memsci.2014.02.034

Lorite, G.S., Rodrigues, C.M., de Souza, A.A., Kranz, C., Mizaikoff, B., Cotta, M.A., (2011). The role of conditioning film formation and surface chemical changes on Xylella fastidiosa adhesion and biofilm evolution. J. Colloid Interface Sci. 359, 289-295. https://doi.org/10.1016/j.jcis.2011.03.066

Fortunato, L., Li, M., Chenga, T., Rehman,U, Z., Heidrich,W., Leiknes, T., (2019). Cake layer charachterization in Activated Sludge Membrane Bioreactors: Real-time analysis. J. Memb. Sci. 578, 163-171. https://doi.org/10.1016/j.memsci.2019.02.026

Luo, J., Lv, P., Zhang, J., Fane, A.G., McDougald, D., Rice, S.A., (2017). Succession of biofilm communities responsible for biofouling of membrane bioreactors (MBRs). PLoS One 12, 1–23. https://doi.org/10.1371/journal.pone.0179855

Ma, J., Wang, Z., Li, H., Park, H. D., & Wu, Z. (2016). Metagenomes reveal microbial structures, functional potentials, and biofouling-related genes in a membrane bioreactor. Applied microbiology and biotechnology, 100(11), 5109-5121.

Miura, Y., Watanabe, Y., Okabe, S., (2007). Membrane biofouling in pilot-scale membrane bioreactors (MBRs) treating municipal wastewater: Impact of biofilm formation. Environ. Sci. Technol. 41, 632–638. https://doi.org/10.1021/es0615371

Neoh, C.H., Yung, P.Y., Noor, Z.Z., Razak, M.H., Aris, A., Md Din, M.F., Ibrahim, Z., (2017). Correlation between microbial community structure and performances of membrane bioreactor for treatment of palm oil mill effluent. Chem. Eng. J. 308, 656–663. https://doi.org/10.1016/j.cej.2016.09.063

Sena-Vélez, M., Redondo, C., Graham, J. H., & Cubero, J. (2016). Presence of extracellular DNA during biofilm formation by Xanthomonas citri subsp. citri strains with different host range. PLoS One, 11(6), e0156695.

Sweity, A., Ying, W., Ali-Shtayeh, M.S., Yang, F., Bick, A., Oron, G., Herzberg, M., (2011). Relation between EPS adherence, viscoelastic properties, and MBR operation: Biofouling study with QCM-D. Water Res. 45, 6430-6440. https://doi.org/10.1016/j.watres.2011.09.038

Takada, K., Shiba, T., Yamaguchi, T., Akane, Y., Nakayama, Y., Soda, S., Inoue, D., Ike, M., (2018). Cake layer bacterial communities during different biofouling stages in full-scale membrane bioreactors. Bioresour. Technol. 259, 259–267. https://doi.org/10.1016/j.biortech.2018.03.051

Takimoto, Y., Hatamoto, M., Ishida, T., Watari, T., Yamaguchi, T., (2018). Fouling Development in A/O-MBR under Low Organic Loading Condition and Identification of Key Bacteria for Biofilm Formations. Sci. Rep. 8, 1–9. https://doi.org/10.1038/s41598-018-29821-9

Toyofuku, M., Inaba, T., Kiyokawa, T., Obana, N., Yawata, Y., Nomura, N., (2016). Environmental factors that shape biofilm formation. Biosci. Biotechnol. Biochem. 80, 7–12. https://doi.org/10.1080/09168451.2015.1058701

Vanysacker, L., Boerjan, B., Declerck, P., Vankelecom, I.F.J., (2014). Biofouling ecology as a means to better understand membrane biofouling. Appl. Microbiol. Biotechnol. 98, 8047–8072. https://doi.org/10.1007/s00253-014-5921-2

Vuong, C., Otto, M., (2002). Staphylococcus epidermidis infections. Microbes Infect. 4, 481-489. https://doi.org/10.1016/S1286-4579(02)01563-0

Wingender, J., Flemming, H.C., (2011). Biofilms in drinking water and their role as reservoir for pathogens. Int. J. Hyg. Environ. Health 214, 417–423. https://doi.org/10.1016/j.ijheh.2011.05.009

Yun, M.A., Yeon, K.M., Park, J.S., Lee, C.H., Chun, J., Lim, D.J., (2006). Characterization of biofilm structure and its effect on membrane permeability in MBR for dye wastewater treatment. Water Res. 40, 45-52. https://doi.org/10.1016/j.watres.2005.10.035

Zhang, T., Shao, M.F., Ye, L., (2012). 454 Pyrosequencing reveals bacterial diversity of activated sludge from 14 sewage treatment plants. ISME J. 6, 1137–1147. https://doi.org/10.1038/ismej.2011.188

Ziegler, A.S., McIlroy, S.J., Larsen, P., Albertsen, M., Hansen, A.A., Heinen, N., Nielsen, P.H., (2016). Dynamics of the fouling layer microbial community in a membrane bioreactor. PLoS One 11, 1–14. https://doi.org/10.1371/journal.pone.0158811

Chapter 5

Maintaining microbial diversity mitigates membrane fouling of an anoxic/oxic membrane bioreactor under starvation condition

Yuya Takimoto, Masashi Hatamoto, Toru Soga, Daiki Kuratate, Takahiro Watari and Takashi Yamaguchi (2021). Maintaining microbial diversity mitigates membrane fouling of an anoxic/oxic membrane bioreactor under starvation condition. *Science of the Total Environment*, 759, 143474.

5.1. Background and objectives

MBR has potential as an alternative wastewater treatment system to the conventional activated sludge (AS) process because of its higher nutrient removal efficiency, smaller footprint with high MLSS sludge concentration. The MBR is one of the most innovative biological system for municipal wastewater treatment. However, membrane fouling development remains a main obstacle for sing larger-scale MBR plants. Membrane fouling development by an extracellular polymeric substance (EPS) and soluble microbial product (SMP), which are largely known as cause of primary membrane fouling, has been investigated in several MBRs under various conditions (Johir et al., 2011; Nguyen et al., Yigit et al., 2008; Yao et al., 2011). Besides, biomass associated product (BAP) and utilization associated product (UAP) of SMPs have been identified as essential byproducts in mixed liquor of MBR and contributed membrane fouling development (Jiang et al., 2010; Jacquin et al., 2018; Shi et al., 2018). EPS macro-molecules, which are loosely bound to the AS, are crucial for membrane fouling as they accumulate on a membrane surface (Wang and Wu, 2009; Wang et al., 2009). Previous studies indicated that the degradation of a higher molecular weight organic matter into lower molecules effectively mitigates membrane fouling (Huang et al., 2008; Wei et al., 2016; Zhou et al., 2016). Thus, a simple way to mitigate membrane fouling is to degrade and reduce macro-molecules into micro-molecules that can easily pass through the membrane pores.

Several studies have focused on microbial communities and key players in the AS of MBR involving EPS or SMP production and membrane fouling development with biofilm formation under various conditions (Ma et al., 2013a; Gao et al., 2013; Gao et al., 2014; Guo et al., 2015; Neoh et al., 2017). Recently, a few reports compared the difference of microbial consortium and dynamics between the AS and membrane biofilm in MBR (Takimoto et al., 2018; Takada et al., 2018). These studies have identified significant differences in the microbial consortium between the AS and the biofilm or cake layer on the membrane in a reactor. Moreover, candidate phyla radiation (CPR) group and Firmicutes are dominant in the biofilm or cake layer. However, these phyla are minority in a bulk sludge, indicating that the bacteria are relevant to development of a biofouling layer on the membrane surface.

In contrast, some studies reported that membrane fouling development attributed to AS microbial community structures (Ma et al., 2013b; Sepehri and Sarrafzadeh, 2018; Liu et al., 2019). Enrichment of nitrifiers in the microbial community of AS mitigated membrane fouling

(Sepehri and Sarrafzadeh, 2018). Moreover, Chloroflexi played an important role in mitigating membrane biofouling in MBRs because they contributed degradation of SMPs and cell materials (Miura et al., 2007; Watanabe et al., 2017). Thus, the results of previous studies suggest that there is an appropriate composition of microbial community in MBRs for fouling mitigation. There has been limited information on the critical bacteria responsible for maintaining homeostasis against endogenous SMP productions and membrane fouling. Certain bacteria responsible for fouling could be identified by increasing abundance during membrane fouling, however, the behavior of specific members responsible for membrane fouling mitigation is still unknown.

Previously, an operation of MBR under prolonged starvation condition induced microbial cell lysis and SMP production, leading to biofilm growth on the membrane surface and severe membrane biofouling (Palmarin et al., 2020; Takimoto et al., 2018). We got inspired by these reports and thought about the use of starvation conditions, which could be useful for membrane fouling research. The aim of chapter 5 was to evaluate the contribution of dissolved organic carbon (DOC) and microbial community dynamics to membrane fouling development for an endogenous respiration of MBR. Here, we operated anoxic/oxic (A/O)-MBRs under prolonged starvation conditions at three times to reveal microbial-driven fouling mechanisms and to explore the important players in the AS of fouled and fouling-mitigated AO-MBRs.

Table 5.1 Characteristics of the influent sewage during starvation conditions in each reactor

Parameters	Unit	H1	H2	L
pH	-	6.7 ± 0.1	6.6 ± 0.1	6.8 ± 0.1
DO	mg/L	0.1 ± 0.1	0.2 ± 0	1.0 ± 0.4
$sCOD_{cr}$	mg/L	163 ± 45	162 ± 24	111 ± 22
TN	mg-N/L	29 ± 8	28 ± 2	20 ± 5
TP	mg-P/L	2.6 ± 0.5	3.3 ± 0.4	1.8 ± 0.5
NH_4^+	mg-N/L	22 ± 6	32 ± 12	17 ± 4

5.2. Materials and methods

5.2.1. A/O-MBR operations

The laboratory-scale A/O-MBR systems have already been described in our previous study (Takimoto et al., 2018). It consisted of a 6 L of anoxic tank and a 6 L of aerobic tank. All MBRs were operated in duplicate under same operational parameters (initial mixed liquor suspended solids (MLSS) concentrations, hydraulic retention time (HRT), solid retention time (SRT)) in different seasons: 2017 summer (H1 #1, #2), 2017 winter (L #1, #2) and 2018 summer (H2 #1, #2). A flat sheet membrane (chlorinated polyvinyl chloride: CPVC) of 0.20 μm mean pore size (KUBOTA, Osaka, Japan) and with a filtration area of 0.11 m^2 was used. Air at 5 L/min was supplied by a diffuser at the bottom of a reactor. Internal recycling of anoxic and aerobic sludge was conducted to remove the nitrite. Municipal sewage wastewater after sedimentation was used as the influent into the anoxic tank. **Table 5.1** shows the characteristics of influent sewage. Conventional AS that the initial concentration of mixed liquor solids concentration was approximately 4000 mg/L taken from a sewage treatment facility was inoculated in each MBR. Each reactor was operated under the following conditions: a membrane suction cycle of 9 min on and 1 min off was adopted and an average operating membrane flux of 11.8 $L \cdot m^{-2} \cdot h^{-1}$ (LMH).

All reactors (H1 #1, #2; H2 #1, #2; L #1, #2) were operated for more than one month under standard HRT conditions of 8.0 hours with 60 days of SRT to stabilize the reactor performance and acclimatization of the microbial community. Under standard conditions, the average organic loading rate (OLR) was 0.42 kg-chemical oxygen demand (COD)$\cdot m^{-3} \cdot day^{-1}$, and the average soluble COD and total nitrogen (TN) removal efficiencies in all reactors were 86 ± 1% and 60 ± 15%, respectively. Until starvation conditions, the membrane in the aerobic tank were physically washed using sponges with ultra-pure water or replaced by a new membrane. The average transmembrane pressure (TMP) and flux were 6.1 ± 2.6 kPa and 12.3 ± 1.2 LMH, respectively, during the starting of a starvation condition for each reactor.

Starvation operations were then started in all MBRs to develop the membrane fouling. To induce membrane fouling, the permeate effluent of the reactors was supplied into the anoxic tank instead of influent sewage to generate a low OLR starvation condition. And 200 mL of sewage wastewater was fed as an influent to compensate for the 200 mL of AS sample taken daily from the aerobic tank, accounting for approximately 0.002 kg-COD$\cdot m^{-3} \cdot day^{-1}$. In this study, day 1 was

defined as the first day of starvation conditions in all reactors. H1, H2, and L reactors were operated at 26.2 ± 0.5°C, 26.0 ± 0.9°C, and 12.1 ± 0.9°C, respectively, during starvation.

5.2.2 Analytical methods

Temperature and dissolved oxygen (DO) of the AS in the aerobic tank were determined using a DO meter (DM-32P, TOA DKK, Tokyo, Japan). The permeate flow rate was measured by a measuring cylinder for 30 min. TMP was measured using a pressure transducer (ZSE50F, SMC, Tokyo, Japan) set in the permeate line. Soluble CODcr, TN and total phosphorus (TP) of samples were determined using a water-quality analyzer (DR2800, Hach, Loveland, CO, USA). MLSS and mixed liquor volatile suspended solids (MLVSS) were determined using APHA standard methods. DOC (soluble TOC) concentrations were determined using a TOC analyzer (TOC-V CSN, SHIMADZU, Kyoto, Japan). Soluble samples were filtered by 0.22 μm filter paper.

5.2.3 Biofilm sampling and 16 S rRNA gene sequencing

After membrane fouling development in H2 and L reactors (H2: TMP: 68.4 (#1) and 59.0 kPa (#2) on day 30, L: TMP: 88.9 (#1) and 89.9 kPa (#2) on day 23), a severe fouled membrane were taken from the aerobic tank and the membrane surface was rinsed with ultra-pure water to remove the AS loosely attached to the membrane. A tightly bonded biofilm on the membrane has been obtained and used as a biofilm sample. Samples were immediately stored at −20 °C.

For microbial community analysis, AS of the aerobic tank and biofilm samples were used. DNA was extracted from each sample using FastDNA Spin Kit for Soil (MP Biomedicals, Santa Ana, CA, USA) and following instructions from the manufacturer. The microbial 16S rRNA genes of each sample were amplified using universal forward (Univ515F: 5′-GTGCCAGCMGCCGCGGTAA-3′) and reverse (Univ806R: 5′-GGACTACHVGGGTWTCTAAT-3′) primers. The conditions of PCR amplification were as follows: one cycle of 94 °C (3 min), 25 cycles of 94 °C (45 s), 50 °C (60 s) and 72 °C (90 s), and a final cycle of 72 °C (10 min). The products were purified using a QIAquick PCR Purification Kit (QIAGEN, Hilden, Germany). The 16S rRNA gene sequencing of purified products was performed as described by Caporaso et al. (2012). DNA sequencing was performed using a MiSeq Reagent Kit v2 and the MiSeq System (Illumina Inc., San Diego, CA, USA).

5.2.4. Data analysis

Sequences were processed using Quantitative Insights Into Microbial Ecology (QIIME) version 1.9.1 (Caporaso et al., 2010). Operational taxonomic units (OTUs) clustering at 97% of identity were collected using UCLUST. Taxonomic classifications were determined using the Greengenes database ver. 13_8 and BLAST searches in the National Center for Biotechnology Information (NCBI) (http://blast.ncbi.nlm.nih.gov/Blast.cgi). The Venn diagrams of microbial communities of AS samples were constructed using Venny 2.1.0 online tool (https://bioinfogp.cnb.csic.es/tools/venny/). The microbial community structure changes in the AS and biofilm samples were evaluated by a plot of principal component analysis (PCA), visualized by using Sequence Tag-based Analysis of Microbial Population dynamics (STAMP) software. Raw sequence data obtained in this study were deposited in the DDBJ Sequence Read Archive (DRA) with an accession number of DRA010111.

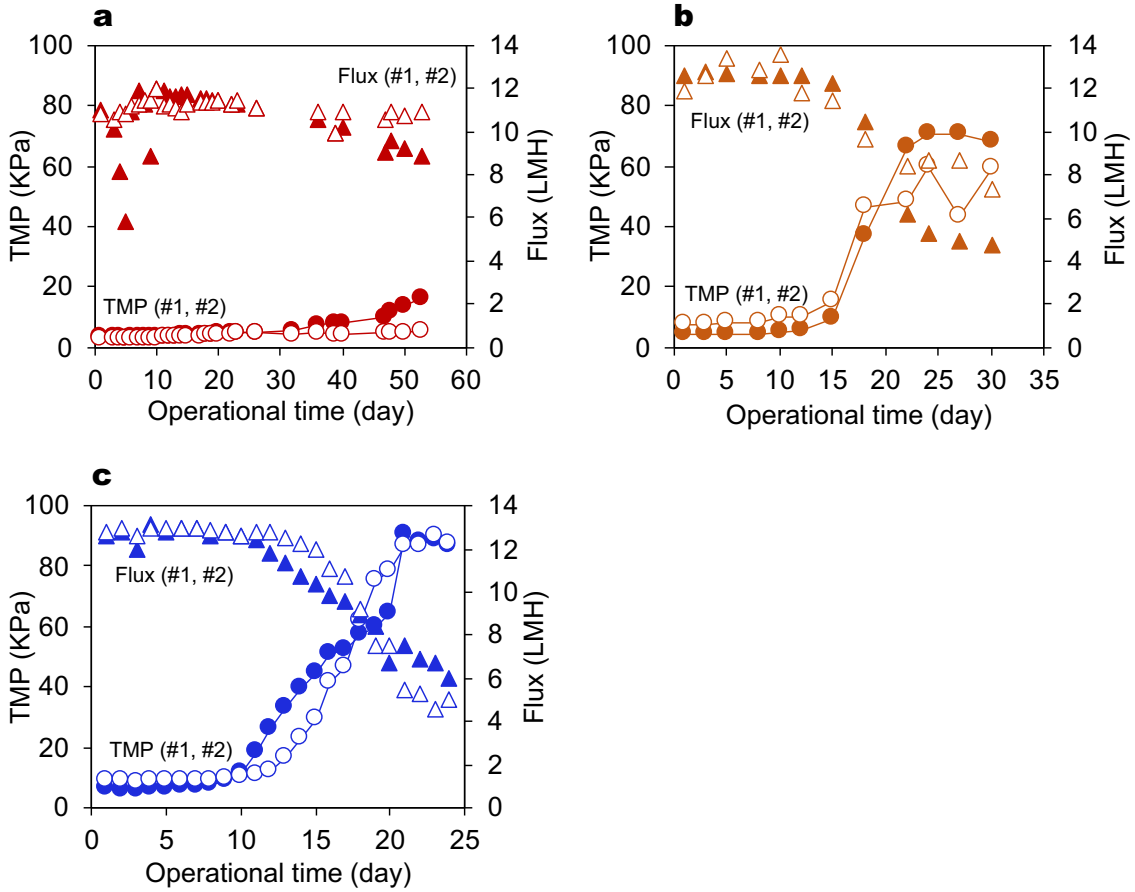

Fig. 5.1 TMP and flux profiles of a) fouling-mitigated H1 (#1, #2), b) fouled H2 (#1, #2), and c) fouled L (#1, #2) reactors during starvation conditions. Filled and open circles indicate TMP transition of #1 and #2, respectively. Filled and open triangles indicate a flux transition of #1 and #2, respectively.

5.3. Results

5.3.1. Membrane fouling development in H2 and L reactors and fouling mitigation in H1 reactor

The progression of fouling in each reactor was evaluated by monitoring an TMP increase and a flux decline (**Fig. 5.1**). In H2 and L reactors, TMP started to increase, and flux decreased from day 15 and 10 onwards under starvation conditions, respectively. Subsequently, TMP reached at 65.9 kPa (#1) and 48.2 kPa (#2) on day 22 in H2 reactor, and 64.3 kPa (#1) and 78.3 kPa (#2) on day 20 in L reactors, respectively. Visible biofilm formation on the membrane in both MBRs was observed; however, it could not be removed by physical water treatment, suggesting that severe membrane fouling had developed in H2 and L reactors.

In contrast, in H1 reactor, TMP increased on day 53 (#1: 16.1, #2: 5.7 kPa) under starvation conditions. Furthermore, the visible biofilm could not be observed on the membrane surface, resulting in a mitigation in membrane fouling of H1 reactor even under starvation conditions.

TN and TP concentrations increased in the aerobic tank of all reactors after starting starvation conditions (**Fig. 5.2**). After TP concentrations reached 76 (#1) and 110 mg/L (#2) on days 17 and 10, respectively, the concentrations became stable in H1 and H2 reactor. Conversely, TN and TP concentrations continuously increased in L reactor during the condition. However, MLSS and MLVSS concentrations decreased in all reactors during starvation conditions (**Fig. 5.3**). Initially, TMP increased in H2 and L reactors (R2: day 15, L: day 11) by decreasing MLSS concentrations from 2900 to 3000 mg/L. In H1 reactor, the MLSS concentrations decreased from an initial value and reached 2700 mg/L on day 22. The sCOD removal rates for H1, H2, and L reactors were 63 ± 21%, 67 ± 12%, and 66 ± 12%, respectively, during starvation conditions (data not shown). DOC in the supernatant AS and permeate effluent showed different behavior between all reactors (**Fig. 5.4**). The DOC concentrations in the AS supernatant increased in all reactors with starvation conditions, whereas the DOC concentration of effluent was constant in the fouled L reactor (**Fig. 5.4c**). In the fouled H2 reactor, the difference between DOC concentration of AS supernatant and effluent (ΔDOC) increased to 20.1 mg/L on day 18, corresponding to an increase of TMP to 41.8 kPa. Conversely, the DOC concentration of effluent in the fouling-mitigated H1 reactor increased, reflecting the DOC concentration of the AS supernatant in this reactor (**Fig. 5.4a**). In the end of the operation of H1 reactor, ΔDOC started to rise from day 36.

The fouled H2 and L reactors showed similar DO behavior; at the beginning of a starvation operation, DO concentrations were rapidly increased and became stable in each reactor at even

different temperatures (**Fig. 5.5b and c**). In contrast, in the fouling-mitigated H1 reactor, DO concentration was unstable and decreased during a starvation operation (**Fig. 5.5a**).

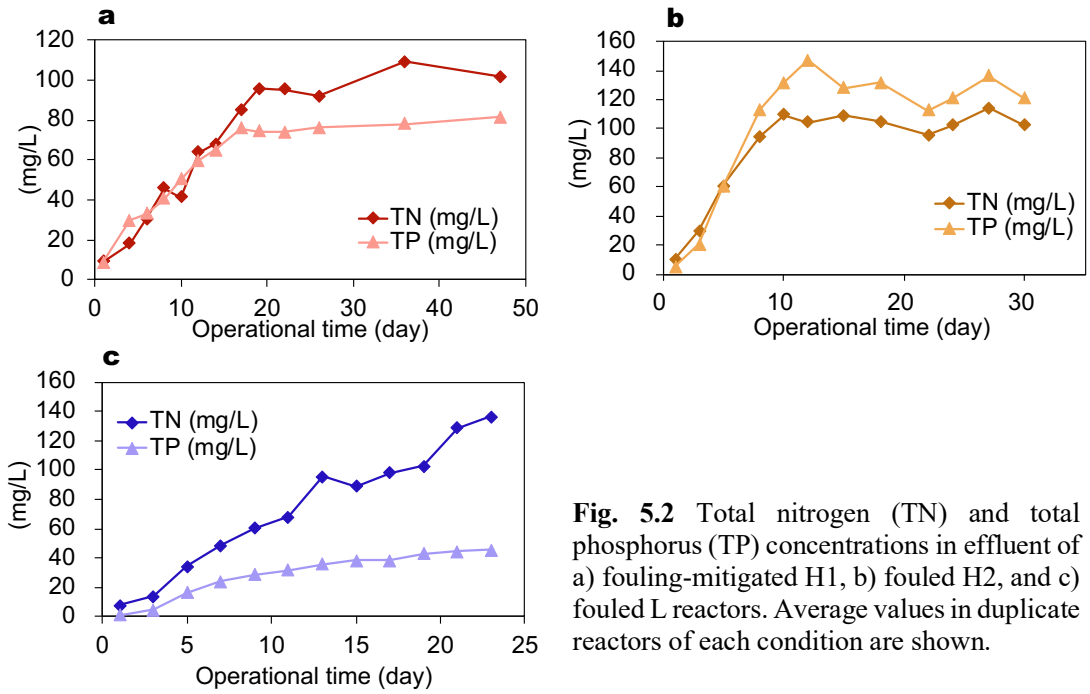

Fig. 5.2 Total nitrogen (TN) and total phosphorus (TP) concentrations in effluent of a) fouling-mitigated H1, b) fouled H2, and c) fouled L reactors. Average values in duplicate reactors of each condition are shown.

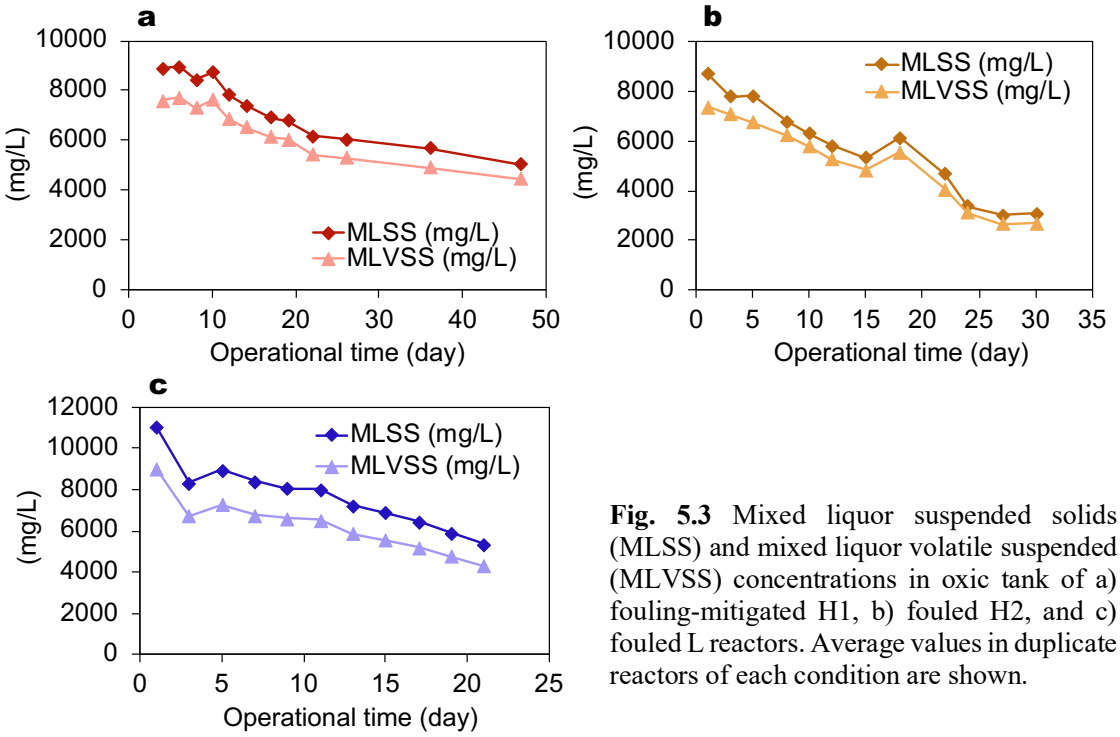

Fig. 5.3 Mixed liquor suspended solids (MLSS) and mixed liquor volatile suspended (MLVSS) concentrations in oxic tank of a) fouling-mitigated H1, b) fouled H2, and c) fouled L reactors. Average values in duplicate reactors of each condition are shown.

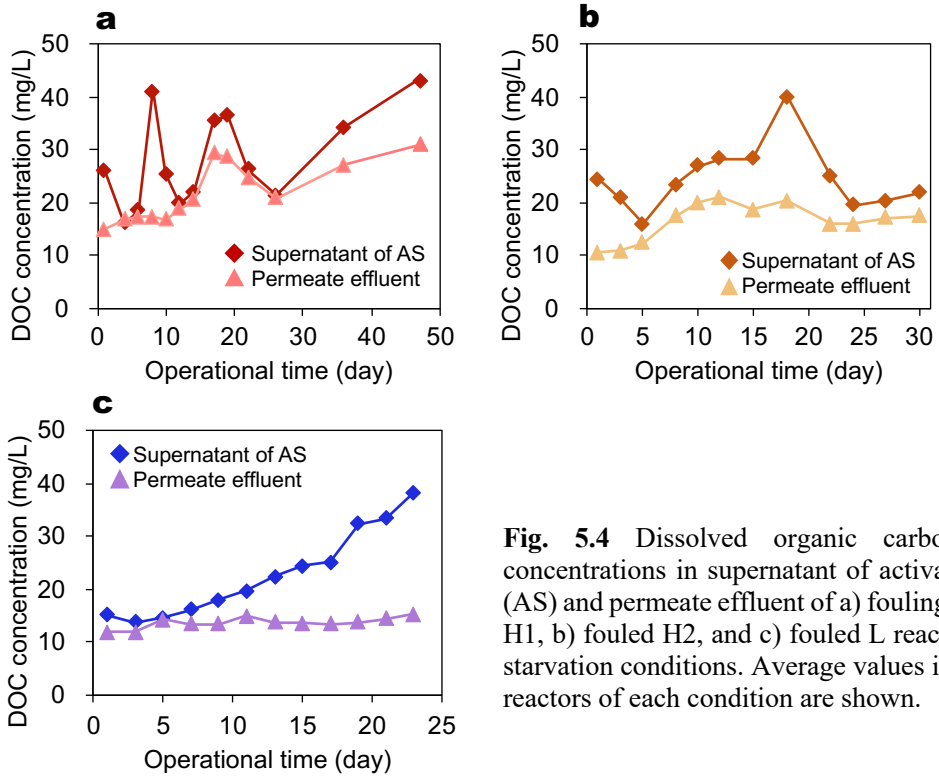

Fig. 5.4 Dissolved organic carbon (DOC) concentrations in supernatant of activated sludge (AS) and permeate effluent of a) fouling-mitigated H1, b) fouled H2, and c) fouled L reactors during starvation conditions. Average values in duplicate reactors of each condition are shown.

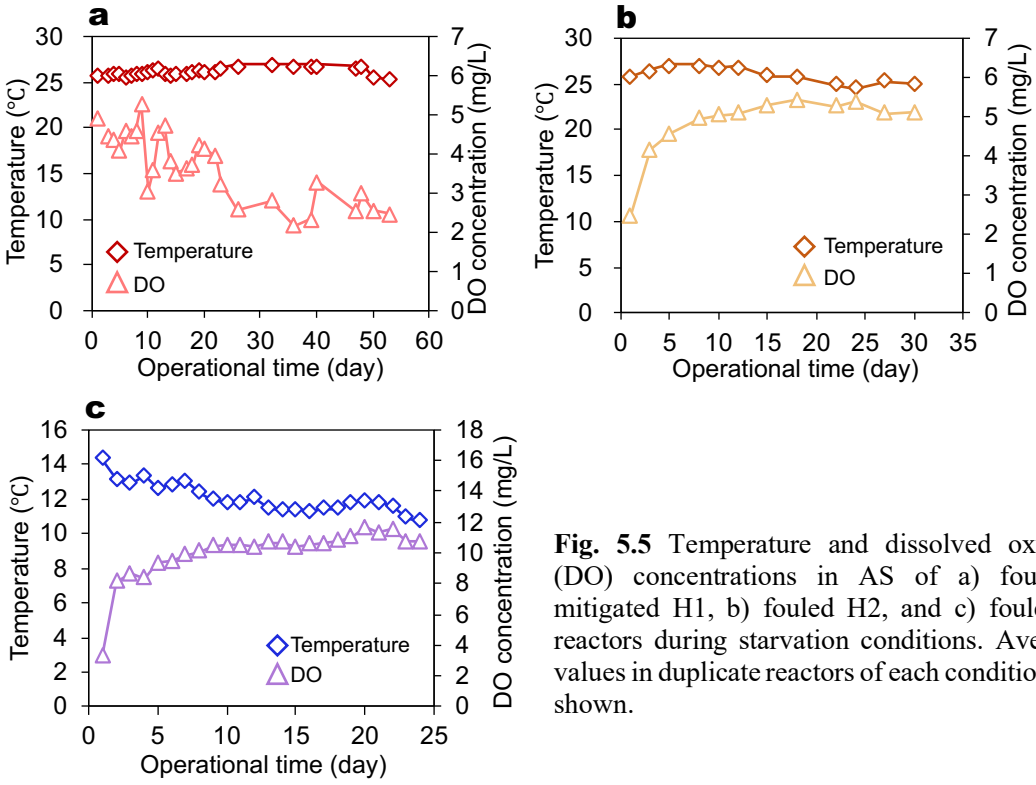

Fig. 5.5 Temperature and dissolved oxygen (DO) concentrations in AS of a) fouling-mitigated H1, b) fouled H2, and c) fouled L reactors during starvation conditions. Average values in duplicate reactors of each condition are shown.

5.3.2. Comparison of microbial community in AS and biofilm

The results of microbial community analysis in AS and biofilm during operation under each condition showed that Proteobacteria and Bacteroidetes were the dominant phyla and were continuously present in all samples (**Fig. 5.6**). There were significant differences in community structures between AS and biofilm in H2 and L reactors, where fouling occurred (**Fig. 5.7b and c**). Interestingly, uncultured TM6 (#1; 13.2% and #2; 25.4% in H2 reactor) and OD1 (#1; 18.8% and #2; 7.2% in L reactor) were the predominant phyla in the biofilm on the membrane surface of H2 and L reactors, respectively. The relative abundance of Chlamydiae in biofilm of H2 and L reactors was higher than that in the AS of each reactor. In the AS of H1 and H2 reactors, relative abundances of Betaproteobacteria, Deltaproteobacteria, Bacteroidetes, Chlorobi, and Nitrospirae decreased from day 8 to day 22. However, relative abundances of Gammaproteobacteria, Firmicutes, Acidobacteria, Armatimonadetes increased from days 8–22 in the AS of H1 and H2 reactors, whereas Chloroflexi increased in abundance only in H1 reactor. The relative abundances of Deltaproteobacteria and Bacteroidetes were marginally decreased in the AS of L reactor.

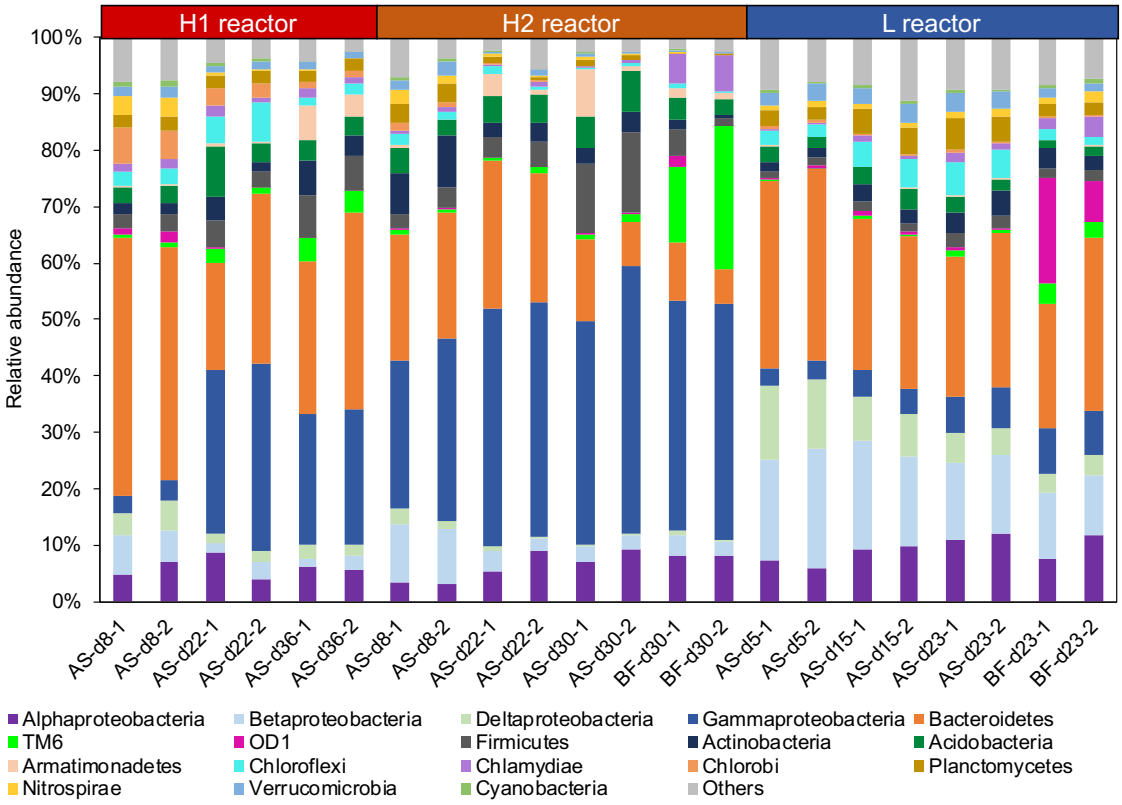

Fig. 5.6 Microbial community structures of activated sludge (AS) in aerobic tank and biofilm (BF) on membrane surface in each reactor during starvation conditions.

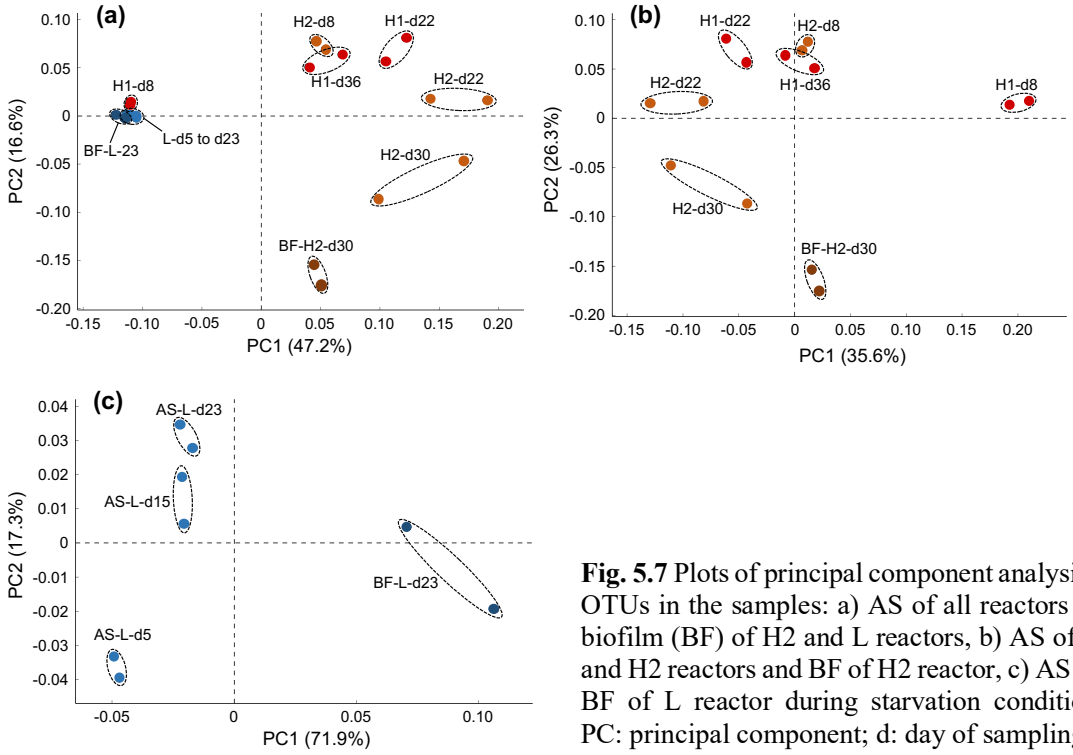

Fig. 5.7 Plots of principal component analysis of OTUs in the samples: a) AS of all reactors and biofilm (BF) of H2 and L reactors, b) AS of H1 and H2 reactors and BF of H2 reactor, c) AS and BF of L reactor during starvation conditions. PC: principal component; d: day of sampling.

5.3.3. Comparison of AS microbial communities among H1, H2 and L reactors

Changes in the top 30 OTUs detected in AS samples of all reactors are shown in **Table 5.2**. Four OTUs (Nos. 15, 16, 25 and 26) gradually decreased during starvation operations in the fouled L reactor. The remaining OTUs were present at low abundance in the AS of L reactor compared to those in H1 and H2 reactors. Although the microbial community structure of the AS in L reactor was stable, the communities in AS of H1 and H2 reactors changed drastically during the starvation operation (**Fig. 5.7a**). The change in abundance of the top 30 OTUs in AS of H1 and H2 reactors was divided into three groups (population I, II, and III) based on the changes in directions: population I had a relative abundance, which constantly decreased during starvation condition; population III had a relative abundance, which constantly increased during the condition; and population II had a stable the relative abundance, as compared to populations I and III (**Figs. 5.8 and 5.9**).

Population I drastically decreased during starvation conditions in which 11 OTUs (Nos. 3, 8, 15, 16, 19, 21, 23, 24, 25, 26, and 28) and 12 OTUs (Nos. 3, 8, 10, 11, 15, 16, 19, 21, 23, 24,

26, and 28) in H1 and H2 reactors, respectively. The total percentage of population I decreased from 30.4% (day 8) to 1.3% (day 36) in H1 reactor and from 17.9% (day 8) to 0.6% (day 30) in H2 reactor. 77% of total OTUs, which belonged to population I, shared between H1 and H2 reactors (**Fig. 5.10a**).

Population II increased after starting the starvation condition and then decreased or remained relatively stable during prolonged starvation operation (**Figs. 5.8 and 5.9**). Seven OTUs (Nos. 1, 2, 6, 11, 14, 17, and 20) and 10 OTUs (Nos. 1, 4, 5, 6, 7, 17, 18, 20, 22, and 29) were included in population II in H1 and H2 reactors, respectively. The total percentage of population II increased from 1.5% (day 8) to 34.9% (day 22) and then dropped to 17.5% (day 36) in H1 reactor. In H2 reactor, the percentage increased from 23.7% (day 8) to 53.1% (day 22) and then dropped to 29.6% (day 30).

Population III continuously increased even in prolonged starvation operation, and 12 OTUs (Nos. 4, 5, 7, 9, 10, 12, 13, 18, 2, 27, 29, and 30) and 7 OTUs (Nos. 2, 9, 12, 14, 20, 27, and 30) were detected in H1 and H2 reactors, respectively. The total percentage of population III increased from 1.5% (day 8) to 7.1% (day 14) in H1 reactor and from 2.2% (day 8) to 9.9% (day 15) in H2 reactor, respectively. The increasing trend showed a remarkable effect from day 22 in both reactors.

Table 5.3 shows alpha diversity indices of 3600 reads extracted from all DNA sequences of each AS sample. The Shannon index value decreased from day 8 to day 22, respectively, by 15% and 24% on average for AS in H1 and H2 reactors. The Chao1 index values also decreased by 30% and 47% on average for H1 and H2 reactors, respectively, from day 8 to day 22. All indices decreased over time in both reactors. However, H1 reactor had the higher microbial diversity (**Table 5.3**). On the other hand, the diversity indices in L reactor increased slightly with the operational term.

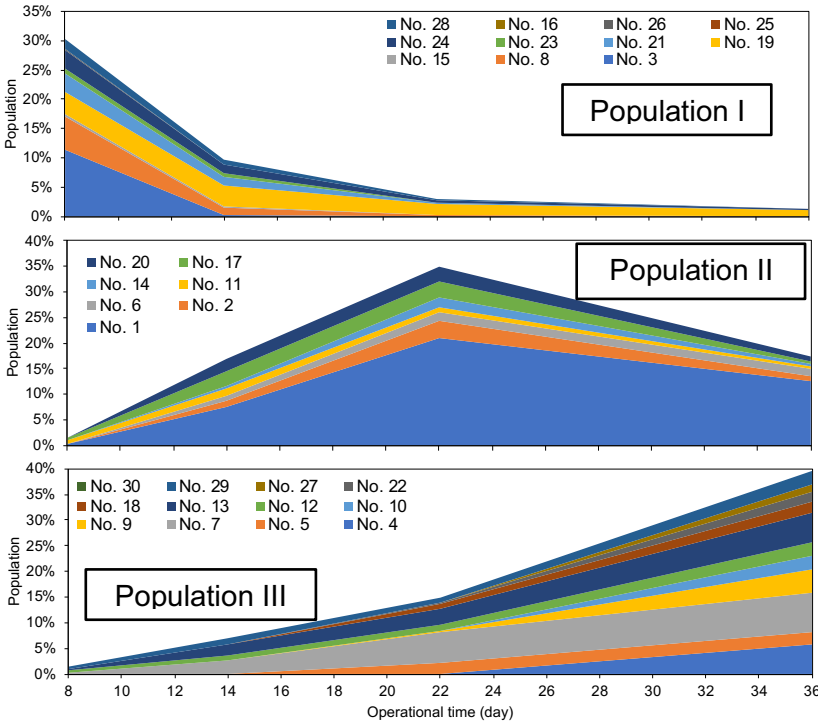

Fig. 5.8 Changes in OTUs of different populations in the AS of fouling-mitigated H1 reactor. Average values in duplicate reactors of each condition are shown.

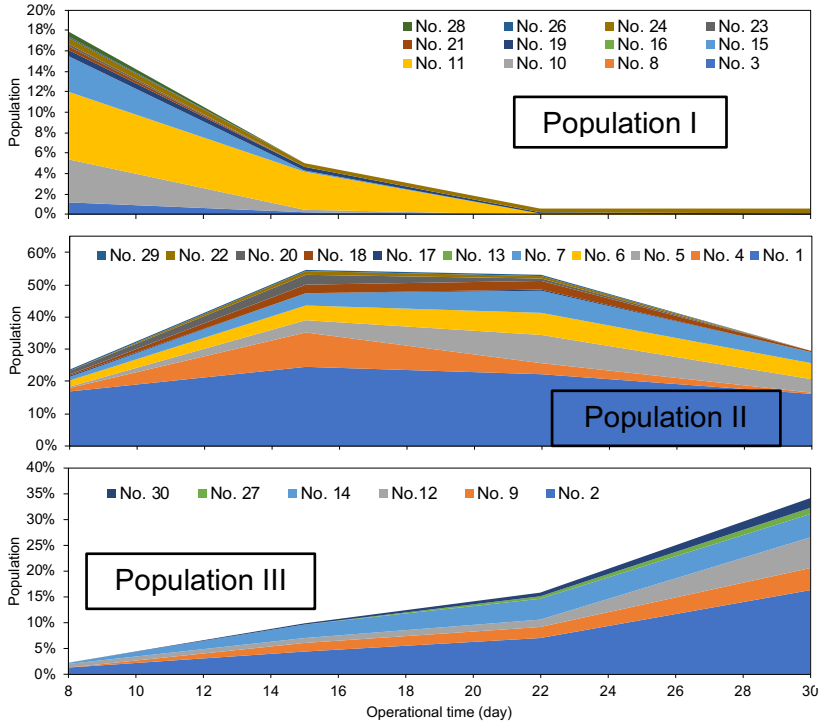

Fig. 5.9 Changes in OTUs of different populations in the AS of fouled H2 reactor. Average values in duplicate reactors of each condition are shown.

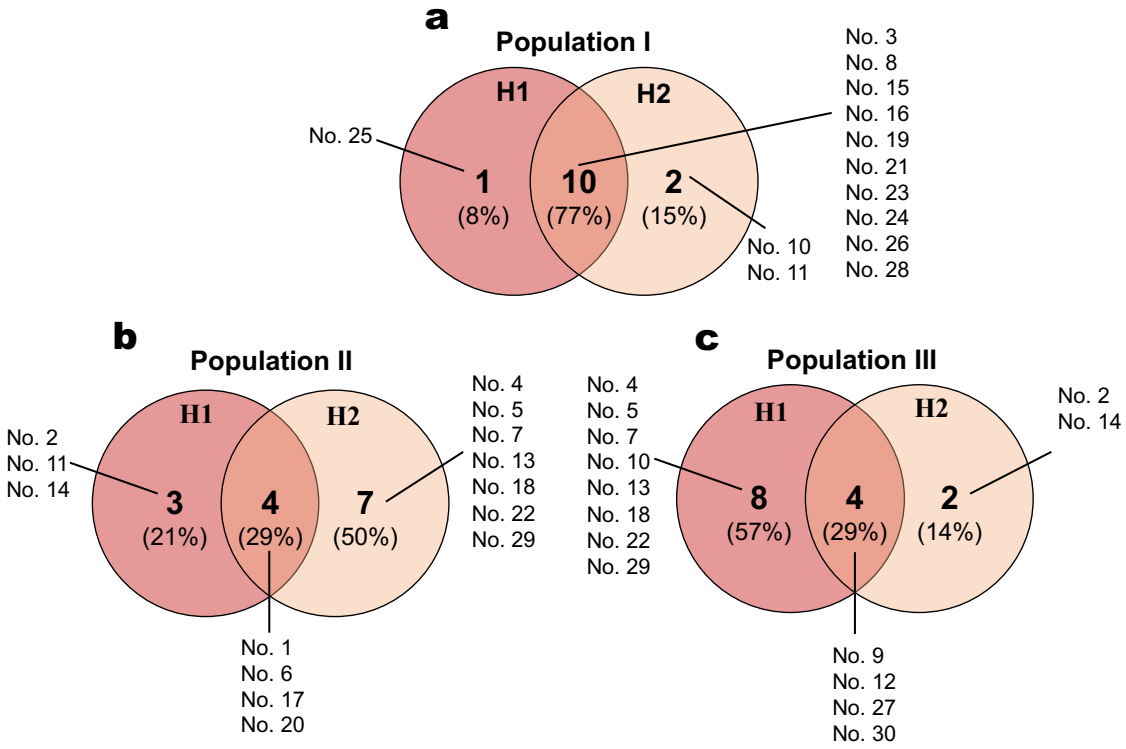

Fig. 5.10 Venn diagram between OTUs of H1 and H2 reactors in a) population I, b) population II, and c) population III. Average values in duplicate reactors of each condition are used

5.4. Discussion

5.4.1. Reactor performances in terms of fouling development and mitigation

An extremely low OLR starvation condition rapidly induced membrane fouling over a short period (two weeks) in our previous study (Takimoto et al., 2018) even under standard flux operations (11.8 LMH). In the present study, increasing TN and TP concentrations of effluent and decreasing MLSS concentrations of all MBRs suggested that starvation conditions induced fast and severe membrane fouling through the development of cell-lyse-derived SMPs (BAP). Previous studies have shown that when an influent COD was limited, the sludge microorganisms might release more SMPs under starvation conditions (Shen et al., 2012). In the present study, cell decay substances have been released from microbial cell walls affected by extremely low food to microorganism ratio conditions, resulting in fast and severe membrane fouling development. The rapid increase in TP and decrease of MLSS concentration in H2 reactor suggests severe microbial lysis, releasing more BAP.

The DOC concentration in the AS supernatant increased in all reactors (**Fig. 5.4**), suggesting a release of endogenous organic substances from microbial cell bodies under starvation conditions, as mentioned above. While the DOC concentration of effluent was stable for fouled H2 and L reactors, the DOC concentration of the fouling-mitigated H1 reactor followed that of the AS supernatant (**Fig. 5.4a**). The DO and DOC transitions suggested that an extremely low food to microorganism ratio decreased the microbial activities; thus, endogenous substances, which could be released by cell lysis, were not degraded and then accumulated in fouled H2 and L reactors. In contrast, the fouling-mitigated H1 reactor maintained some aerobic microbial activity and degraded the large molecules of endogenous substances into smaller molecules that could pass through the membrane pore. The difference in DOC concentration between the AS supernatant and permeate effluent suggested that size exclusion was a major fouling mechanism. Besides, a larger molecule (>100 kDa) was retained in an aerobic tank in earlier reports (Zhao et al., 2010; Shen et al., 2012). Teng et al. (2020) also suggested that large molecules (>100 kDa) has potential for making cross-linking structure and gelation on the membrane surface. Under lower OLR (approximately 0.06 g-COD·g-MLSS^{-1}·day^{-1}), although the SMP concentrations were lower than high OLR condition (approximately 0.13 g-COD·g-MLSS^{-1}·day^{-1}), protein-like and large sized substances were more abundant (Maqbool et al., 2017). The results suggested that the endogenous substances were relatively large molecules (i.e. biopolymer) as BAP and had higher membrane retention. Thus, the larger molecules might be main components of BAP and cause membrane fouling development. In addition, the present study showed that the behavior of DOC and DO was significant in predicting fouling development. In other words, fouling development could be predicted by monitoring the difference between the DOC concentrations in AS supernatant and permeate effluent (ΔDOC), which was negatively correlated with permeability in fouled H2 and L reactors (**Fig. 5.11**). Even in H1 reactor, increase of ΔDOC concentration on day 47 might affect TMP rise from the day. Under the same starvation conditions to induce membrane fouling development in all MBRs, only H1 reactor mitigated fouling development. Thus, we presumed that microbial community structures might be different in each reactor and the fouling-mitigated H1 reactor holds specific bacterial communities, which was supposed to degrade a DOC component. And thus, we have compered the microbial community structures as discussed below section 5.4.3. in depth.

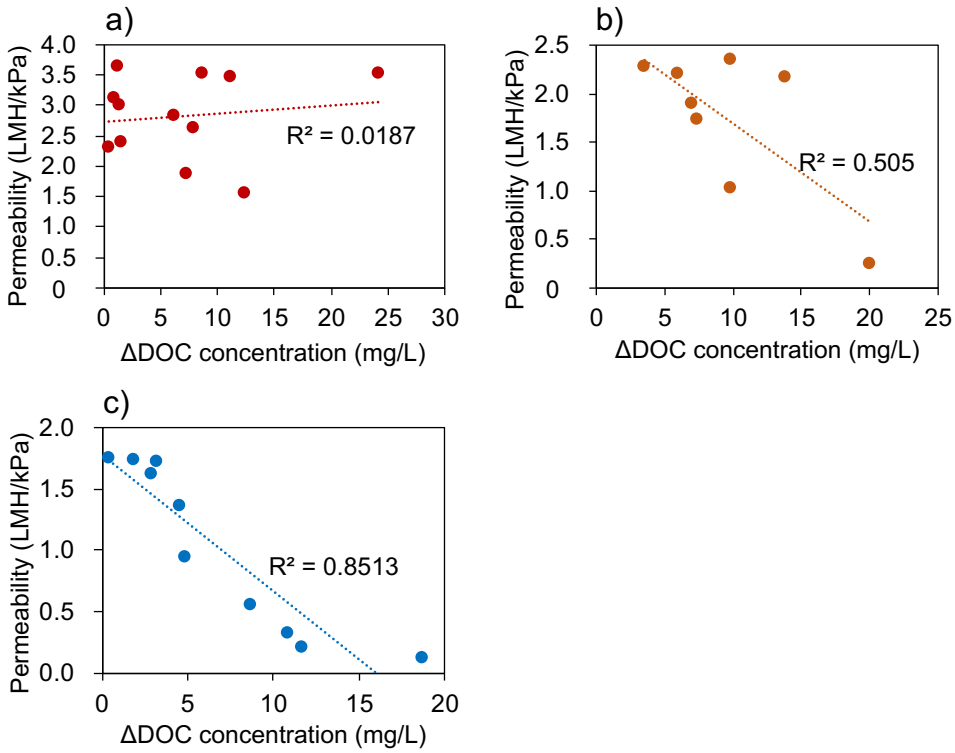

Fig. 5.11 Correlation between permeability and ΔDOC concentrations of a) fouling-mitigated H1, b) fouled H2, and c) fouled L reactors during membrane fouling development under starvation conditions. ΔDOC indicates the difference between DOC concentrations of supernatant AS and permeate effluent. Average values in duplicate reactors of each condition are shown.

5.4.2. Microbial community of AS and biofilm in fouled H2 and L reactors

PCA analysis has shown the changes in AS and biofilm microbial communities based on OTUs (**Fig. 5.7**). Microbial community structures of the AS and biofilm in L reactor were almost stable during starvation operation; however, substantial changes were observed in the AS communities of H2 reactor (**Fig. 5.7a**). There was a significant difference between the AS and biofilm microbial community structure in H2 reactor, whereas no significant difference was observed for L reactor (**Fig. 5.6 and Fig. 5.7b and c**). Both biofilms were composed of uncultured phyla of TM6, OD1 and Chlamydiae bacteria. These results suggested that temperature conditions with seasons did not affect the biofilm development and microbial communities of biofilm. Since the accumulated DOC might create the same environment on the membrane surface, similar microbial communities were developed in H2 and L reactors. Several previous studies have reported that uncultured TM6 and OD1 bacteria were predominant in membrane attached samples and that Chlamydiae was found to be twice the relative abundance at an early stage of biofilm formation

than in AS (Takimoto et al., 2018; Neoh et al., 2016; Rehman et al., 2020). In this study, these phyla probably played an important role in biofilm development.

Under low temperature conditions in L reactor, AS microbial communities did not change substantially; however, MLSS decreased, suggesting that almost all AS bacteria were influenced and lysed by starvation conditions. Moreover, the accumulated DOC in AS was not degraded as the microbial community could not adapt to a prolonged starvation environment due to low temperature. As a result, a lower activity of the AS microbial community does not cause any shift of microbial diversity indices in the L reactor (**Table 5.3**).

5.4.3. Comparison of AS microbial community between fouling-mitigated H1 and fouled H2 reactors

The populations of Gammaproteobacteria, Firmicutes, Acidobacteria, and Armatimonadetes increased under starvation conditions, and these trends were comparable between H1 and H2 reactors; however, the output of the reactor differed considerably in terms of the fouling development. The difference between the AS microbial communities of H1 and H2 reactors was primarily reflected by the phylum Chloroflexi. The population of Chloroflexi increased from day 8 (2.4% in #1, 2.8% in #2) to day 22 (4.9% in #1, 7.1% in #2) and then decreased to day 36 (1.2% in #1, 2.0% in #2) in the AS of H1 reactor, whereas in H2 reactor, the population (day 8; 1.9% in #1, 1.0% in #2) was stably low during starvation operation. Chlorofexi are frequently detected in AS of MBR and are considered to contribute to the degradation of SMPs and cell material (Miura et al., 2007; Watanabe et al., 2017).

The decrease in abundance of the population I have suggested that bacteria have been lysed or negatively influenced by starvation conditions. As a result, these bacteria might be the source of SMPs that led to fouling development in both H1 and H2 reactors. Furthermore, some BAP components derived from cell lysis might be used as carbon sources for ordinary heterotrophic bacteria in populations II and III.

The increase in abundance of population III has suggested that bacteria have been well adapted for prolonged starvation conditions and could utilize the BAPs. OTUs belonging to family *Chitinophagaceae* (OTUs Nos. 5, 7, 13, and 22) were dominant and unique OTUs of population III found in H1 reactor (**Fig. 5.10c**). The *Chitinophagaceae* were reported as quorum sensing bacteria (Hong et al., 2019) and might play a role in membrane fouling (Xiong et al.,

2015). However, they also had the potential for chitin hydrolysis (Kämpfer et al., 2011). Moreover, researchers have shown that the *Chitinophagaceae* family acted as a hydrolyzer of SMP, BAP, and EPS (Szabó et al., 2017); thus, the family might be able to degrade BAPs derived from a microorganism (not only bacteria but also fungi) in H1 reactor. Conversely, *Xanthomonadaceae* (OTU No. 2) was detected as a unique and dominant OTU in population III of H2 reactor. The *Xanthomonadaceae* family, which were frequently detected in MBRs, was reported as quorum sensing bacteria, which is related to fouling development (Ishizaki et al., 2016; Hong et al., 2019). Moreover, *Xanthomonadaceae* has been identified as an EPS producer and can produce xanthan, which is a sticky polysaccharide polymer, and has resistance of cellulose backbone for hydrolysis with high membrane fouling potential (Szabó et al., 2017; Nataraj et al., 2008). As a consequence, these bacteria may be related to the membrane fouling development in H2 reactor.

Rhodanobacteraceae (OTU No. 1) was dominant in population II. *Rudaea* sp., which belongs to *Rhodanobacteraceae*, was implicated in the degradation of aromatic compounds for producing EPS (Qu et al., 2015). *Xanthomonadaceae* (OTU No. 6) has been observed at a higher proportion in H2 than in H1 reactor (**Table 5.2**). In contrast, phylum Chloroflexi (*Candidatus* Promineofilum: OTU No. 17) was found at higher proportions in the AS of H1 reactor than in H2 reactor. While this OTU was predominant in the biofilm and Chloroflexi was previously reported as a filamentous bacteria causing bulking (Ziegler et al., 2016; Nierychlo et al., 2019), it has also reported as capable of degrading complex polymers in anaerobic environments (Speirs et al., 2019). Thus, OTU members may have led to the mitigation of fouling in H1 reactor. These findings suggested that *Xanthomonadaceae* triggered the fouling development in H2 reactor. Besides, a low abundance of *Xanthomonadaceae*, enrichment of *Chitinophagaceae* and *Candidatus* Promineofilum contributed to fouling mitigation in H1 reactor.

Diversity decreased with decrease in MLSS with both H1 and H2 reactors, but the trend was more significant in H2, with a higher diversity of H1 reactor (**Fig. 5.3 and Table 5.3**). In contrast, the diversity of population in H1 reactor facilitated adaptation to starvation conditions and resulted in higher numbers of OTUs in population III than H2 reactor (**Fig. 5.10c**), leading fouling mitigation. Zhang et al. (2017) reported that microbial diversity and SMP degrading bacteria were increased by adding bamboo charcoal to MBR, contributing to fouling mitigation. Under the long SRT of MBR, microbial communities can become more complex and these conditions are conducive to the consumption of macro-molecules and low production of

biopolymer (Duan et al., 2009). Conversely, a decrease in microbial diversity resulted in reducing the number of usable carbon sources (Yang et al., 2011). Thus, in the present study, the consumption of DOC, mainly BAPs, by heterotrophic bacteria might have been facilitated by high diversity in H1 reactor. Higher diversity in the AS microbial community led to an increase in critical bacteria at low abundance at an early stage of fouling, playing a key role in the degradation of complex foulants and mitigated membrane fouling. The present study has shown that suitable conditions with higher microbial diversity and development of heterotrophic organisms are tolerant of prolonged starvation environment, and could increase important bacteria (*Chitinophagaceae*, *Candidatus* Promineofilum) and could mitigate membrane fouling development.

Table 5.2 Comparison of the AS microbial communities at the OTUs level in each reactor under starvation conditions.

				Reactor Name	H1 reactor						H2 reactor						L reactor						
				Sampling day	8 day		22 day		36 day		8 day		22 day		30 day		5 day		15 day		23 day		
				Sample Name	AS-d8-1	AS-d8-2	AS-d22-1	AS-d22-2	AS-d36-1	AS-d36-2	AS-d8-1	AS-d8-2	AS-d22-1	AS-d22-2	AS-d30-1	AS-d30-2	AS-d5-1	AS-d5-2	AS-d15-1	AS-d15-2	AS-d23-1	AS-d23-2	
No.	OTU ID	Phylum (Class)	Family	Genera																			
1	denovo6135	(Gammaproteobacteria)	*Rhodanobacteraceae*	*Rudaea*	0.1	0.3	19.6	22.5	11.0	14.2	17.6	16.4	24.5	20.2	11.0	21.6	0.0	0.0	0.0	0.0	0.1	0.1	30%
2	denovo12388	(Gammaproteobacteria)	*Xanthomonadaceae*	*Chujaibacter*	0.0	0.0	3.4	3.0	1.0	1.0	1.8	0.7	9.8	4.0	15.0	17.3	0.1	0.1	0.2	0.4	0.4	0.9	25%
3	denovo10402	Bacteroidetes	*Lewinellaceae*	*Lewinella*	7.2	15.7	0.0	0.0	0.0	0.0	1.8	0.6	0.0	0.0	0.0	0.0	0.0	0.0	0.0	0.0	0.0	0.0	20%
4	denovo10937	Bacteroidetes	*Prolixibacteraceae*	*Sunxiuqinia*	0.0	0.0	0.1	0.0	0.5	11.3	0.9	1.3	0.8	6.3	0.4	0.3	0.0	0.0	0.0	0.0	0.0	0.0	15%
5	denovo3949	Bacteroidetes	*Chitinophagaceae*	*Taibaiella*	0.0	0.0	2.3	1.7	2.1	2.5	0.2	0.0	10.3	7.0	5.5	2.4	0.0	0.0	0.0	0.0	0.0	0.0	10%
6	denovo5665	(Gammaproteobacteria)	*Xanthomonadaceae*	*Thermomonas*	0.0	0.0	1.8	1.8	1.4	1.5	1.5	2.8	4.0	9.3	8.2	2.2	0.0	0.0	0.0	0.0	0.0	0.0	9%
7	denovo9505	Bacteroidetes	*Chitinophagaceae*	*Ferruginibacter*	0.1	0.2	5.6	6.7	9.1	6.0	0.8	1.1	8.7	5.0	3.4	3.0	0.0	0.0	0.0	0.0	0.1	0.1	8%
8	denovo10408	Bacteroidetes	*Lewinellaceae*	*Lewinella*	9.0	2.3	0.3	0.0	0.0	0.0	0.0	0.0	0.0	0.0	0.0	0.0	0.1	0.1	0.1	0.0	0.1	0.0	7%
9	denovo5928	Armatimonadetes	*Fimbriimonadaceae*	*Fimbriimonas*	0.0	0.0	0.5	0.1	5.7	3.7	0.1	0.0	3.7	0.4	8.1	0.6	0.0	0.0	0.0	0.0	0.0	0.0	6%
10	denovo6098	(Gammaproteobacteria)	*Yersiniaceae*	*Rouxiella*	0.0	0.0	0.0	0.0	5.2	0.0	0.8	7.5	0.0	0.0	0.0	0.0	0.0	0.0	0.0	0.0	0.0	0.0	5%
11	denovo12303	Actinobacteria	*Iamiaceae*	Unclassified	0.7	0.8	1.6	0.3	0.1	0.6	5.7	7.5	0.0	0.1	0.0	0.0	0.2	0.2	0.3	0.2	0.3	0.2	4%
12	denovo7558	Firmicutes	*Alicyclobacillaceae*	*Tumebacillus*	0.5	0.8	1.4	1.0	1.7	3.3	0.4	0.8	1.2	1.9	4.9	7.0	0.0	0.0	0.1	0.0	0.1	0.1	3%
13	denovo9308	Bacteroidetes	*Chitinophagaceae*	*Lacibacter*	0.2	0.3	2.2	3.7	6.2	5.7	0.1	0.1	0.0	0.2	0.0	0.0	0.1	0.0	0.1	0.1	0.0	0.0	2%
14	denovo7284	(Alphaproteobacteria)	*Micropepsaceae*	*Micropepsis*	0.0	0.0	3.5	0.0	0.6	0.5	0.3	0.0	2.2	5.9	3.5	5.6	0.0	0.0	0.0	0.0	0.0	0.0	1%
15	denovo13714	Bacteroidetes	*Cytophagaceae*	*Ohtaekwangia*	0.4	0.3	0.0	0.0	0.0	0.0	1.5	5.4	0.0	0.0	0.0	0.0	3.4	3.4	2.2	2.1	1.9	2.5	0%
16	denovo8436	Bacteroidetes	*Lewinellaceae*	*Lewinella*	0.0	0.0	0.0	0.0	0.0	0.0	0.1	0.0	0.0	0.0	0.0	0.0	5.2	5.4	1.0	2.5	0.5	0.8	
17	denovo5300	Chloroflexi	*Ardenticatenaceae*	*Candidatus Promineofilum*	0.3	0.6	2.5	4.2	0.2	0.6	0.3	0.2	0.7	0.0	0.0	0.1	0.1	0.0	0.2	0.3	0.3	0.1	
18	denovo1135	(Gammaproteobacteria)	*Alcanivoracaceae*	*Alcanivorax*	0.0	0.0	0.6	1.4	0.1	4.1	0.2	0.9	1.3	3.9	0.2	0.4	0.0	0.0	0.0	0.0	0.0	0.0	
19	denovo8738	(Betaproteobacteria)	*Zoogloeaceae*	*Thauera*	4.1	3.4	2.3	1.7	1.0	1.0	0.5	0.5	0.1	0.2	0.0	0.1	0.0	0.0	0.0	0.0	0.1	0.0	
20	denovo9398	Acidobacteria	*Holophagaceae*	*Geothrix*	0.0	0.0	4.1	1.5	1.4	0.7	1.7	0.8	0.4	1.3	0.0	0.1	0.0	0.0	0.0	0.0	0.0	0.0	
21	denovo5637	Bacteroidetes	*Haliscomenobacteraceae*	*Phaeodactylibacter*	2.6	3.8	0.1	0.0	0.0	0.0	0.6	0.2	0.0	0.0	0.0	0.0	0.0	0.0	0.0	0.0	0.0	0.0	
22	denovo13594	Bacteroidetes	*Chitinophagaceae*	*Edaphobaculum*	0.0	0.0	0.5	0.0	3.5	0.1	0.1	0.0	0.8	1.0	0.0	0.0	0.0	0.0	0.0	0.0	0.0	0.0	
23	denovo13209	(Betaproteobacteria)	*Sterolibacteriaceae*	*Georgfuchsia*	1.0	0.9	0.1	0.2	0.0	0.1	0.3	0.1	0.0	0.0	0.0	0.0	1.9	1.9	3.5	2.4	2.3	1.8	
24	denovo6136	Nitrospirae	*Nitrospiraceae*	*Nitrospira*	3.3	3.1	0.6	0.1	0.5	0.1	0.8	0.4	0.5	0.2	0.6	0.4	0.0	0.0	0.0	0.0	0.1	0.0	
25	denovo5301	(Deltaproteobacteria)	*Kofleriaceae*	*Kofleria*	0.0	0.0	0.0	0.0	0.0	0.0	0.0	0.0	0.0	0.0	0.0	0.0	3.1	2.8	0.1	0.2	0.0	0.0	
26	denovo5270	(Betaproteobacteria)	*Azonexaceae*	*Azonexus*	0.2	0.2	0.0	0.0	0.0	0.0	0.1	0.1	0.0	0.0	0.0	0.0	3.1	2.6	2.5	2.2	1.6	1.3	
27	denovo3269	Actinobacteria	*Iamiaceae*	*Iamia*	0.0	0.0	0.0	0.0	2.9	0.2	0.0	0.0	0.5	0.5	1.2	1.1	0.0	0.0	0.0	0.0	0.0	0.0	
28	denovo1105	Bacteroidetes	*Chitinophagaceae*	*Terrimonas*	2.0	1.4	0.2	0.1	0.0	0.0	0.8	0.4	0.0	0.0	0.0	0.0	2.5	1.7	2.9	2.6	2.8	2.7	
29	denovo6810	TM6	Unclassified	Unclassified	0.4	0.4	1.5	0.5	2.3	2.9	0.1	0.4	0.3	0.3	0.2	0.1	0.0	0.0	0.0	0.0	0.0	0.0	
30	denovo200	Bacteroidetes	*Chitinophagaceae*	*Cnuella*	0.0	0.0	0.1	0.0	0.1	0.0	0.0	0.0	1.0	0.5	2.8	0.8	0.0	0.0	0.0	0.0	0.0	0.0	

Table 5.3 Microbial diversity indices in the activated sludge (AS) and biofilm (BF) of all reactors during starvation conditions

Reactor	*Sample Name*	*Sampling day*	*Shannon*	*PD whole tree*	*Chao1*	*Ace*	*Species*	*OTUs*	*Goods coverage*
H1	AS-d8-1	8	7.64 ± 0.05	164.0 ± 5.0	2117 ± 110	2230 ± 111	862 ± 20	862 ± 20	0.85 ± 0.01
	AS-d8-2	8	7.51 ± 0.06	148.5 ± 5.2	1772 ± 123	1932 ± 103	827 ± 16	827 ± 16	0.86 ± 0.00
	AS-d22-1	22	6.53 ± 0.03	134.5 ± 10.4	1535 ± 153	1660 ± 118	632 ± 11	632 ± 11	0.89 ± 0.00
	AS-d22-2	22	6.30 ± 0.02	124.5 ± 3.5	1197 ± 96	1309 ± 88	577 ± 10	577 ± 10	0.91 ± 0.00
	AS-d36-1	36	6.47 ± 0.04	123.2 ± 4.3	1350 ± 149	1433 ± 85	567 ± 10	567 ± 10	0.90 ± 0.00
	AS-d36-2	36	6.09 ± 0.03	97.6 ± 5.5	1284 ± 171	1302 ± 80	504 ± 10	504 ± 10	0.91 ± 0.00
H2	AS-d8-1	8	6.99 ± 0.03	73.3 ± 0.8	782 ± 27	809 ± 21	552 ± 6	552 ± 6	0.94 ± 0.00
	AS-d8-2	8	6.42 ± 0.04	70.8 ± 1.6	738 ± 28	804 ± 24	487 ± 7	487 ± 7	0.94 ± 0.00
	AS-d22-1	22	4.99 ± 0.02	41.8 ± 1.0	427 ± 17	426 ± 10	273 ± 3	273 ± 3	0.97 ± 0.00
	AS-d22-2	22	5.23 ± 0.02	48.0 ± 3.5	377 ± 13	389 ± 14	268 ± 4	268 ± 4	0.97 ± 0.00
	AS-d30-1	30	5.27 ± 0.03	53.3 ± 3.2	399 ± 28	448 ± 27	261 ± 5	261 ± 5	0.97 ± 0.00
	AS-d30-2	30	5.09 ± 0.01	57.6 ± 3.0	404 ± 14	412 ± 12	273 ± 2	273 ± 2	0.97 ± 0.00
	BF-d30-1	30	5.63 ± 0.02	42.9 ± 1.1	367 ± 15	383 ± 15	272 ± 1	272 ± 1	0.97 ± 0.00
	BF-d30-2	30	4.91 ± 0.02	43.5 ± 2.0	301 ± 21	313 ± 15	209 ± 4	209 ± 4	0.98 ± 0.00
L	AS-d5-1	5	8.06 ± 0.04	180.1 ± 8.5	1654 ± 114	1730 ± 86	821 ± 15	821 ± 15	0.87 ± 0.00
	AS-d5-2	5	8.01 ± 0.02	147.6 ± 5.4	1646 ± 114	1668 ± 86	804 ± 13	804 ± 13	0.87 ± 0.00
	AS-d15-1	15	8.37 ± 0.03	165.2 ± 4.9	1724 ± 75	1781 ± 74	873 ± 16	873 ± 16	0.87 ± 0.00
	AS-d15-2	15	8.42 ± 0.04	199.1 ± 5.0	1696 ± 68	1843 ± 59	883 ± 18	883 ± 18	0.86 ± 0.00
	AS-d23-1	23	8.55 ± 0.03	177.9 ± 5.9	1663 ± 107	1748 ± 113	889 ± 15	889 ± 15	0.87 ± 0.01
	AS-d23-2	23	8.50 ± 0.04	198.6 ± 9.2	1832 ± 145	1921 ± 119	910 ± 19	910 ± 19	0.86 ± 0.01
	BF-d23-1	23	8.02 ± 0.04	163.1 ± 8.3	1691 ± 121	1771 ± 97	813 ± 18	813 ± 18	0.87 ± 0.01
	BF-d23-2	23	7.77 ± 0.02	144.0 ± 5.2	1556 ± 83	1656 ± 69	800 ± 11	800 ± 11	0.88 ± 0.00

5.5. Summary of chapter 5

Laboratory-scale A/O-MBRs treating actual municipal sewage at different seasons have been operated under the same starvation conditions to induce membrane fouling development. Interestingly, one of the MBRs has been stably operated, even under prolonged starvation conditions, without fouling development. Hence, we hypothesized that specific bacteria would degrade BAPs released from endogenous respiration, which was supposed to lead to membrane fouling mitigation in the fouling-mitigated reactor. In the fouled reactor, specific bacteria would increase abundance, contributing to SMP production and fouling development. Moreover, the certain fouling-mitigating bacteria were low abundant in fouled reactor. In this study, higher microbial diversity indices and a number of unique bacteria have been identified in the fouling-mitigated MBR. ΔDOC, which is the difference in DOC concentrations between AS supernatant and permeate effluent, was negatively correlated with permeability and could be used as a fouling development parameter. On the other hand, biofilms in the fouled MBRs have formed different microbial communities from the AS communities. TM6, OD1, and Chlamydiae were detected as a predominant phylum in the biofilm and might have important roles in biofilm formation. *Chitinophagaceae* and *Candidatus* Promineofilum increased in abundance in the fouling-mitigated MBR, suggesting that they played an essential role in fouling mitigation associated with BAP degradation. *Xanthomonadaceae* were detected as the dominant family in the fouled reactor and might be related to the membrane fouling development. The microbial community of the fouling-mitigated reactor has shown a high diversity; thus, maintaining and improving microbial diversity may be a significant parameter for fouling control. While microbial diversity was stable with a high level, at a lower temperature, lower microbial activities might be related to BAP accumulation.

References

Caporaso, J.G., Kuczynski, J., Stombaugh, J., Bittinger, K., Bushman, F.D., Costello, E.K., Fierer, N., Peña, A.G., Goodrich, J.K., Gordon, J.I., Huttley, G.A., Kelley, S.T., Knights, D., Koenig, J.E., Ley, R.E., Lozupone, C.A., Mcdonald, D., Muegge, B.D., Pirrung, M., Reeder, J., Sevinsky, J.R., Turnbaugh, P.J., Walters, W.A., Widmann, J., Yatsunenko, T., Zaneveld, J., Knight, R., 2010. correspondence QIIME allows analysis of high- throughput community sequencing data Intensity normalization improves color calling in SOLiD sequencing. Nat. Publ. Gr. 7, 335–336. https://doi.org/10.1038/nmeth0510-335

Caporaso, J.G., Lauber, C.L., Walters, W.A., Berg-Lyons, D., Huntley, J., Fierer, N., Owens, S.M., Betley, J., Fraser, L., Bauer, M., Gormley, N., Gilbert, J.A., Smith, G., Knight, R., 2012. Ultra-high-throughput microbial community analysis on the Illumina HiSeq and MiSeq platforms. ISME J. 6, 1621–1624. https://doi.org/10.1038/ismej.2012.8

Duan, L., Moreno-Andrade, I., Huang, C. lin, Xia, S., Hermanowicz, S.W., 2009. Effects of short solids retention time on microbial community in a membrane bioreactor. Bioresour. Technol. 100, 3489–3496. https://doi.org/10.1016/j.biortech.2009.02.056

Gao, D.W., Wang, X.L., Xing, M., 2014. Dynamic variation of microbial metabolites and community involved in membrane fouling in A/O-MBR. J. Memb. Sci. 458, 157–163. https://doi.org/10.1016/j.memsci.2014.01.064

Gao, D.W., Wen, Z.D., Li, B., Liang, H., 2013. Membrane fouling related to microbial community and extracellular polymeric substances at different temperatures. Bioresour. Technol. 143, 172–177. https://doi.org/10.1016/j.biortech.2013.05.127

Guo, X., Miao, Y., Wu, B., Ye, L., Yu, H., Liu, S., Zhang, X. xiang, 2015. Correlation between microbial community structure and biofouling as determined by analysis of microbial community dynamics. Bioresour. Technol. 197, 99–105. https://doi.org/10.1016/j.biortech.2015.08.049

Hong, P.N., Noguchi, M., Matsuura, N., Honda, R., 2019. Mechanism of biofouling enhancement in a membrane bioreactor under constant trans-membrane pressure operation. J. Memb. Sci. 592, 117391. https://doi.org/10.1016/j.memsci.2019.117391

Huang, X., Leal, M., Li, Q., 2008. Degradation of natural organic matter by TiO2 photocatalytic oxidation and its effect on fouling of low-pressure membranes. Water Res. 42, 1142–1150. https://doi.org/10.1016/j.watres.2007.08.030

Ishizaki, S., Fukushima, T., Ishii, S., Okabe, S., 2016. Membrane fouling potentials and cellular properties of bacteria isolated from fouled membranes in a MBR treating municipal wastewater. Water Res. 100, 448–457. https://doi.org/10.1016/j.watres.2016.05.027

Jacquin, C., Gambier, N., Lesage, G., Heran, M., 2018. New insight into fate and fouling behavior of bulk Dissolved Organic Matter (DOM) in a full-scale membrane bioreactor for domestic wastewater treatment. J. Water Process Eng. 22, 94–102. https://doi.org/10.1016/j.jwpe.2018.01.014

Jiang, T., Kennedy, M.D., Schepper, V. De, Nam, S.N., Nopens, I., Vanrolleghem, P.A., Amy, G., 2010. Characterization of soluble microbial products and their fouling impacts in membrane bioreactors. Environ. Sci. Technol. 44, 6642–6648. https://doi.org/10.1021/es100442g

Kämpfer, P., Lodders, N., Falsen, E., 2011. Hydrotalea flava gen. nov., sp. nov., a new member of the phylum Bacteroidetes and allocation of the genera Chitinophaga, Sediminibacterium, Lacibacter, Flavihumibacter, Flavisolibacter, Niabella, Niastella, Segetibacter, Parasegetibacter, Terrimonas, Fer. Int. J. Syst. Evol. Microbiol. 61, 518–523. https://doi.org/10.1099/ijs.0.023002-0

Liu, J., Liang, X., Yang, C., Yu, S., Guo, H., 2019. Tracing membrane biofouling to the microbial community structure and its metabolic products: An investigation on the three-stage MBR combined with worm reactor process. Bioresour. Technol. 278, 165–174. https://doi.org/10.1016/j.biortech.2019.01.069

Ma, J., Wang, Z., Yang, Y., Mei, X., Wu, Z., 2013. Correlating microbial community structure and composition with aeration intensity in submerged membrane bioreactors by 454 high-throughput pyrosequencing. Water Res. 47, 859–869. https://doi.org/10.1016/j.watres.2012.11.013

Ma, Z., Wen, X., Zhao, F., Xia, Y., Huang, X., Waite, D., Guan, J., 2013. Effect of temperature variation on membrane fouling and microbial community structure in membrane bioreactor. Bioresour. Technol. 133, 462–468. https://doi.org/10.1016/j.biortech.2013.01.023

Maqbool, T., Cho, J., & Hur, J. (2017). Dynamic changes of dissolved organic matter in membrane bioreactors at different organic loading rates: Evidence from spectroscopic and chromatographic methods. Bioresource technology, 234, 131-139.

Miura, Y., Watanabe, Y., Okabe, S., 2007. Significance of Chloroflexi in performance of submerged membrane bioreactors (MBR) treating municipal wastewater. Environ. Sci. Technol. 41, 7787–7794. https://doi.org/10.1021/es071263x

Nataraj, S., Schomäcker, R., Kraume, M., Mishra, I.M., Drews, A., 2008. Analyses of polysaccharide fouling mechanisms during crossflow membrane filtration. J. Memb. Sci. 308, 152–161. https://doi.org/10.1016/j.memsci.2007.09.060

Neoh, C.H., Yung, P.Y., Noor, Z.Z., Razak, M.H., Aris, A., Md Din, M.F., Ibrahim, Z., 2017. Correlation between microbial community structure and performances of membrane bioreactor for treatment of palm oil mill effluent. Chem. Eng. J. 308, 656–663. https://doi.org/10.1016/j.cej.2016.09.063

Nierychlo, M., Miłobędzka, A., Petriglieri, F., McIlroy, B., Nielsen, P.H., McIlroy, S.J., 2019. The morphology and metabolic potential of the Chloroflexi in full-scale activated sludge wastewater treatment plants. FEMS Microbiol. Ecol. 95, 1–11. https://doi.org/10.1093/femsec/fiy228

Palmarin, M.J., Young, S., Chan, J., 2020. Recovery of a hybrid and conventional membrane bioreactor following long-term starvation. J. Water Process Eng. 34, 101027. https://doi.org/10.1016/j.jwpe.2019.101027

Qu, Y., Ma, Q., Deng, J., Shen, W., Zhang, X., He, Z., Nostrand, J.D.V., Zhou, Jiti, Zhou, Jizhong, 2015. Responses of microbial communities to single-walled carbon nanotubes in phenol wastewater treatment systems. Environ. Sci. Technol. 49, 4627–4635. https://doi.org/10.1021/es5053045

Rehman, Z.U., Fortunato, L., Cheng, T., Leiknes, T.O., 2020. Metagenomic analysis of sludge and early-stage biofilm communities of a submerged membrane bioreactor. Sci. Total Environ. 701, 134682. https://doi.org/10.1016/j.scitotenv.2019.134682

Sepehri, A., Sarrafzadeh, M.H., 2018. Effect of nitrifiers community on fouling mitigation and nitrification efficiency in a membrane bioreactor. Chem. Eng. Process. - Process Intensif. 128, 10–18. https://doi.org/10.1016/j.cep.2018.04.006

Shen, Y.X., Xiao, K., Liang, P., Sun, J.Y., Sai, S.J., Huang, X., 2012. Characterization of soluble microbial products in 10 large-scale membrane bioreactors for municipal wastewater treatment in China. J. Memb. Sci. 415–416, 336–345. https://doi.org/10.1016/j.memsci.2012.05.017

Shi, Y., Huang, J., Zeng, G., Gu, Y., Hu, Y., Tang, B., Zhou, J., Yang, Y., Shi, L., 2018. Evaluation of soluble microbial products (SMP) on membrane fouling in membrane bioreactors (MBRs) at the fractional and overall level: a review. Rev. Environ. Sci. Biotechnol. 17, 71–85. https://doi.org/10.1007/s11157-017-9455-9

Speirs, L.B.M., Rice, D.T.F., Petrovski, S., Seviour, R.J., 2019. The Phylogeny, Biodiversity, and Ecology of the Chloroflexi in Activated Sludge. Front. Microbiol. 10. https://doi.org/10.3389/fmicb.2019.02015

Szabó, E., Liébana, R., Hermansson, M., Modin, O., Persson, F., Wilén, B.M., 2017. Microbial population dynamics and ecosystem functions of anoxic/aerobic granular sludge in sequencing batch reactors operated at different organic loading rates. Front. Microbiol. 8, 1–14. https://doi.org/10.3389/fmicb.2017.00770

Takada, K., Shiba, T., Yamaguchi, T., Akane, Y., Nakayama, Y., Soda, S., Inoue, D., Ike, M., 2018. Cake layer bacterial communities during different biofouling stages in full-scale membrane bioreactors. Bioresour. Technol. 259, 259–267. https://doi.org/10.1016/j.biortech.2018.03.051

Takimoto, Y., Hatamoto, M., Ishida, T., Watari, T., Yamaguchi, T., 2018. Fouling Development in A/O-MBR under Low Organic Loading Condition and Identification of Key Bacteria for Biofilm Formations. Sci. Rep. 8, 1–9. https://doi.org/10.1038/s41598-018-29821-9

Teng, J., Shen, L., Xu, Y., Chen, Y., Wu, X. L., He, Y., ... & Lin, H. (2020). Effects of molecular weight distribution of soluble microbial products (SMPs) on membrane fouling in a membrane bioreactor (MBR): Novel mechanistic insights. Chemosphere, 248, 126013.

Wang, Z., Wu, Z., 2009. Distribution and transformation of molecular weight of organic matters in membrane bioreactor and conventional activated sludge process. Chem. Eng. J. 150, 396–402. https://doi.org/10.1016/j.cej.2009.01.018

Wang, Z., Wu, Z., Tang, S., 2009. Extracellular polymeric substances (EPS) properties and their effects on membrane fouling in a submerged membrane bioreactor. Water Res. 43, 2504–2512. https://doi.org/10.1016/j.watres.2009.02.026

Watanabe, R., Nie, Y., Wakahara, S., Komori, D., Li, Y.Y., 2017. Investigation on the response of anaerobic membrane bioreactor to temperature decrease from 25 °C to 10 °C in sewage treatment. Bioresour. Technol. 243, 747–754. https://doi.org/10.1016/j.biortech.2017.07.001

Wei, D., Tao, Y., Zhang, Z., Zhang, X., 2016. Effect of pre-ozonation on mitigation of ceramic UF membrane fouling caused by algal extracellular organic matters. Chem. Eng. J. 294, 157–166. https://doi.org/10.1016/j.cej.2016.02.110

Xiong, Y., Harb, M., Hong, P.Y., 2015. Characterization of biofoulants illustrates different membrane fouling mechanisms for aerobic and anaerobic membrane bioreactors. Sep. Purif. Technol. 157, 192–202. https://doi.org/10.1016/j.seppur.2015.11.024

Yang, C., Zhang, W., Liu, R., Li, Q., Li, B., Wang, S., Song, C., Qiao, C., Mulchandani, A., 2011. Phylogenetic diversity and metabolic potential of activated sludge microbial communities in full-scale wastewater treatment plants. Environ. Sci. Technol. 45, 7408–7415. https://doi.org/10.1021/es2010545

Zhang, W., Liu, X., Wang, D., Jin, Y., 2017. Effects of bamboo charcoal on fouling and microbial diversity in a flat-sheet ceramic membrane bioreactor. Bioresour. Technol. 243, 1020–1026. https://doi.org/10.1016/j.biortech.2017.07.084

Zhao, W.T., Shen, Y.X., Xiao, K., Huang, X., 2010. Fouling characteristics in a membrane bioreactor coupled with anaerobic-anoxic-oxic process for coke wastewater treatment. Bioresour. Technol. 101, 3876–3883. https://doi.org/10.1016/j.biortech.2009.12.141

Zhou, Z., He, X., Zhou, M., Meng, F., 2017. Chemically induced alterations in the characteristics of fouling-causing bio-macromolecules – Implications for the chemical cleaning of fouled membranes. Water Res. 108, 115–123. https://doi.org/10.1016/j.watres.2016.10.065

Ziegler, A.S., McIlroy, S.J., Larsen, P., Albertsen, M., Hansen, A.A., Heinen, N., Nielsen, P.H., 2016. Dynamics of the fouling layer microbial community in a membrane bioreactor. PLoS One 11, 1–14. https://doi.org/10.1371/journal.pone.0158811

Chapter 6

Conclusion remarks

6.1. Summary of this thesis

This thesis focused on membrane biofouling developed by microbes and biofilm forming bacteria in A/O-MBR. Full-scale plant is practiced under lower F/M conditions influenced by stopping influent or rain event. Thus, this thesis also focused on the influence of low OLR conditions on membrane fouling, and A/O-MBR was operated under prolonged extremely low OLR conditions. The experimental outcomes and conclusions in each chapter are as follows;

In chapter 3, A/O-MBR was operated under extremely low organic loading rate condition (R_L reactor; OLR: 0.002 kg-COD·m^{-3}·day^{-1}), and membrane fouling and biofilm were drastically developed compared to the A/O-MBR under normal conditions (R_N reactor; OLR: 0.42 kg-COD·m^{-3}·day^{-1}). This phenomenon was explained that the microbes were lysed by affecting starvation environment and the lysed microbes released significant substances such as SMP on membrane fouling development. The microbial community analysis based on 16S rRNA genes sequencing revealed that composition between the bulk sludge and biofilm was considerably different, and characteristic bacteria found in BF were thought to important for biofilm formation on the membrane surface in A/O-MBR. Candidate TM6 showed specific presence on the fouled membrane surface as a biofilm in the R_L reactor. On the other hand, Candidate OD1 was the predominant phylum in the fouled membrane surface of the R_N reactor. In this chapter, these uncultured bacteria was decided as biofilm-forming bacteria.

Since two A/O-MBRs operated under extremely low OLR condition could induce severe membrane fouling and biofilm formation, chapter 4 focused on initiation and progression of membrane fouling by microbes to monitor fouled membrane surface by non-destructive observation and microbial community analysis. In the initial fouling stage, dead cell or red-stained nucleic acid were attached on the membrane surface with no living bacteria and the dead cell might play conditioning film which enhance to microbial adherence to the membrane. In the middle fouling stage, live cells formed microcolonies on the dead cells and these colony resulted in decreased permeability. 16S rRNA genes analysis showed that the specific bacteria formed biofilm on the membrane. In addition, unclassified *Neisseriaceae* was detected largely in middle-stage biofilm. The results indicated that specific pioneer bacteria might play a role in forming microcolonies and then triggering further biofilm development.

In chapter 5, three A/O-MBRs were operated under the low OLR condition in different seasons. Interestingly, an A/O-MBR at higher temperature mitigated membrane fouling although

low OLR condition induced membrane fouling at lower temperature as shown in chapter 3 and 4. Thus, we hypothesized that cell decayed substances (so called BAP) derived from microbial cell lysis were utilized by specific bacteria which could adapt the starvation condition in the fouling-mitigated MBR. Comparing the reactor performances between fouled and fouling-mitigated MBR at higher temperature, dissolved organic carbon (DOC) played an important role on membrane fouling. In the fouled MBR, DOC was accumulated in the MBR suggesting that endogenously developed DOC was higher molecular weight and bacteria in the fouled MBR could not utilize the DOC component. Conversely, in the fouling-mitigated MBR, the DOC behavior in the activated sludge was similar to the effluent sample. This result suggested that the DOC was degraded into lower molecules which could easily pass through the membrane pores. Based on the microbial community analysis in depth, *Chitinophagaceae* and *Candidatus* Promineofilum increased in abundance in the fouling-mitigated MBR, suggesting that they played an essential role in fouling mitigation associated with BAP degradation. Conversely, *Xanthomonadaceae* were detected as the dominant family in the fouled reactor and might be related to the membrane fouling development. The microbial community of the fouling-mitigated reactor has shown a high diversity; thus, maintaining and improving microbial diversity may be an important parameter for fouling control. While microbial diversity was stable with a high level, at a lower temperature, microbial activities might be related to BAP degradation. This chapter indicated that ΔDOC which is DOC concentration between activated sludge and permeate effluent could be used ad indicator positively correlating for permeability.

This thesis revealed impact of low OLR condition on membrane fouling and biofilm forming bacteria in A/O-MBR treating actual municipal sewage. The practical low OLR operational conditions indicated that biofilm forming bacteria formed live-cell microcolony on the dead-cell conditioning film and was specifically grown on the membrane. In addition, these bacteria were seemed to be CPR bacteria or related to pathogenic bacteria. Furthermore, SMP especially BAP derived from cell lysis showed significant role on membrane fouling development and DOC could be use as important indicator for expecting fouling development (**Fig. 6.1**). Finally, higher microbial diversity enhanced degradation of BAP into lower molecules less than membrane pore. In conclusion, BAP has primary role on initial membrane fouling and CPR and biofilm forming bacteria attached on the conditioning film formed by BAP (**Fig. 6.2**). In the final

fouling stage, biofilm consisted by BAP, these bacteria, and EPS contributed to generate cake layer.

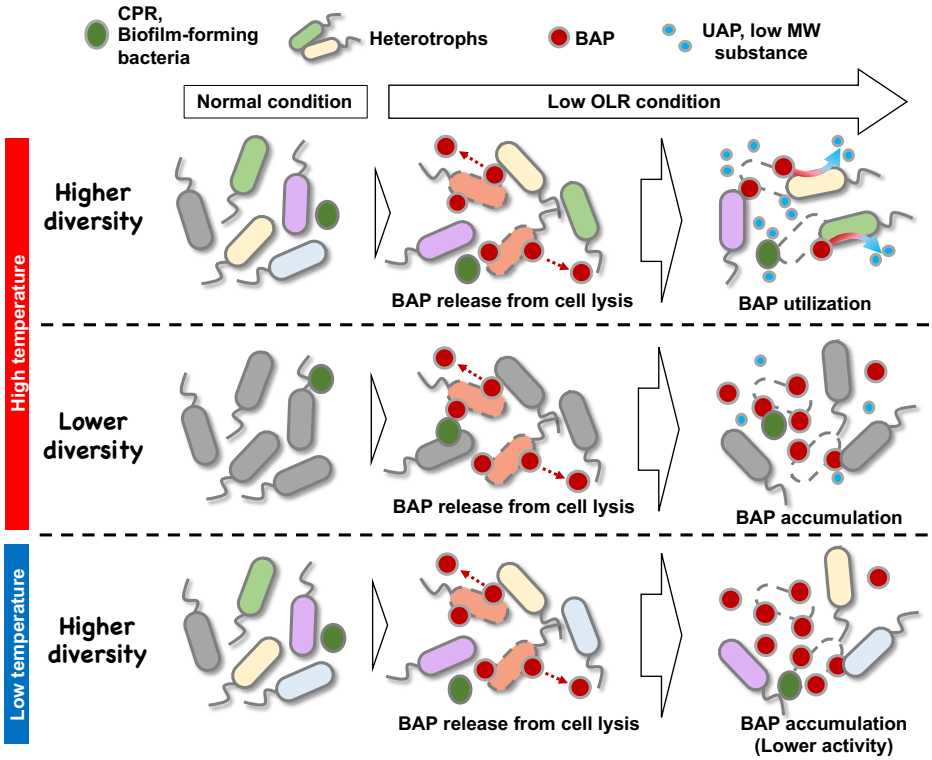

Fig. 6.1 Estimated mechanisms of BAP degradation and accumulation in activated sludge of A/O-MBR under low organic loading rate conditions.

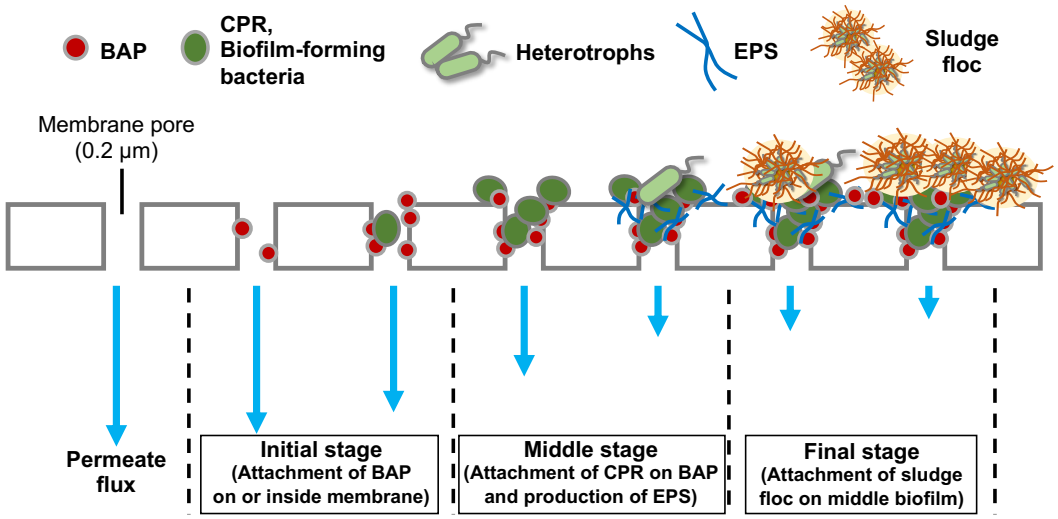

Fig. 6.2 Hypothetical role of BAP and uncultured bacteria (candidate phylum radiation: CPR) on biofilm formation and estimated membrane fouling mechanism in A/O-MBR under low organic loading rate condition.

6.2. Future outlook

In chapter 3 and 4, uncultured or pathogenic bacteria (OD1, TM6, *Neisseriaceae*) were identified as biofilm-forming bacteria based on 16S rRNA gene sequencing for analyzing biofilm developed on the membrane surface under low OLR conditions. **Fig. 6.3** shows the distribution of the biofilm-forming bacteria under various organic loading rate conditions. The biofilm-forming bacteria were enrichment on the biofilm or bio-cake on the membrane surface compared to bulk sludge community. Many studies operated under lower or standard conditions (0.02-0.06 g-COD·g-MLSS^{-1}·day^{-1}). Under the condition including this thesis, CPR and uncultured bacteria have increased the relative abundance in biofilm from activated sludge community. Moreover, anaerobic bacteria were frequently detected on the membrane surface. Thus, the biofilm might crate partial anaerobic or anoxic zone inside the pores of membrane and these biofilm-forming bacteria could penetrate into the membrane. However, since each bacteria has not been isolated as pure culture, physiological ecology of these bacteria on the membrane or aquatic environment are still unknown. Thus, biofilm formation mechanism in depth might be explained through pure culture for these biofilm-forming bacteria. In addition, the relationship between bacteria, bacteria and protozoa or metazoan might be important to understand biofilm formation. To control these biofilm-forming bacteria and protozoa or metazoan could lead to fouling mitigation strategy.

The study in chapter 5 showed that DOC accumulated in activated sludge of MBR was mainly consisted from BAP, and induced membrane fouling development in low OLR MBRs. The distribution of molecular size in BAP should be analyzed to reveal main component affecting membrane fouling development. On the other hand, diversity and activity of microbial community in activated sludge of MBR for degrading non-degradable substances (i.e. BAP) was important to mitigate membrane fouling. Optimal operational parameters of MBR should be investigated to maintain microbial diversity based on this study. Finally, combination of controlling non-degradable substance content and biofilm-forming bacteria will contribute to establish continuous operation of MBR with no fouling development in the future.

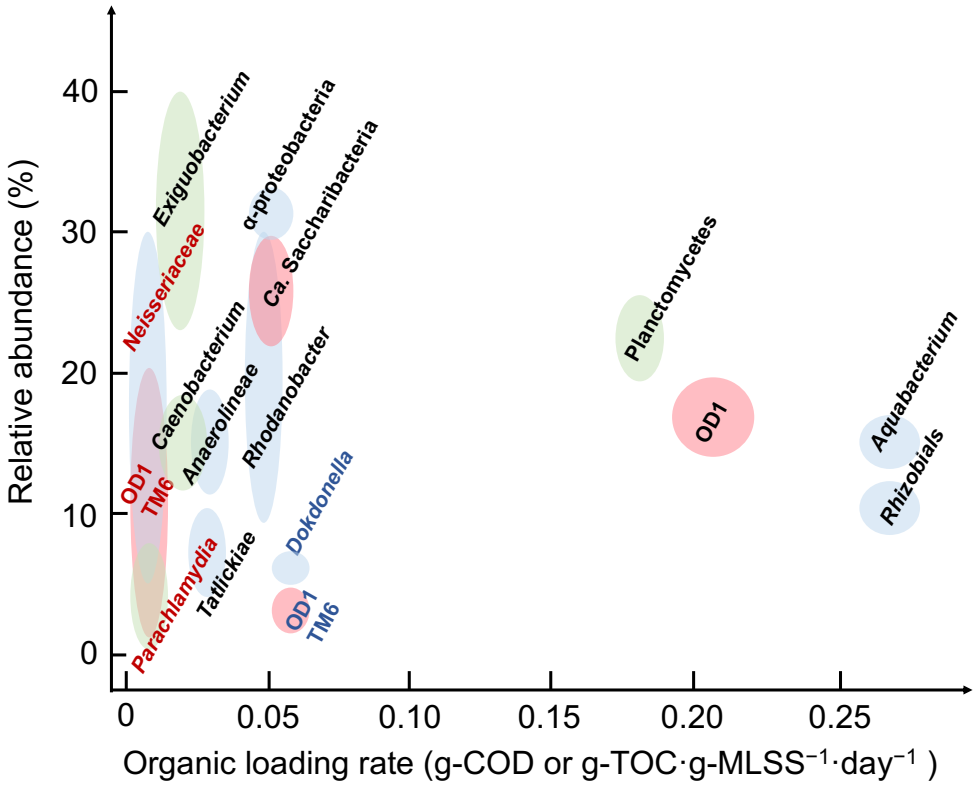

Fig. 6.3 Relative abundance of biofilm-forming bacteria detected on membrane surface based on 16S rRNA gene sequencing under various organic loading rate conditions shown in **Table 2.1**. Red and blue letters indicate the biofilm-forming bacteria determined in this study under low OLR and standard conditions, respectively. Red, green, and blue circles indicate uncultured bacteria, Chlamydiae/Firmicutes/Chloroflexi, and Proteobacteria, respectively.

謝辞

本博士学位論文は，長岡技術科学大学大学院 5 年一貫制博士課程 技術科学イノベーション専攻に在籍した 5 年間の研究成果をまとめたものです．本研究の遂行と本論文の作成にあたり，多くの方々から多大なご支援とご指導を賜りました．

新居浜工業高等専門学校 生物応用化学専攻で修了した専門分野とは大きく異なる分野で，排水処理について全く知識・経験の乏しい筆者に対して，長岡技術科学大学 山口隆司 教授には温かく受け入れて頂き，研究に対する姿勢や本質的な考え方をご指導頂いただけでなく，様々な機会やチャンス・出会いを設けて頂きました．同大学 幡本将史 准教授には，本研究の実施から論文の執筆に至るまで，絶えず懇切丁寧にご指導いただきました．実験結果に対して様々な観点で深く考察する重要性，そこから新たな研究の方向性を創出する楽しさをまさに体感しながら学ばせて頂きました．山口 教授，幡本 准教授の排水処理に関わる微生物に真摯に向き合う姿勢，環境微生物学・排水処理工学を修める面白さを教えていただいたことはとても大切な時間となりました．ここに深く感謝申し上げます．

長岡技術科学大学 小笠原渉 教授，牧慎也 准教授には，学位審査にあたりまして，副査の労を担って頂き，本論文の完成に非常に建設的なご意見・ご助言をいただくだけでなく，今後の研究の方針や研究者として社会貢献をする意義についてご指導を賜りました．筆者の新居浜工業高等専門学校在学時の指導教員でもある牧准教授には，研究をマネージメントする重要性や，研究者としてまた社会人として生き抜く上で大切なことを時に厳しく絶えずご指導下さいました．これまで様々な場面で研究生活を支えて下さり，改めて深く感謝申し上げます．同じく，副査を務めて頂いた広島大学 金田一智則 准教授には，本学位論文の根幹となる貴重なご助言を賜り，今後の進展についても考察する機会を頂戴しました．ここに記して感謝申し上げます．

阿南工業高等専門学校 川上周司 講師，産業技術総合研究所 黒田恭平 博士，和歌山工業高等専門学校 青木仁孝 准教授には，実験技術に関する適切なアドバイスから申請書の書き方まで，研究者としてのあり方をご指導いただきました．また，チュラロンコン大学 Wiboonluk 准教授，Jenyuk 講師には，タイ国滞在時に全面的な支援を頂戴し，充実した留学生活を支えて頂きました．技術職員 渡邉高子氏，スタッフ 重野晶子氏，黒崎香織氏，丸山奈都子氏には，学生生活において研究だけでなく私生活においても多大なご支援を頂きました．また，株式会社クボタの皆様には本研究を円滑に進めるために非常に多くの技術的・設備的なご支援と建設的なご意見を賜りました．ここに記して深く感謝申し上げます．

筆者が在学時に同研究室に在学されていた渡利高大氏（現 長岡技術科学大学 助教），段下剛志氏（現 徳山工業高等専門学校 助教），中原望氏（現 産業技術総合研究所），平片悠河氏（現 産業技術総合研究所），Adlin 氏（現 長岡技術科学大学 助教）や，同研究室 池田匠児氏，Thao 氏，惣中英章氏，鞍立大喜氏，三輪徹氏，徳田裕二郎氏，水田裕貴氏には，日々の研究に関するディスカッションやご助言をいただくことや，日常生活においても様々な場面でご支援をいただき，楽しく充実した日々を送ることができました．ここに記して深く感謝いたします．

最後に，遠い愛媛の地からいつも温かく見守り，研究生活での身体的，精神的な部分にまで常に気遣い，支えてくれた両親と祖父，祖母，弟たちに深く感謝の意を表し，本学位論文の結びと致します.

令和 3 年 3 月 25 日

滝本祐也